Mathematics of Transmission Dynamics and Control of HIV/AIDS in an MSM
Population

by

Queen Tollett

A Dissertation Presented in Partial Fulfillment
of the Requirements for the Degree
Doctor of Philosophy

Approved June 2023 by the
Graduate Supervisory Committee:

Abba B. Gumel, Chair
Sharon Crook
John Fricks
Carl Gardner
John Nagy

ARIZONA STATE UNIVERSITY

August 2023

ABSTRACT

The human immunodeficiency virus (HIV) pandemic, which causes the syndrome of opportunistic infections that characterize the late stage HIV disease, known as the acquired immunodeficiency syndrome (AIDS), remains a major public health challenge to many parts of the world. This dissertation contributes in providing deeper qualitative insights into the transmission dynamics and control of the HIV/AIDS disease in Men who have Sex with Men (MSM) community. A new mathematical model (which is relatively basic), which incorporates some of the pertinent aspects of HIV epidemiology and immunology and fitted using the yearly new case data of the MSM population from the State of Arizona, was designed and used to assess the population-level impact of awareness of HIV infection status and condom-based intervention, on the transmission dynamics and control of HIV/AIDS in an MSM community. Conditions for the existence and asymptotic stability of the various equilibria of the model were derived. The numerical simulations showed that the prospects for the effective control and/or elimination of HIV/AIDS in the MSM community in the United States are very promising using a condom-based intervention, provided the condom efficacy is high and the compliance is moderate enough. The model was extended in Chapter 3 to account for the effect of risk-structure, staged-progression property of HIV disease, and the use of pre-exposure prophylaxis (PrEP) on the spread and control of the disease. The model was shown to undergo a PrEP-induced *backward bifurcation* when the associated control reproduction number is less than one. It was shown that when the compliance in PrEP usage is 50%(80%) then about 19.1%(34.2%) of the yearly new HIV/AIDS cases recorded at the peak will have been prevented, in comparison to the worst-case scenario where PrEP-based intervention is not implemented in the MSM community. It was also shown that the HIV pandemic elimination is possible from the MSM community even for the scenario when the effective contact rate is

increased by 5-fold from its baseline value, if low-risk individuals take at least 15 years before they change their risky behavior and transition to the high-risk group (regardless of the value of the transition rate from high-risk to low-risk susceptible population).

DEDICATION

"I can do all things through Christ which strengtheneth me"

Philippians 4:13.

I thank God for life and sending a comforter.

I am thankful to my parents, Frederick Sr, and Josephine Wiggs and my three

brothers (Frederick Jr, Larry and Emmitt Wiggs) who I am certain are looking

down from heaven with smiles on their faces.

I thank my son, Kenneth Tollett, Jr and my Sister Hildred Wiggs for their

encouragement and support.

ACKNOWLEDGEMENT

TABLE OF CONTENTS

LIST OF TABLES

LIST OF FIGURES

Chapter 1

INTRODUCTION

1.1 General Overview

Since its emergence early in the 1980s, the *human immunodeficiency virus* (HIV) pandemic, which causes the syndrome of opportunistic infections that characterize the late stage HIV disease, known as the *acquired immunodeficiency syndrome* (AIDS), remains a major public health challenge to many parts of the world [66, 58, 72, 107, 32]. It has, as of July 2022, caused over 84.2 million cases and 40.1 million deaths globally [135, 113]. Recent data from the Joint United Nations Program on HIV/AIDS (UN-AIDS) shows that 38.4 million people currently live with HIV/AIDS (in the year 2021 alone, HIV caused 1.5 million new infections and 650,000 deaths globally [113, 133]). Of the 38.4 million people who are currently living with HIV/AIDS, 36.7 million are adults (15 years and older), 1.7 million are children (ages $0 - 14$ years) and 54% are women and girls [133]. Figure 1.1 depicts the global map of HIV/AIDS for the year 2020. The first cases of HIV/AIDS were reported in the United States on June 5, 1981 (among five homosexual men in Los Angeles) [56]. The Centers for Disease Control and Prevention (CDC) estimates that 1.2 million Americans are currently living with the virus, and 15,820 Americans have succumbed to the deadly virus [27]. At least three people are infected with HIV every hour in the United States [43]. UNAIDS estimate that $29 billion will be required globally to get on track to end AIDS as a global public health threat in 2025 [113] (similarly, more than $28 billion is spent per year in the United States to curtail the spread of HIV/AIDS in the U.S. [118]). The map for the prevalence of HIV/AIDS in the United States for the year 2022, is
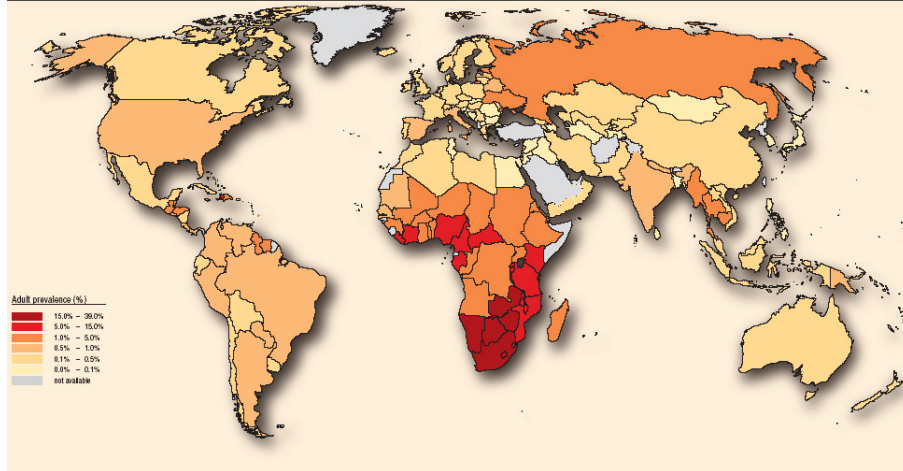
Figure 1.1: Global Map of HIV/AIDS for the Year 2020 [98].

depicted in Figure 1.2.

1.1.1 HIV in the MSM Population

Globally, the risk of acquiring an HIV infection is 26 times higher among *men who have sex with men* (MSM), compared to the general HIV-infected population [134]. The majority of people in the United States who are infected and living with HIV/AIDS are members of the MSM community [17, 119]. For instance, data from the CDC showed that the MSM population accounted for 68% of all new HIV diagnoses in the United States and dependent areas, whereas heterosexuals accounted for 22%, and *intravenous drug users* (IDUs), MSM-IDUs, and others account for the remaining 10% [17, 39, 123, 113]. The global data for HIV/AIDS cases by age and gender (as of July 2022) is summarized in Figure 1.3. The percentages of new HIV cases by mode of transmission for the United States (and dependent areas) are summarized in Figure 1.4. Although the African American population represents about 13.4% of the total population of the United States [127], they disproportionately account for more cases of the HIV/AIDS pandemic. For example, data from the CDC for HIV infections during 2019, depicted in Figure 1.5, showed that this population accounted for about
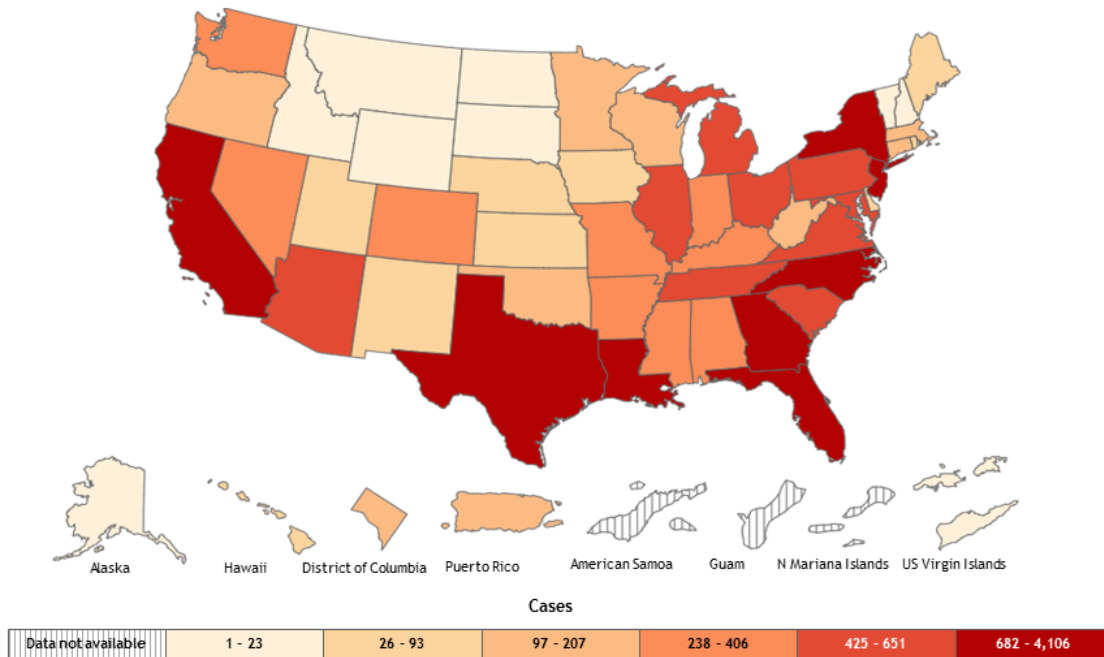
Figure 1.2: Prevalence of HIV/AIDS in the United States for the Year 2022 [3].
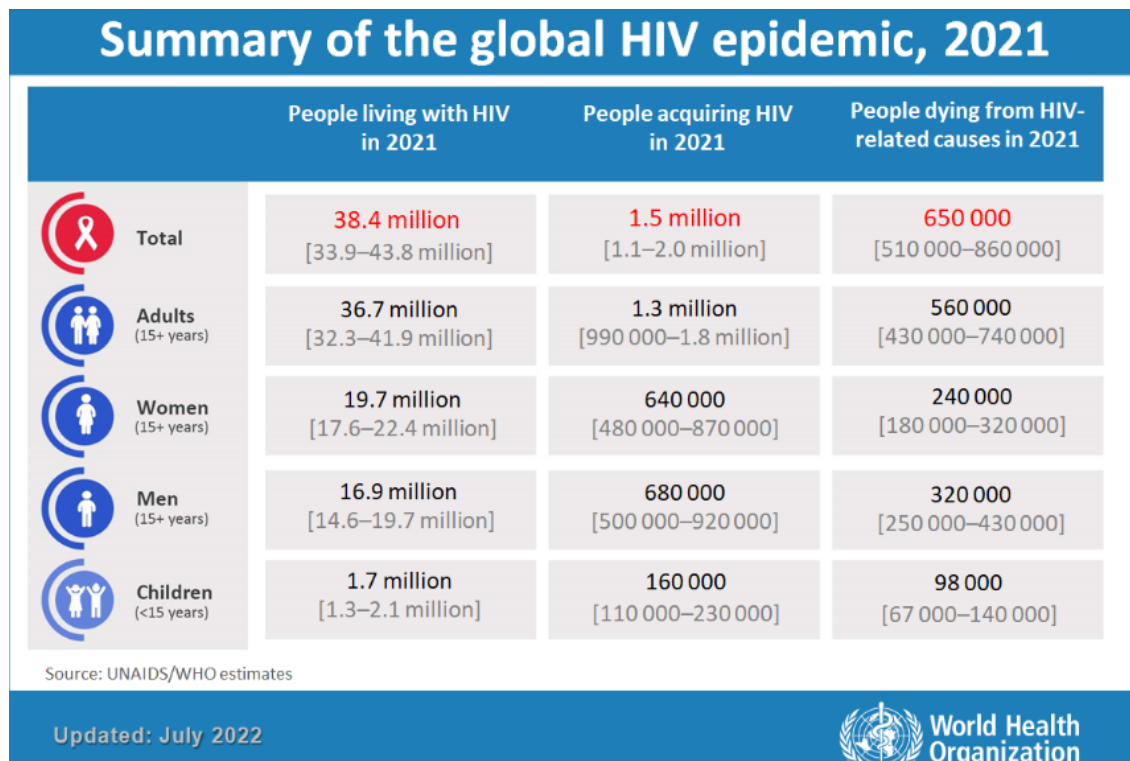
Figure 1.3: Summary of the Global HIV Epidemic by Age and Gender, as of July, 2022 [135].

New HIV Diagnoses in the US and Dependent Areas by Transmission Category, 2020*

Transmission Category	Percentage
Male-to-Male Sexual Contact	68% (20,758)
Heterosexual Contact	22% (6,626)
Injection Drug Use	7% (2,055)
Male-to-Male Sexual Contact and Injection Drug Use	4% (1,109)
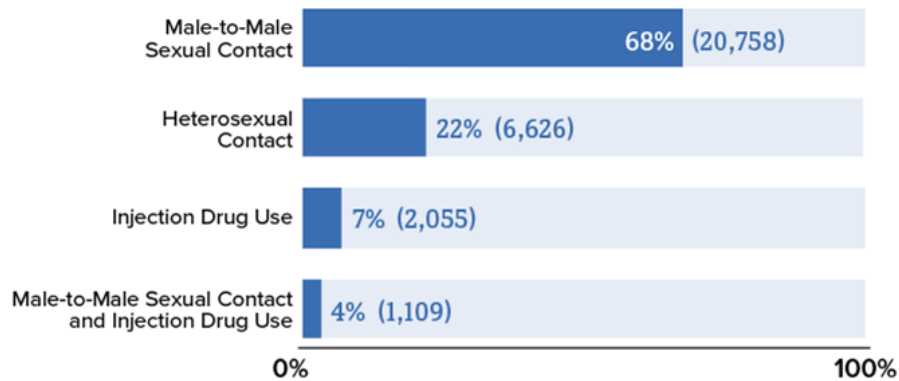
Figure 1.4: Proportion (Number) of New HIV Cases in the United States and Dependent Areas by Transmission Mode for the Year 2020 [17].

40.3% of all new HIV cases in the United States during that year [57, 41]. Figure 1.5

Race/Ethnicity	% of People with HIV, 2019[11]	% of U.S. Population, 2019[14]
Black/African American	**40.3%**	**13.4%**
White	28.5%	60.1%
Hispanic/Latino	**24.7%**	**18.5%**
Asian	1.5%	5.9%
American Indian/Alaska Native	0.3%	1.3%
Native Hawaiian and Other Pacific Islander	0.09%	0.2%

Figure 1.5: Proportion of People with HIV by Race/Ethnicity Compared to the Pro- portion of U.S. Population in 2019 [127].

further shows that the White American population (which represents about 60% of the United States population) accounted for only about 29% of the new HIV cases that year. However, the Hispanic American population (which represents about 19% of the United States population) accounted for about 25% of new HIV cases during 2019. Figure 1.6 depicts the distribution of new HIV cases in the United States by race, gender and mode of HIV transmission during 2019 [127].

4
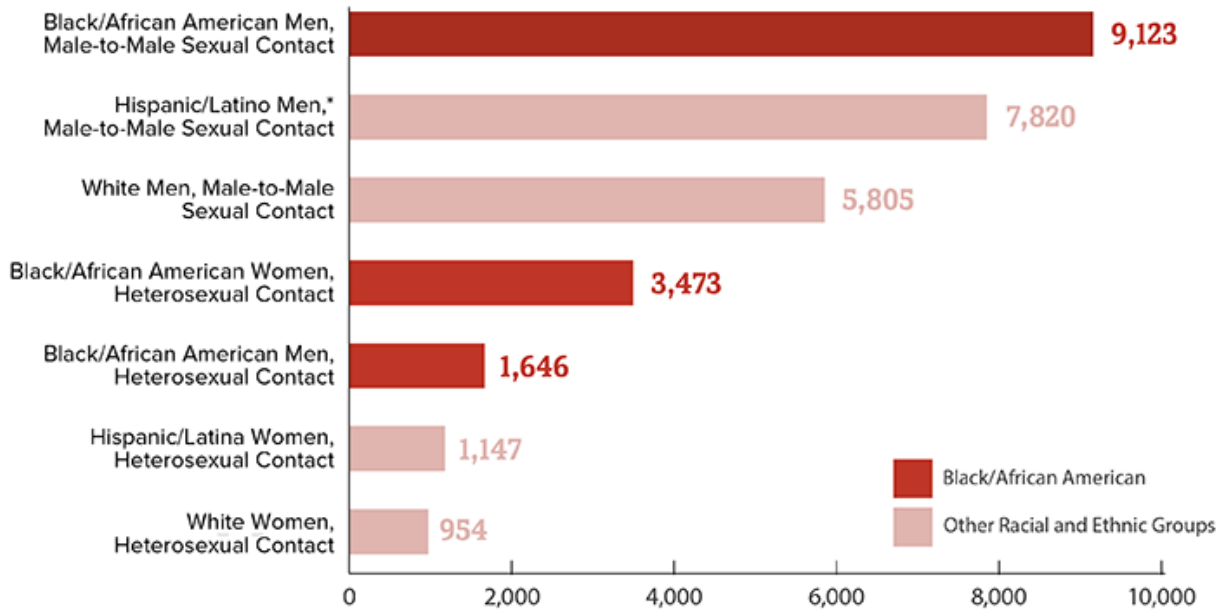
Figure 1.6: The Number of New HIV Cases by Race/Ethnicity, Gender and Transmission Category (I.E., Homosexual Vs. Heterosexual) in the United States in 2019 [42].

1.1.2 HIV in the State of Arizona

Data from the Arizona Department of Health Services (AZDHS) [8] showed that, in the year 2021, MSM accounted for the overwhelming percentage (61.7%) of the prevalence of new cases in the state. Figure 1.7 depicts the annual HIV incidence for the state of Arizona for the period 1982-2020. This figure shows the other risk groups that contributed to the prevalence in the state during the period from 1982 to 2020, namely IDUs (8.2%), MSM-IDU (7.7%), high-risk heterosexuals (10.9%), no-risk-reported (10.2%) and perinatal/blood/other population (1.3%) [8]. During the year 2020, the state of Arizona recorded 662 new HIV cases (of those, 85.6% were male and 14.4% were female) and 280 HIV-infected individuals died of the disease (of which 86.8% were male and 13.2% were female) [5]. Furthermore, in the year 2021, about 6,530 Arizonians (with 94.4% males and 5.4% females) used *pre-exposure prophylaxis* (PrEP) [5]. Figure 1.8 depicts the number of PrEP users in Arizona from

5

HIV incidence among persons aged ≥13 years by risk, Arizona 1982 - 2020
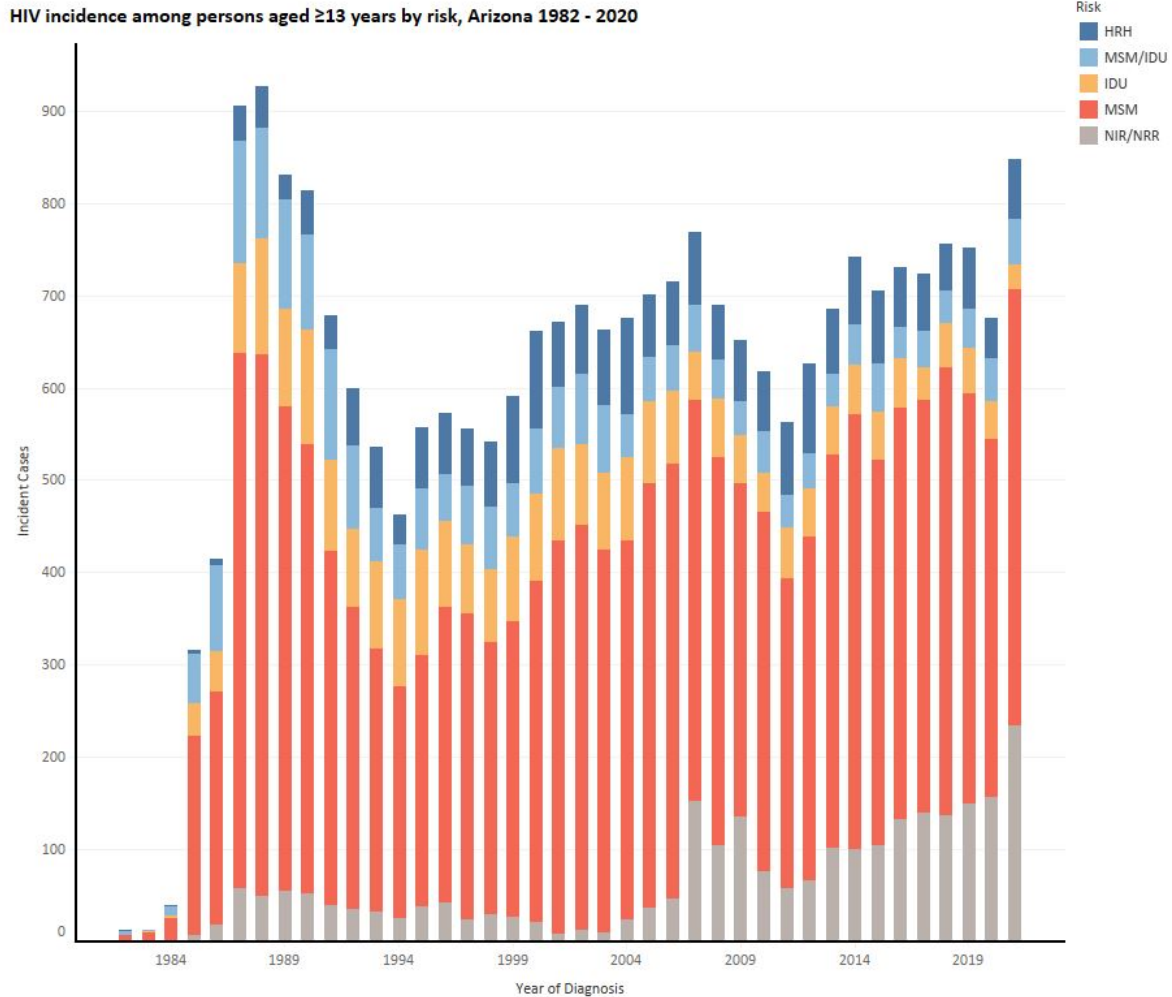
Figure 1.7: Number of New HIV Cases in Arizona among the Persons Aged 13 Years and above, by Risk, from 1982 to 2020 [8]. HRH Represents High-risk Heterosexual And NIR/NRR Represents No Indicated Risk/No Risk Reported.

2012 till 2021.

1.2 Modes of HIV Transmission

The primary mode of HIV transmission in humans is sexual (particularly *via* contact with infected bodily fluids, such as blood, semen, pre-seminal fluid, rectal fluids, and vaginal fluids) [19, 107]. Other modes of transmission (which are now less common) include mother to-child vertical transmission (during pregnancy or child birth or
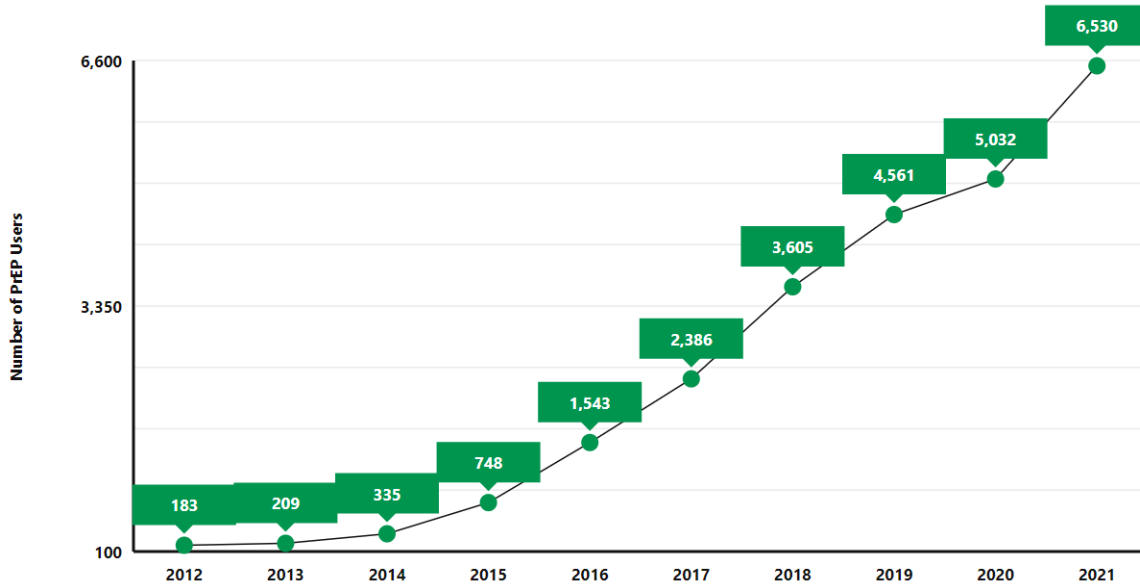
Figure 1.8: Number of PrEP Users in Arizona, 2012-2021 [5].

through breast feeding), sharing contaminated needles and organ transplantation or blood transfusion [22, 107]. For the disease transmission to occur, the infected bodily fluids must come in contact with mucous membranes or damaged tissue or be directly injected into the bloodstream of the susceptible person [107, 116, 22]. HIV infection transmission in the United States is primarily through; *men who have sex with men* (MSM), *intravenous drug users* (IDUs), heterosexual individuals, and *men who have sex with men* that are also *intravenous drug users* (MSM-IDUs) [18, 107]. In fact, current data shows that MSM, of all races and ethnicities, account for the highest percentage of new HIV infections in the United States (in addition to being the risk group that is most severely affected by the burden of the disease) [40]. Of the 30,635 new HIV infections in the year 2020, 90% were acquired sexually (and 24.44% of these were heterosexual) [40]. A well-known feature of HIV disease is the staged-progression property of the transmission process, where a typical HIV-infected individual passes through the three sequential infection stages, namely the primary, the secondary and the AIDS stages. During the primary stage, which typically lasts 2 to 4 weeks,
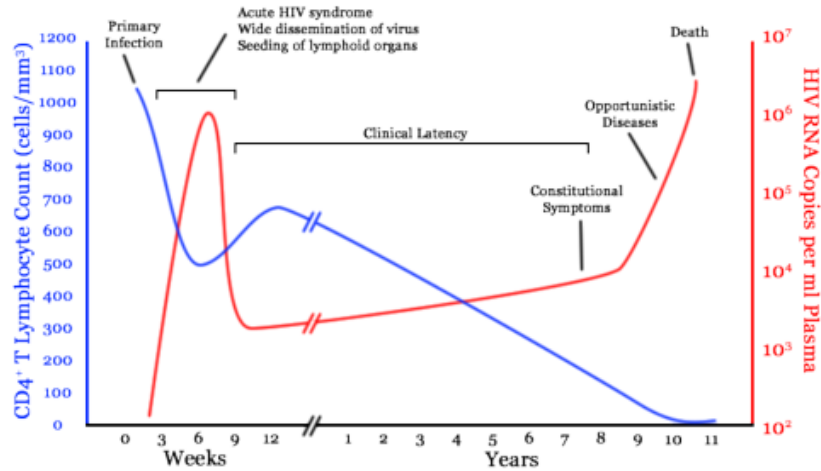
Figure 1.9: Progression of HIV Infection [89].

the virus is rapidly replicating in the body of the infected individual. The affected individual may experience flu-like symptoms (sero-conversion illness) and, owing to his/her high viral load (*viremia*), is highly infectious [69, 2]. The secondary stage (also known as asymptomatic or chronic, or clinically-latent) stage may last 8 to 10 years [69, 2]. During this stage, the immune system is vigorously working to suppress the virus, and the affected individual is less infectious (because their viral load had been greatly suppressed to, in some cases, non-detectable levels). At the end of this stage, (particularly in untreated HIV-infected individuals) the immune system weakens, and the viral load begins to rise (while the target CD4$^+$ T cell count begins to drastically decrease). This leads to the AIDS stage of infection. In this stage, the immune system is essentially defected by the virus (i.e., it is unable to suppress viral replication). The infected individual is highly infectious during this stage, and fatally succumbs to opportunistic infections [2, 114] (Figure 1.9 depicts a typical course of HIV infection in an infected individual). This feature is crucial to be included in models for HIV transmission dynamics [107, 74, 67].

1.3 Public Health Interventions Against HIV/AIDS

Numerous preventive and therapeutic measures have been, and are currently, used in an effort to control and mitigate the burden of the HIV/AIDS pandemic in the affected areas. The preventive measures notably include *pre-exposure prophylaxis* (PrEP), condom use, voluntary HIV testing, public health education and counseling against risky behavior, and providing access to sterile needles to injection drug users (IDUs) [115, 46, 85]. The therapeutic measures adopted are based on using drugs (notably highly-active antiretroviral therapy [51]) to treat HIV infected individuals.

PrEP was first approved by the FDA in 2012 [28, 37, 75]. It is given daily to high-risk individuals who are currently HIV-negative, aimed at minimizing their chance of acquiring an HIV infection (individuals on PrEP are also required to follow-up with their healthcare provider and get tested for HIV regularly, typically every three months). PrEP is generally administered to people who are: (i) in an ongoing sexual relationship with an HIV-positive person; (ii) in a non-mutually monogamous sexual relationship and is a gay or bisexual man that has had unprotected anal sex or have been diagnosed with a sexually transmitted disease (STD) in the last six months; (iii) in a non-mutually monogamous sexual relationship and is a heterosexual man or woman who does not regularly use condoms during sex with a partner of unknown HIV status; or (iv) have injected illicit drugs in the past six months using shared equipment or who have been in a treatment program for intravenous drug users [107, 94, 64, 128, 28]. Some of the drugs approved by the Food and Drug Administration (FDA) for use in PrEP are *Truvada*® , and *Descovy* ® [30]. The drugs in PrEP are designed to block the transmission pathways of the virus in the human body [124]. *Truvada* was designed for people at risk through sex or intravenous drug use. *Descovy* was designed for people at risk through sex. Recent data shows that

PrEP is 99% effective in blocking HIV transmission [36, 44]. It should, however, be stressed that the effectiveness of PrEP depends on compliance in its usage. Since PrEP is not 100% effective in blocking HIV infection, PrEP users should also combine their PrEP usage with other preventive measures (such as the use of condoms, avoiding or reducing risky sexual practices, using sterile needles and getting tested for HIV regularly) [34, 44]. In December of 2021, the FDA approved an injection drug, *Apretude* ®, for use in at-risk adults and adolescents weighing at least 77 pounds for PrEP [1]. This new drug is injected every two months. The Food and Drug Administration reported that two clinical trials were conducted. The fist clinical trial consisted for 4,566 cisgender men and transgender women who have sex with men received either *Apretude* or *Truvada* [129]. The trial measured the rate of HIV infections among the participants. The participants who took *Apretude* had 69% less risk of getting infected with HIV than those who took *Truvada*. The second clinical trial consisted of 3,224 cisgender women [129]. The trial measured the rate of HIV infections in participants who took cabotegravir in addition to *Apretude* or *Truvada*. The participants who took cabotegravir in addition to *Apretude* had 90% less risk of getting infected with HIV than those who took *Truvada* [129].

The National Institute of Allergy and Infectious Diseases(NIAID) announced a new initiative for combating the HIV/AIDS pandemic in the United States in 2019 [90, 117]. The initiative is based on four main control pillars, namely testing (data shows that 15% of people living with HIV in the United States are unaware of their infection status [122]), the use of drug treatment (using antiretroviral therapy), PrEP and respond quickly to potential HIV outbreaks [117]. Lack of compliance has been identified as a major stumbling block for the successful implementation of this initiative. For instance, it is known that 50% of people taking antiretroviral treatment in the United States have interruptions during a one-year period (i.e., they do not

strictly adhere to the specified treatment regimen during the one-year duration) [120]. Furthermore, although the majority of high–risk individuals who should be on PrEP are actually not on PrEP, the lack of compliance among those who are on PrEP is common in the U.S. (this is largely due to the high cost of PrEP) [126].

1.4   Outline of the Dissertation

This Dissertation contains two main chapters. Below is a brief description of the content of the two main chapters. In Chapter 2 of the dissertation, a mathematical model was developed and used to assess the population-level impact of a public health education campaign (or awareness of HIV infection status), as a sole intervention and mitigation strategy, on the transmission dynamics and control of HIV/AIDS in an MSM community. The model was rigorously analysed to gain insight into its dynamical features. The rigorous analyses of the model revealed that its disease-free equilibrium is locally- and globally-asymptotically stable whenever a certain epidemiological threshold, known as the *reproduction number* of the model, is less than one. It was also shown that the model has a unique endemic equilibrium, for a special case, whenever the associated reproduction number exceeds one. This equilibrium (when it exists) was also shown to be locally-asymptotically stable by using a Krasnoselskii sub-linearity approach [71, 53, 105, 82]. Furthermore, the unique endemic equilibrium was shown to be globally-asymptotically stable for a special case of the model, using the non-linear Lyapunov function of the Goh-Volterra type. The model was fitted with the cumulative yearly new HIV case data for the MSM population in the State of Arizona for the period from 1990 to 2019. The fitted model was used to estimate the unknown parameters of the model. Detailed global sensitivity analyses were carried out to determine the parameters of the model that have the highest impact in driving the disease dynamics. Finally, numerical simulations were carried out, using the fixed

and fitted parameter values, to assess the population-level impact of a condom use strategy for curtailing the spread of the disease in the MSM population.

Chapter 3 of the dissertation is based on extending the model in Chapter 2 to account for the effect of risk-structure, the staged-progression property of HIV disease, and the use of pre-exposure prophylaxis (PrEP) on the spread and control of HIV/AIDS in an MSM population. The resulting risk-structured model, which takes the form of a 9-dimensional, two-group (low-risk and high-risk), deterministic system of nonlinear differential equations, was also rigorously analysed, with respect to the existence and asymptotic stability properties of its equilibria. The disease-free equilibrium of the model is shown to be locally-asymptotically stable whenever its associated reproduction number is less than one. Using center manifold theorem, it was shown that the model undergoes a PrEP-induced *backward bifurcation* (when the reproduction number is less than one) if the PrEP efficacy and compliance are not perfect. For the special case of the model where the *backward bifurcation* does not occur, the disease-free equilibrium of the model was shown to be globally-asymptotically stable when the associated reproduction number is less than one. Detailed global sensitivity and uncertainty analyses were carried out to determine the parameters of the model that have the highest impact on the control reproduction number of the model, (hence, disease burden in the MSM community). Some numerical simulation results are reported.

Chapter 2

SINGLE GROUP MODEL FOR HIV DYNAMICS IN AN MSM POPULATION

2.1   Introduction

The human immunodeficiency virus (HIV), the causative agent of acquired immun-odeficiency syndrome (AIDS), remains a significant global public health and socio-economic concern since its emergence in June, 1981 [56]. AIDS results in a gradual decline and failure of the immune system of the infected individual, resulting in significant weight loss, often accompanied by diarrhea, chronic weakness, fever and eventually increases the risk of life-threatening infections (such as Tuberculosis (TB), Pneumocystis pneumonia (PCP) and Cryptococcal meningitis) and cancers (such as Lymphoma, Kaposi's sarcoma and Human Papillomavirus (HPV)-related cancers) [48]. HIV/AIDS is one of the world's most fatal infectious diseases. Each year almost 1 million people die from HIV/AIDS and in some countries it's the leading cause of death (particularly across Sub-Saharan Africa) [96]. In addition to accounting for nearly 38.4 million people currently living with HIV/AIDS, over 650,000 people have died of the disease and 1.5 million people were newly infected with HIV globally. Ap-proximately 40% of new HIV infections are transmitted by people who are unaware that they have HIV [21].

HIV is a sexually-transmitted infection (via contact with infected bodily fluids such as blood, semen, pre-seminal fluid, rectal fluids, and vaginal fluids) [23]. However, HIV can also be transmitted vertically (from a mother to her child, during pregnancy or childbirth, or through breastfeeding). Non-sexual transmission can also occur through the sharing of injection equipment such as needles (among *intravenous drug*

users (IDUs) or within healthcare settings) and through blood transfusions [23]. For transmission to occur, the infected bodily fluids must come in contact with mucous membranes or damaged tissue or be directly injected into the bloodstream of the susceptible person [107]. HIV infection transmission in the U.S. is primarily through; *men who have sex with men* (MSM), *intravenous drug users* (IDUs), heterosexual individuals, and *men who have sex with men* that are also *intravenous drug users* (MSM-IDUs) [18, 107]. According to the Sexually Transmitted Infections Treatment Guidelines provided by the Center for Disease Control and Prevention (CDC), MSM of all races and ethnicities currently have the largest number of new HIV infections and remain the group most severely affected by HIV/AIDS [25]. Furthermore, in the U.S., the estimated lifetime risk for HIV/AIDS infection among the MSM population is one in six, compared with heterosexual men at one in 524 and heterosexual women at one in 253 [25, 86].

Numerous preventive and therapeutic strategies appear promising, and are implemented for retarding the progression and control the spread of HIV/AIDS epidemic in the United States [23]. The most effective preventive strategies include; the usage of condoms, mass testing to detect HIV-infected individuals (including those who remain asymptomatic), HIV screening for pregnant women as part of a routine antenatal screening to avoid the chances of passing HIV to their baby during pregnancy, birth or breastfeeding, public health education and counseling related to protection against HIV and other sexually transmitted infections (STIs), access to sterile needles and injecting equipment (such as spoons or swabs) [92, 23]. However, the most promising therapeutic treatment strategies include; the usage of *antiretroviral treatment* (ART), taking *pre-exposure prophylaxis* (PrEP) medicine (even if an individual is tested negative for HIV/AIDS, to reduce the risks of getting the virus) and taking *post-exposure prophylaxis* (PEP) medicine within 72 hours after a recent possible ex-

posure to HIV [92, 23]. Although these control strategies have helped in curbing the spread of the disease but still HIV/AIDS remains a major socio-economic challenge in the United States [107] (the CDC estimates that the lifetime treatment cost for an individual infected with HIV in the United States is $379,668 (in 2010) [33, 11]). Several mathematical models (mostly of the form of deterministic systems of non-linear differential equations) have been used to provide insight and understanding on the impacts of various preventive and therapeutic strategies against HIV/AIDS [84, 136, 111, 100, 59, 14, 61]. For instance, a deterministic model was used to study the effect of condom use as a singular intervention for HIV/AIDS prevention in the absence of any other treatment [84]. This study showed that for populations with reasonable average numbers of HIV-infected partners, HIV/AIDS epidemic could be stopped by using condoms only. Yusuf *et al.* [136] presented a model for controlling the spread of the disease using change in sexual habits and antiretroviral therapy (ART), as control measures, in South Africa. The results of this study predicted that the implementation of the proposed strategy (based on aforementioned two control measures) would drive new cases of the disease towards eradication in 10 years. Tripathi *et al.* [111] found how the screening of infectives and resulting preventive measures could reduce the spread of HIV/AIDS. Podder *et al.* [100] showed that the use of combined testing and treatment strategy is more effective than the use of the standard antibody test (such as the Enzyme Linked Immunosorbent Assay (ELISA)) with ARV (antiretroviral) treatment, even for the use of condoms as a singular strategy. Granich *et al.* [59] reported that implementing universal voluntary HIV testing with immediate antiretroviral therapy (if diagnosed HIV positive) as a strategy, could lead to the elimination of HIV transmission. Similarly, Broder [14] and Lundgren *et al.* [61] respectively highlighted the significance of antiretroviral therapy (ART) and its impact on the HIV/AIDS pandemic.

This chapter introduces a basic model (also of the form of deterministic system of nonlinear differential equations) to provide an insight into the transmission dynamics of the disease in an MSM population and to assess the population-level impact of awareness of HIV/AIDS infection amongst the populace on the dynamics and control of the disease in an MSM community in the United States. The focus of this chapter is on using mathematical modeling approaches together with data on new yearly confirmed and cumulative HIV/AIDS cases for the State of Arizona to assess the population-level impacts of the treatment of symptomatic and asymptomatic individuals (i.e., those individuals who are detected, *via* random testing) on curtailing and mitigating the burden of the HIV/AIDS pandemic in the United States. Further, the population-level impact of the use of condom-based intervention will also be assessed for the effective control and/or elimination of HIV in the MSM community. This chapter is organized as follows. The basic model for HIV/AIDS transmission in the MSM population is formulated in Section 2.2. Basic qualitative analysis of the model and the parameters of the model are also estimated, based on fitting the model with yearly new case data (i.e., for the State of Arizona), are also presented in this section. The model is rigorously analyzed, with respect to the asymptotic stability properties of its equilibria (disease-free and endemic), in Section 2.3. Global parameter sensitivity analysis is carried out in Section 2.4. Numerical simulations are reported in Section 2.5. The theoretical and numerical simulations results generated in this chapter are discussed in Section 2.6.

2.2   Model Formulation

To construct a basic mathematical model for assessing the impact of HIV testing on the transmission dynamics of HIV/AIDS in an MSM (*men-who-have-sex-with-men*) population, we stratify the total MSM population at time t, denoted by $N(t)$, into the

mutually-exclusive compartments of susceptible $(S(t))$, infected individuals with no clinical symptoms of AIDS who are unaware of their infection status $(I_u(t))$, infected individuals with no clinical symptoms of AIDS who are aware of their infection status $(I_d(t))$, individuals at AIDS stage of infection who are unaware of their infection status $(A_u(t))$, individuals at AIDS stage of infection who are aware of their infection status $(A_d(t))$ and effectively-treated individuals $(T(t))$, so that:

$$N(t) = S(t) + I_u(t) + I_d(t) + A_u(t) + A_d(t) + T(t) \tag{2.1}$$

and the *force of infection* is given by

$$\lambda = (\beta) \left[\frac{I_u + \eta_d I_d + \eta_A (A_u + \eta_d A_d)}{N} \right]. \tag{2.2}$$

The equations for the basic model are given by the following deterministic system of nonlinear differential equations (a flow diagram of the model is depicted in Figure 2.1; the state variables and parameters of the model are tabulated in Table 2.1):

$$
\begin{aligned}
\frac{dS}{dt} &= \Pi - (\lambda + \mu)S, \\
\frac{dI_u}{dt} &= f\lambda S - (\psi_u + \sigma_u + \mu + \delta_I)I_u, \\
\frac{dI_d}{dt} &= (1 - f)\lambda S + \psi_u I_u - (\sigma_d + \tau_d + \mu + \delta_I)I_d, \\
\frac{dA_u}{dt} &= \sigma_u I_u - (\psi_u + \mu + \delta_A)A_u, \\
\frac{dA_d}{dt} &= \sigma_d I_d + \psi_u A_u - (\tau_d + \mu + \delta_A)A_d, \\
\frac{dT}{dt} &= \tau_d(I_d + A_d) - \mu T,
\end{aligned}
\tag{2.3}
$$

where Π is the recruitment rate into the MSM population, β is the effective contact rate, $\eta_d < 1$ is the modification parameter accounting for the assumption that HIV-infected individuals who are aware of their infection status are less likely to transmit

17

infection than infected individuals who are unaware of their infection status, $\eta_A > 1$ is a modification parameter accounting for the assumption that individuals with clinical symptoms of AIDS are more infectious than HIV-infected individuals who do not display clinical symptoms of AIDS (this is to account for the fact that, in HIV biology, infectiousness is correlated with viral load, and individuals in the AIDS stage of HIV infection have much higher viral load than those in the asymptomatic stage of HIV infection [97]), μ is the natural death rate and $0 < f < 1$ is the proportion of new HIV-infected individuals who are unaware of their HIV infection status. Furthermore, $\sigma_u(\sigma_d)$ is the rate at which asymptomatic individuals who are unaware (aware) of their HIV infection progress to the AIDS stage of HIV infection, τ_d is the treatment rate of individuals who are aware of their infection status, ψ_u is the rate at which infected individuals who are unaware of their infection status become aware of their infection (by detection, via random testing) and $\delta_I(\delta_A)$ is the disease-induced mortality for individuals in the asymptomatic (AIDS) stage of HIV infection.
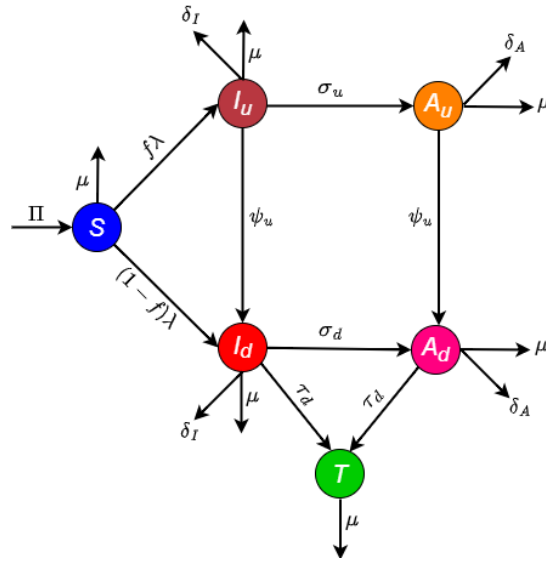
Figure 2.1: Flow Diagram of the Model (2.3).

Parameter	Description
S	Population of susceptible individuals
I_u	Population of infected individuals with no clinical symptoms of AIDS who are unaware of their infection status
I_d	Population of infected individuals with no clinical symptoms of AIDS who are aware of their infection status
A_u	Population of individuals at AIDS stage of infection who are unaware of their infection status
A_d	Population of individuals at AIDS stage of infection who are aware of their infection status
T	Population of effectively-treated individuals
Parameter	**Description**
Π	Recruitment rate into the MSM population
β	Effective contact rate
$\eta_d < 1$	Modification parameter accounting for the assumption that HIV-infected individuals who are aware of their infection status are less likely to transmit infection than infected individuals who are unaware of their infection status
$\eta_A > 1$	Modification parameter accounting for the assumption that individuals with clinical symptoms of AIDS are more infectious than HIV-infected individuals who do not display clinical symptoms of AIDS
μ	Natural death rate

$0 < f < 1$	Proportion of new HIV-infected individuals who are unaware of their HIV infection status
$\sigma_u \, (\sigma_d)$	Rate at which asymptomatic individuals who are unaware (aware) of their HIV infection progress to the AIDS state of HIV infection
τ_d	Treatment rate of individuals who are aware of their infection status
ψ_u	Rate at which infected individuals who are unaware of their infection status become aware of their infection (by detection, *via* random testing)
$\delta_I \, (\delta_A)$	Disease-induced mortality for individuals in the asymptomatic (AIDS) stage of HIV infection

Table 2.1: Description of the State Variables and Parameters of the Model (2.3).

The main assumptions made in the formulation of the model (2.3) are:

1. Homogeneous mixing (i.e., a well-mixed MSM population, where every member of the population has equal likelihood of mixing with every other member; and that individuals are indistinguishable).

2. Exponentially-distributed waiting time in each epidemiological compartment.

3. Individuals in the primary and asymptomatic stage of HIV infection are lumped into one compartment (I_u or I_d), based on whether they are aware of their infection status, for mathematical tractability.

4. Effectively-treated infected individuals do not transmit infection or die of the disease.

Parameter	Baseline Values	Source
Π	1,379 year^{-1}	[6], [60]
β	0.105124 year^{-1}	Obtained from the data fitting
η_d	0.43 (dimensionless)	[100]
η_A	1.5 (dimensionless)	[107]
μ	0.0125 year^{-1}	[31]
f	0.9 (dimensionless)	[24]
σ_u	0.5 year^{-1}	[101]
σ_d	0.2223 year^{-1}	[47]
τ_d	26 year^{-1}	[119]
ψ_u	0.0150808 year^{-1}	Obtained from the data fitting
δ_I	0.0047 year^{-1}	[20]
δ_A	0.09 year^{-1}	[101]

Table 2.2: Baseline Values of the Parameters of the Model (2.3).

The basic qualitative features of the model (2.3) will now be explored.

2.2.1   Basic Qualitative Properties

Before carrying out asymptotic analysis of the basic model (2.3), it is instructive that we explore the basic qualitative properties of the model (2.3). It is convenient to define the following biologically- feasible region for the basic model (2.3):

$$\Omega = \left\{ (S, I_u, I_d, A_u, A_d, T) \in \mathbb{R}_+^6 : 0 \leq N \leq \frac{\Pi}{\mu} \right\},$$

where $N(t)$ is the total population. For the model (2.3) to be mathematically- and biologically-meaningful, it is necessary that the solutions of the basic model (2.3) remain non-negative for all non- negative initial conditions (i.e., solutions that start

in Ω remain in Ω for all time $t > 0$). We claim the following result:

Theorem 2.2.1. *All solutions of the model* (2.3) *with non-negative initial data re-main non-negative for all time $t > 0$.*

Proof. It follows from the first equation of the model (2.3) that

$$\frac{dS}{dt} = \Pi - (\lambda + \mu)S \geq -(\lambda + \mu)S, \tag{2.4}$$

so that,

$$\frac{dS}{dt} + (\lambda + \mu)S \geq 0. \tag{2.5}$$

Multiplying the inequality (2.5) by the integrating factor,
$\rho(t) = \exp\left[\int_0^t (\lambda(u) + \mu)du\right]$ gives

$$\rho(t)\left[\frac{dS}{dt} + (\lambda + \mu)S\right] = \frac{d(S\rho)}{dt} \geq 0, \tag{2.6}$$

from which it follows that $S(t) \geq 0$ for all $t \geq 0$. Using the positivity of $S(t)$, it can, similarly, be shown that the remaining state variables of the model (2.3) are non-negative (for all non-negative initial conditions) for $t \geq 0$. Consequently, all the solutions of the model (2.3), with non-negative initial conditions, remain non-negative for all time $t \geq 0$ (see also [108]). $\qquad\square$

Theorem 2.2.2. *The region Ω is positively-invariant and attracts all solutions of the model* (2.3).

Proof. Adding all the equations of the model (2.3) gives:

$$\frac{dN}{dt} = \Pi - \mu N - \delta_I(I_u + I_d) - \delta_A(A_u + A_d), \tag{2.7}$$

from which it follows that (since all state variables and parameters of the model are non-negative)

$$\frac{dN}{dt} \leq \Pi - \mu N. \tag{2.8}$$

It follows from (2.7) that if $N(t) > \dfrac{\Pi}{\mu}$, then $\dfrac{dN}{dt} < 0$. Furthermore, it follows from (2.8), by applying a standard comparison theorem [65, 104, 91], on (2.7), we get the following inequality:

$$N(t) \leq \frac{\Pi}{\mu} + \left(N_0 - \frac{\Pi}{\mu} \right) e^{-\mu t}. \tag{2.9}$$

Therefore, if $N_0 \leq \dfrac{\Pi}{\mu}$, then $N(t) \leq \dfrac{\Pi}{\mu}$. Thus, Ω is positively-invariant. Furthermore, if $N(0) \geq \dfrac{\Pi}{\mu}$, then either the solution enters Ω in finite time or $N(t)$ approaches $\dfrac{\Pi}{\mu}$ asymptotically. Therefore, every solution of the model (2.3) with initial conditions in Ω remains in Ω for all time $t > 0$. $\square$

Since the basic model (2.3) is well-posed in Ω, it is therefore sufficient to study the dynamics of the model (2.3) in Ω [70].

2.2.2   Data Fitting and Parameter Estimation

The model (2.3) was fitted using the yearly new case data of the MSM population from the State of Arizona (Arizona Department of Health Services) for the period $1990 - 2019$ [113]. The results obtained are depicted in Figure 2.2, showing a very good fit. Furthermore, cumulative yearly new cases were plotted confirming a good fit of the model to the yearly data.

2.3   Existence and Asymptotic Stability of Equilibria

In this section, the basic model (2.3) will be rigorously analyzed to explore the conditions for the existence and asymptotic stability of its equilibria.
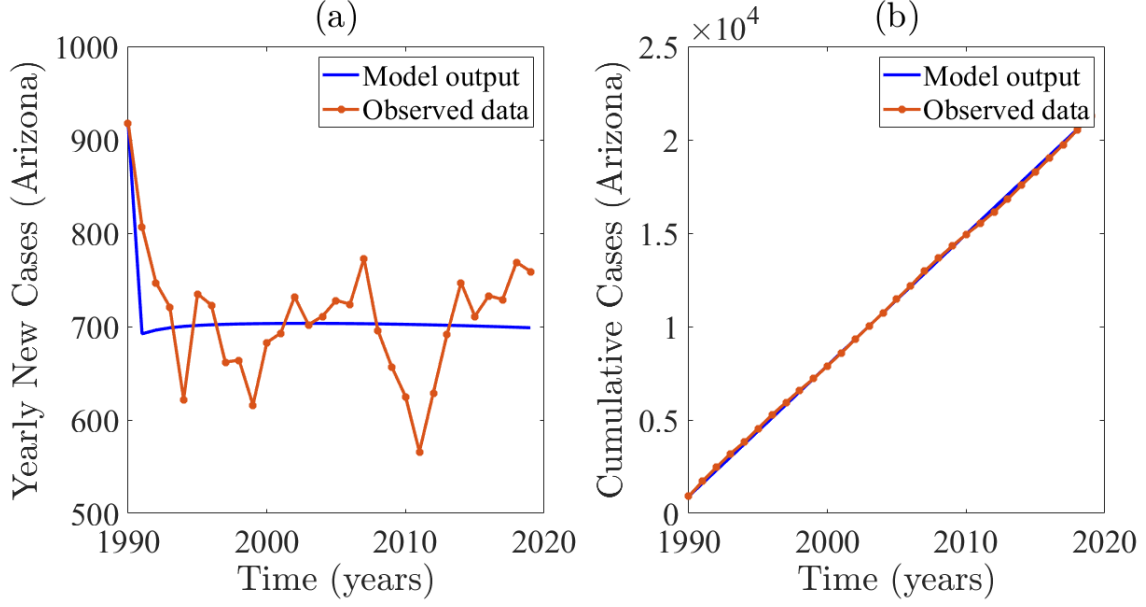
Figure 2.2: Time Series Illustration of the Least Squares Fit of the Model (2.3), Showing the Model's Output (Blue Curve) for the Yearly New Cases for the Msm Population Compared To The Observed Confirmed New Cases (Brown Curve) for the State of Arizona for the Period from 1990 to 2019 (B) Simulation Result of the Model (2.3), Showing Cumulative Yearly New Cases (Blue Curve) Compared to the Observed Yearly Confirmed Cases for the MSM Population in the State of Arizona (Brown Curve) Using the Baseline and the Estimated Parameter Values Given In Table 2.2.

2.3.1 Disease-Free Equilibrium

The model (2.3) has a disease-free equilibrium (DFE), given by:

$$\mathcal{E}_0 = (S^*, I_u^*, I_d^*, A_u^*, A_d^*, T^*) = \left(\frac{\Pi}{\mu}, 0, 0, 0, 0, 0\right).$$

The local asymptotic stability of the DFE will be explored using the next generation operator method [50, 131]. Specifically, it follows, using the notation in [131], that the non-negative matrix, F, of new infection terms, and the M-matrix, V, of linear transition terms, associated with the model (2.3), are given, respectively, by:

24

$$F = \begin{bmatrix} f\beta & f\beta\eta_d & f\beta\eta_A & f\beta\eta_A\eta_d \\ (1-f)\beta & (1-f)\beta\eta_d & (1-f)\beta\eta_A & (1-f)\beta\eta_A\eta_d \\ 0 & 0 & 0 & 0 \\ 0 & 0 & 0 & 0 \end{bmatrix}, \quad (2.10)$$

and,

$$V = \begin{bmatrix} K_1 & 0 & 0 & 0 \\ -\psi_u & K_2 & 0 & 0 \\ -\sigma_u & 0 & K_3 & 0 \\ 0 & -\sigma_d & -\psi_u & K_4 \end{bmatrix}, \quad (2.11)$$

where,

$K_1 = \psi_u + \sigma_u + \mu + \delta_I$, $K_2 = \sigma_d + \tau_d + \mu + \delta_I$, $K_3 = \psi_u + \mu + \delta_A$ and $K_4 = \tau_d + \mu + \delta_A$.

It is convenient to define (where ρ is the spectral radius):

$$\mathbb{R}_T = \rho(FV^{-1}) = (f\beta)\,\mathbb{R}_{T_1} + \beta\eta_d(1-f)\mathbb{R}_{T_2},$$

where,

$\mathbb{R}_{T_1} = \dfrac{1}{K_1} + \dfrac{\eta_d\psi_u}{K_1K_2} + \dfrac{\eta_A\sigma_u}{K_1K_3} + (\eta_d\eta_A\psi_u)\left(\dfrac{\sigma_u}{K_1K_3K_4} + \dfrac{\sigma_d}{K_1K_2K_4}\right)$ and

$\mathbb{R}_{T_2} = \left(\dfrac{1}{K_2} + \dfrac{\eta_A\sigma_d}{K_2K_4}\right)$.

The result below follows from Theorem 2 of [131].

Theorem 2.3.1. *The disease-free equilibrium ($\mathcal{E}_0$) of the model (2.3) is locally-asymptotically stable whenever $\mathbb{R}_T < 1$, and is unstable if $\mathbb{R}_T > 1$.*

The epidemiological implication of Theorem 2.3.1 is that a small influx of HIV-infected individuals will not generate a large outbreak in the MSM population if the quantity $\mathbb{R}_T$ can be brought to (and maintained at) a value less than one. The quantity $\mathbb{R}_T$ is the *control reproduction number* of the model (2.3). It measures the average

number of new HIV cases generated by a typical infected individual introduced into the MSM population where a certain proportion of infected individuals receive anti-HIV treatment.

The threshold quantity $\mathbb{R}_T$ can be re-written the following alternative form (in terms of constituent reproduction numbers):

$$\mathbb{R}_T = \mathbb{R}_{I_u} + \mathbb{R}_{I_d} + \mathbb{R}_{A_u} + \mathbb{R}_{A_d}, \tag{2.12}$$

where,

$$
\begin{aligned}
\mathbb{R}_{I_u} &= \frac{f\beta}{K_1} \\[2mm]
\mathbb{R}_{I_d} &= \frac{f\beta\psi_u\eta_d}{K_1K_2} + \frac{(1-f)\beta\eta_d}{K_2} \\[2mm]
\mathbb{R}_{A_u} &= \frac{f\beta\sigma_u\eta_A}{K_1K_3} \\[2mm]
\mathbb{R}_{A_d} &= \frac{f\beta\psi_u\sigma_d\eta_A\eta_d}{K_1K_2K_4} + \frac{f\beta\psi_u\sigma_u\eta_A\eta_d}{K_1K_3K_4} + \frac{(1-f)\beta\sigma_d\eta_A\eta_d}{K_2K_4}.
\end{aligned}
\tag{2.13}
$$

In (2.13), the quantities $\mathbb{R}_{I_u}$, $\mathbb{R}_{I_d}$, $\mathbb{R}_{A_u}$ and $\mathbb{R}_{A_d}$ represent, respectively, the constituent reproduction numbers for individuals in the I_u, I_d, A_u and A_d classes. They measure the average number of new HIV cases generated by individuals in these respective classes.

Interpretation of Control Reproduction Number

The control reproduction number, $\mathbb{R}_T$, of the model (2.3), can be epidemiologically interpreted as follows. It can be seen from (2.12) that $\mathbb{R}_T$ is the sum of the four constituent reproduction numbers $\mathbb{R}_{I_u}$, $\mathbb{R}_{I_d}$, $\mathbb{R}_{A_u}$ and $\mathbb{R}_{A_d}$, which are interpreted as follows.

Interpretation of $\mathbb{R}_{I_u}$

The constituent reproduction number $\mathbb{R}_{I_u}$ is the product of the infection rate of individuals in the I_u class near the disease-free equilibrium $(f\beta)$ and the average duration in the I_u class $\left(\dfrac{1}{K_1}\right)$.

Interpretation of $\mathbb{R}_{I_d}$

There are two routes to get to I_d from S, namely the (i) direct $S \rightarrow I_d$ route and the (ii) indirect $S \rightarrow I_u \rightarrow I_d$ route. Let $\mathbb{R}_{01d}$ and $\mathbb{R}_{02d}$ represent the reproduction number for the first and second route, respectively. It follows that $\mathbb{R}_{01d}$ is the product of the infection rate of I_d near the DFE, for the $S \rightarrow I_d$ transition $(\beta\eta_d(1-f))$ and the average duration in the I_d class $\left(\dfrac{1}{K_2}\right)$. Thus,

$$\mathbb{R}_{01d} = \beta\eta_d\left(1-f\right)\left(\frac{1}{K_2}\right).$$

Similarly, $\mathbb{R}_{02d}$ is the product of the rate (near the DFE) at which an I_d individual transmits the disease to a susceptible individual who is unaware of their infection status $(\beta f \eta_d)$, the proportion that survived the I_u class and moved to the I_d class $\left(\dfrac{\psi_u}{K_1}\right)$ and the average duration in the I_d class $\left(\dfrac{1}{K_2}\right)$. Hence,

$$\mathbb{R}_{02d} = \beta f \eta_d \left(\frac{\psi_u}{K_1}\right)\left(\frac{1}{K_2}\right).$$

The sum of $\mathbb{R}_{01d}$ and $\mathbb{R}_{02d}$ gives $\mathbb{R}_{I_d}$.

Interpretation of $\mathbb{R}_{A_u}$

The constituent reproduction number $\mathbb{R}_{A_u}$ is the product of the infection rate of individuals in the A_u class near the DFE $(f\beta\eta_A)$, the proportion that survived the I_u

compartment and moved to the A_u class $\left(\dfrac{\sigma_u}{K_1}\right)$ and the average duration in the A_u class $\left(\dfrac{1}{K_3}\right)$.

Interpretation of $\mathbb{R}_{A_d}$

There are three routes to get to A_d from S, namely (i) $S \rightarrow I_d \rightarrow A_d$, (ii) $S \rightarrow I_u \rightarrow I_d \rightarrow A_d$, and (iii) $S \rightarrow I_u \rightarrow A_u \rightarrow A_d$. Let $\mathbb{R}_{Ad1}, \mathbb{R}_{Ad2}$ and $\mathbb{R}_{Ad3}$ represent the reproduction numbers for the first, second and third routes, respectively. It follows that $\mathbb{R}_{Ad1}$ is the product of the rate at which an infected individual in the I_d class transmits the disease to a susceptible individual who is aware of their infection status $(\beta(1-f)\eta_A\eta_d)$, the proportion that survived the I_d class and moved to the A_d class $\left(\dfrac{\sigma_d}{K_2}\right)$ and the average duration in the A_d class $\left(\dfrac{1}{K_4}\right)$. Hence,

$$\mathbb{R}_{Ad1} = \beta(1-f)\eta_A\eta_d\left(\frac{\sigma_d}{K_2}\right)\left(\frac{1}{K_4}\right).$$

Similarly, $\mathbb{R}_{Ad2}$ is the product of the rate at which an infected individual in the I_u class transmits the disease to a susceptible individual who is unaware of their infection status $(\beta f \eta_A \eta_d)$, the proportion that survived the I_u class and moved to the I_d class $\left(\dfrac{\psi_u}{K_1}\right)$ and the portion that survived the I_d class and moved to the A_d class $\left(\dfrac{\sigma_d}{K_2}\right)$ and the average duration in the A_d class $\left(\dfrac{1}{K_4}\right)$. Hence,

$$\mathbb{R}_{Ad2} = \beta f \eta_A \eta_d\left(\frac{\psi_u}{K_1}\right)\left(\frac{\sigma_d}{K_2}\right)\left(\frac{1}{K_4}\right).$$

Finally, $\mathbb{R}_{Ad3}$ is the product of $(\beta f \eta_A \eta_d)$, the proportion that survived the I_u class and moved to the A_u class $\left(\dfrac{\sigma_u}{K_1}\right)$ and the proportion that survived the A_u class $\left(\dfrac{\psi_u}{K_3}\right)$ and moved to the A_d class and the average duration in the A_d class $\left(\dfrac{1}{K_4}\right)$. Hence,

$$\mathbb{R}_{Ad3} = \beta f \eta_A \eta_d\left(\frac{\psi_u}{K_3}\right)\left(\frac{\sigma_u}{K_1}\right)\left(\frac{1}{K_4}\right).$$

28

The sum of $\mathbb{R}_{Ad1}$, $\mathbb{R}_{Ad}$, and $\mathbb{R}_{Ad3}$ gives $\mathbb{R}_{Ad}$. Finally, the sum of $\mathbb{R}_{I_u}$, $\mathbb{R}_{I_d}$, $\mathbb{R}_{A_u}$ and $\mathbb{R}_{A_d}$ gives $\mathbb{R}_T$. Theorem 2.3.1 shows that HIV can be effectively controlled in the MSM population, for the case when $\mathbb{R}_T < 1$, if the initial sub-populations of the model lie within the basin of attraction of the disease-free equilibrium. For such effective control to be independent of the initial conditions, it is necessary to show that the disease-free equilibrium is globally-asymptotically stable. This is done below. We claim the following result.

Theorem 2.3.2. *The disease-free equilibrium, $\mathcal{E}_0$, of model (2.3) is globally- asymptotically stable in Ω whenever $\mathbb{R}_T < 1$.*

The proof of Theorem 2.3.2, based on using a comparison theorem argument [80, 105, 159], is given in Appendix A. The epidemiological implication of Theorem 2.3.2 is that, the HIV-disease in MSM population can be eliminated from the community if the threshold quantity, $\mathbb{R}_T$ can be brought to (and maintained at) a value less than unity. In other words, having $\mathbb{R}_T < 1$ is necessary and sufficient for the effective control (or elimination) of the disease. Hence, implementing an intervention and awareness program that can bring (and maintain) $\mathbb{R}_T$ to a value less than one will result in the elimination of the HIV-disease in the United States.

The result in Theorem 2.3.2 is numerically illustrated in Figure 2.3, showing the convergence of multiple initial conditions to the disease-free equilibrium ($\mathcal{E}_0$) when $\mathbb{R}_T < 1$.

2.3.2   Endemic Equilibria

In this section, we explore conditions for the existence and asymptotic stability of endemic equilibria (i.e., equilibria where the infected components of the model are nonzero).
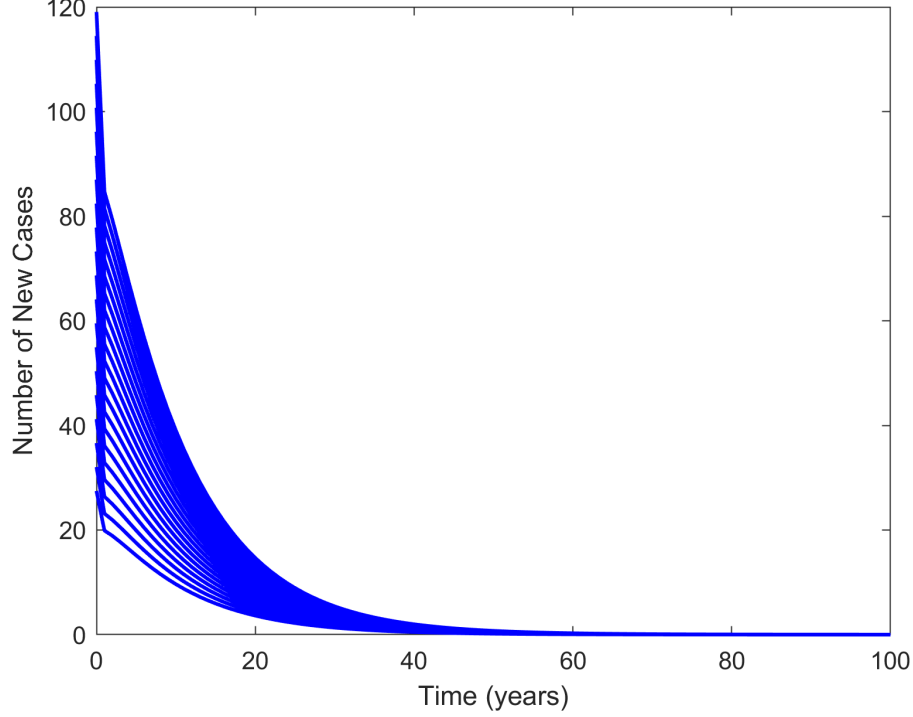
Figure 2.3: Simulations of the Model (2.3), for the Number of New Cases of MSM Population as a Function of Time (in Years), Showing Convergence of Initial Conditions to the Disease-free Equilibrium When $\mathbb{R}_T < 1$. Parameter Values Used Are as given in Table 2.2 with $\beta = 0.01051$ Year^{-1}. With This Set of Parameter Values, $\mathbb{R}_T = 0.1312 < 1$.

Existence:

Let

$$E^{**} = (S^{**}, I_u^{*}, I_d^{**}, A_u^{**}, A_d^{**}, T^{**})$$

represents an arbitrary endemic equilibrium of the model (2.3). It follows then that, at this equilibrium, the force of infection (2.2) becomes

$$\lambda^{**} = (\beta) \left[\frac{I_u^{**} + \eta_d I_d^{**} + \eta_A (A_u^{**} + \eta_d A_d^{**})}{N^{**}} \right], \tag{2.14}$$

with,

$$N^{**} = S^{**} + I_u^{**} + I_d^{**} + A_u^{**} + A_d^{**} + T^{**}. \tag{2.15}$$

30

The components of the arbitrary equilibrium (obtained by solving for each of the state variables of the model (2.3) at the arbitrary endemic equilibrium) are:

$$S^{**} = \frac{\Pi}{\lambda^{**} + \mu}, \quad I_u^{**} = \frac{r_1 \lambda^{**}}{\lambda^{**} + \mu}, \quad I_d^{**} = \frac{r_2 \lambda^{**}}{\lambda^{**} + \mu}, \quad A_u^{**} = \frac{r_3 \lambda^{**}}{\lambda^{**} + \mu},$$

$$A_d^{**} = \frac{r_4 \lambda^{**}}{\lambda^{**} + \mu} \text{ and } T^{**} = \frac{r_5 \lambda^{**}}{\lambda^{**} + \mu},$$

(2.16)

where, $r_1 = \dfrac{f\Pi}{K_1}, \quad r_2 = \dfrac{\Pi}{K_2}\left((1-f) + \dfrac{f\psi_u}{K_1}\right), \quad r_3 = \dfrac{f\sigma_u\Pi}{K_1 K_3}, \quad r_4 = \dfrac{r_2\sigma_d + r_3\psi_u}{K_4}$

and $r_5 = \dfrac{\tau_d(r_2 + r_4)}{\mu}$. It follows, by substituting the expressions in (2.16) into (2.14) (and simplifying), that the solutions of the model (2.3) satisfy the following polynomial:

$$\lambda^{**}\left(a_1 \lambda^{**} + a_0\right) = 0,$$

(2.17)

where, $a_1 = r_1 + r_2 + r_3 + r_4 + r_5$ and $a_0 = \Pi - \beta(r_1 + \eta_d r_2 + \eta_A r_3 + \eta_A \eta_d r_4) = \Pi(1 - \mathbb{R}_T)$. The solutions of (2.17) are $\lambda^{**} = 0$ (which corresponds to the disease-free equilibrium, $\mathcal{E}_0$) and

$$\lambda^{**} = \frac{-a_0}{a_1} = \frac{\beta(\mathbb{R}_T - 1)}{r_1 + r_2 + r_3 + r_4 + r_5} > 0, \text{ whenever } \mathbb{R}_T > 1.$$

(2.18)

Hence, the model (2.3) has a unique positive endemic equilibrium whenever $\mathbb{R}_T > 1$, and no positive endemic equilibrium when $\mathbb{R}_T \leq 1$ (the components of the unique endemic equilibrium can be obtained explicitly by substituting the unique solution of λ^{**}, given in (2.18), into the expressions in (2.14)). Thus, we have established the following result.

Theorem 2.3.3. *The model (2.3) has a unique endemic equilibrium whenever $\mathbb{R}_T > 1$, and no endemic equilibrium otherwise.*

Local Asymptotic Stability of Unique Endemic Equilibrium: Special Case

The local asymptotic stability of the model (2.3) will be explored for the special case with no disease-induced mortality (i.e., we consider the model (2.3) with $\delta_I = \delta_A = 0$). It is convenient to define the following threshold quantity:

$$\tilde{\mathbb{R}}_T = \mathbb{R}_T|_{\delta_I = \delta_A = 0}. \tag{2.19}$$

We claim the following:

Theorem 2.3.4. *The unique endemic equilibrium of the special case of the model (2.3) with $\delta_I = \delta_A = 0$ is locally-asymptotically stable whenever $\tilde{\mathbb{R}}_T > 1$.*

The proof of Theorem 2.3.4 is based on using a Krasnoselskii sub-linearity trick [71, 110, 54, 53, 105, 82], and is given in Appendix B. The epidemiological implication of Theorem 2.3.4, for the special case of the model (2.3) with $\delta_I = \delta_A = 0$, is that the disease will persist in the population (when the threshold quantity, $\tilde{\mathbb{R}}_T$ exceeds one) if the initial sizes of the sub-populations of the model (2.3) are in the basin of attraction of the unique endemic equilibrium.

Global Asymptotic Stability of the Unique Endemic Equilibrium: Special Case

The global asymptotic property of the endemic equilibrium of the model (2.3) is given for the special case when all newly-infected individuals are unaware of their infection status (i.e., $f = 1$) and no disease-induced mortality (i.e., $\delta_I = \delta_A = 0$) and when the modification parameter accounting for the assumption that individuals with symptoms of AIDS are more infectious than those who do not display symptoms of AIDS, is set to zero (i.e., $\eta_A = 0$). Thus, the model (2.3), with $f = 1$ and

$\eta_A = \delta_I = \delta_A = 0$ is reduced to the following system:

$$
\begin{aligned}
\frac{dS}{dt} &= \Pi - (\lambda + \mu)S, \\
\frac{dI_u}{dt} &= f\lambda S - (\psi_u + \sigma_u + \mu)I_u, \\
\frac{dI_d}{dt} &= \psi_u I_u - (\sigma_d + \tau_d + \mu)I_d, \\
\frac{dA_u}{dt} &= \sigma_u I_u - (\psi_u + \mu)A_u, \\
\frac{dA_d}{dt} &= \sigma_d I_d + \psi_u A_u - (\tau_d + \mu)A_d, \\
\frac{dT}{dt} &= \tau_d(I_d + A_d) - \mu T,
\end{aligned}
\tag{2.20}
$$

with λ, now defined as:

$$
\lambda = (\beta)\frac{(I_u + \eta_d I_d)}{N^{**}}
$$

Adding all the equations of the reduced model (2.20) gives

$$
\frac{dN}{dt} = \Pi - \mu N, \tag{2.21}
$$

from which it follows that $N(t) \to \dfrac{\Pi}{\mu}$ as $t \to \infty$. Using $N^{**} = \dfrac{\Pi}{\mu}$ in (2.21) gives a limiting (mass action) system instead of the the standard incidence formulation. Furthermore, the associated reproduction number of the reduced model (2.20) is given as:

$$
\hat{\mathbb{R}}_T = \mathbb{R}_T|_{f=1,\eta_A=\delta_I=\delta_A=0}. \tag{2.22}
$$

It can be easily shown that the reduced model (2.20), has a unique positive EE (as shown in Section 2.3.2) whenever $\hat{\mathbb{R}}_T > 1$. This result is summarized below.

Theorem 2.3.5. *The reduced model (2.20), has a unique (positive) endemic equilibrium whenever $\hat{\mathbb{R}}_T > 1$.*

It is convenient to define the following biologically-feasible region, Ω_0 as:

$$
\Omega_0 = \{(S, I_u, I_d, A_u, A_d, T) \in \Omega : I_u = I_d = A_u = A_d = T = 0\}.
$$

Hence, we claim the following:

Theorem 2.3.6. *The unique endemic equilibrium of the special case of the model (2.3) (i.e. the reduced model (2.20)) with $f = 1$ and $\eta_A = \delta_I = \delta_A = 0$ is globally-asymptotically stable in $\Omega \setminus \Omega_0$ whenever $\hat{\mathbb{R}}_T > 1$.*
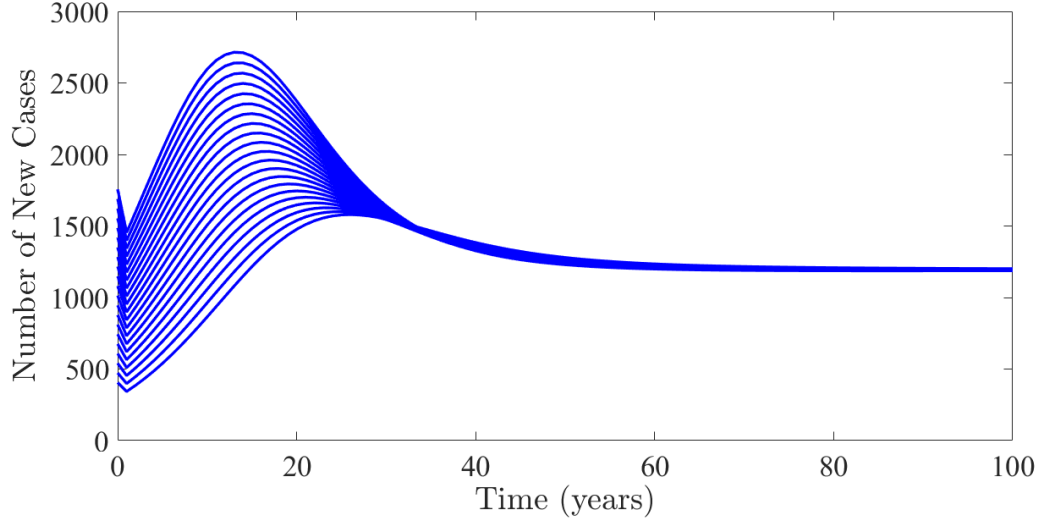
Figure 2.4: Simulations of the Reduced Model (2.20), for the Number of New HIV Cases in MSM Population as a Function of Time, Showing Convergence of Initial Conditions to the Unique Endemic Equilibrium When $\hat{\mathbb{R}}_T > 1$. Parameter Values Used Are as given in Table 2.2 with $\beta = 0.1551$ Year^{-1}. With This Set of Parameter Values, $\hat{\mathbb{R}}_T = 7.4615 > 1$.

The proof of Theorem 2.3.6, is based on using the non-linear Lyapunov function of the Goh-Volterra type, is given in Appendix C. The result of Theorem 2.3.6 is numerically illustrated in Figure 2.4, where multiple initial conditions converged to the unique endemic equilibrium when $\hat{\mathbb{R}}_T > 1$.

2.4   Global Sensitivity Analysis

In this section, the global sensitivity analysis and uncertainty analysis of the model (2.3) will be explored. The model (2.3) contains 12 parameters, and although some of

the parameters were estimated using the MSM data [113], uncertainties are expected to arise in the estimates of some of the other parameters of the model. Hence, it is crucial to assess the impact of the uncertainties of the estimates of the values of the parameters on the outcome of the numerical simulations generated from the model (with respect to a particular response function). In this section, we apply standard uncertainty and sensitivity analysis, using Latin Hypercube Sampling (LHS) technique and partial rank correlation coefficients (PRCCs), to determine the parameters of the model that have the most effect on the chosen response function [79, 13, 81]. The partial rank correlation coefficients (PRCC) approach is a robust sensitivity measure for nonlinear but monotonic relationships between input and output, as long as little to no correlation exists between the inputs [79]. PRCC is considered to be more powerful at determining the sensitivity of a parameter that is strongly monotonic yet highly nonlinear [49]. The magnitude, as well as the statistical significance of the PRCC value of a parameter, indicates that parameter's contribution to the imprecision of the model's prediction of the chosen response function. The parameters with large PRCC values (greater or equal to 0.5 in magnitude) are considered to be the most influential to the response function [102]. Thus, a PRCC approaching -1 or $+1$ indicates a strong effect of the corresponding parameter to the chosen response function. The sign indicates the qualitative relationship between the parameter of the model and the chosen response function. Those with negative (positive) PRCC values are said to be negatively (positively) correlated with the chosen response function.

In this chapter, we choose the control reproduction number ($\mathbb{R}_T$) of the model (2.3) as the response function. We have chosen all of the 12 parameters for the sensitivity analysis. The process of carrying out the sensitivity analysis entails defining a range (lower and upper bound) and distribution for each parameter of the model, and then

splitting each parameter range into 10,000 equal sub-intervals. Parameter sets are drawn from this space without replacement and used to form a $10,000 \times 12$ matrix (hypercube). Each row of this matrix is used to compute the response function (i.e., $\mathbb{R}_T$ in this case) and PRCCs are then computed to assess the contributions of uncertainty and variability in individual parameters to uncertainty and variability in the reproduction number. Parameters with high PRCC values close to -1 or $+1$ are said to be highly correlated with the response function (those with negative(positive) PRCC values are said to be negatively (positively) correlated with the response function). We assume, for simplicity, that each of the 12 parameters of the model (2.3) obeys a uniform distribution, and the range for each parameter is obtained by taking 20% to the left, and then 20% to the right, of its baseline value (given in Table 2.3)

The results of the global sensitivity analysis, depicted in Figure 2.5, show the top four parameters of the basic model (2.3) that have the most effect on the response function ($\mathbb{R}_T$) are the effective contact rate (β), the disease-induced mortality for individuals in the AIDS stage of infection (δ_A), the modification parameter for the infectiousness of individuals in the AIDS stage of infection, in relation to those in the asymptomatic stage (η_A) and the proportion of newly-infected individuals who are unaware of their HIV infection status (f). Hence, it follows from the parameter sensitivity analysis that implementing control interventions and mitigation strategies that:

1. Reduce β (by minimizing number of sexual partners, using condoms during sexual intercourse, minimizing needle-sharing etc.).

2. Reduce f (by implementing effective public health education campaigns and counselling, encouraging minimizing risks, random and frequent HIV testing etc.).

3. Reduce η_A (e.g., via effective treatment and/or discouraging individuals in the

Parameter	Baseline Values	Range	PRCC: $\mathbb{R}_T$
Π	1,379	[1,103, 1,655]	0.020
β	0.105124	[0.0841, 0.1261]	0.97*
η_d	0.43	[0.23, 0.63]	-0.010
η_A	1.5	[1.35, 1.65]	0.86*
μ	0.0125	[0.01, 0.015]	-0.410
f	0.9	[0.8, 1]	0.91*
σ_u	0.5	[0.4, 0.6]	-0.290
σ_d	0.2223	[0.17784, 0.26676]	-0.010
τ_d	26	[20.8, 31.2]	-0.010
ψ_u	0.0150808	[0.0121, 0.0181]	-0.480
δ_I	0.0047	[0.00376, 0.00564]	-0.040
δ_A	0.09	[0.072, 0.108]	-0.94*

Table 2.3: Table of PRCC Values of the Parameters in the Expression for the Control Reproduction Number, $\mathbb{R}_T$, of the Model (2.3). PRCC Values above 0.5 in Magnitude Are Highlighted with a $*$, Implying That These Parameters Are Highly-correlated (i.e., Either Positively Correlated or Negatively Correlated with the Response Function). Apart from The Modification Parameters (i.e., η_d and η_a) and the Proportion "f", Which Are Dimensionless, All the Other Parameters and Their Ranges Have Unit of *per* Year.

AIDS stage from partaking in risky practices that could lead to disease transmission to their susceptible partners)

will be most effective in reducing the control reproduction number (hence, reducing the disease burden, as measured in terms of HIV-related mortality and morbidity). It is noteworthy that the parameter δ_A (for the disease-induced rate for individuals at the AIDS stage of infection) is highly (but negatively) correlated with the response function ($\mathbb{R}_T$). Nonetheless, suggesting a strategy to increase the value of this pa-

rameter (which will, in theory, reduce $\mathbb{R}_T$) is unrealistic epidemiologically.
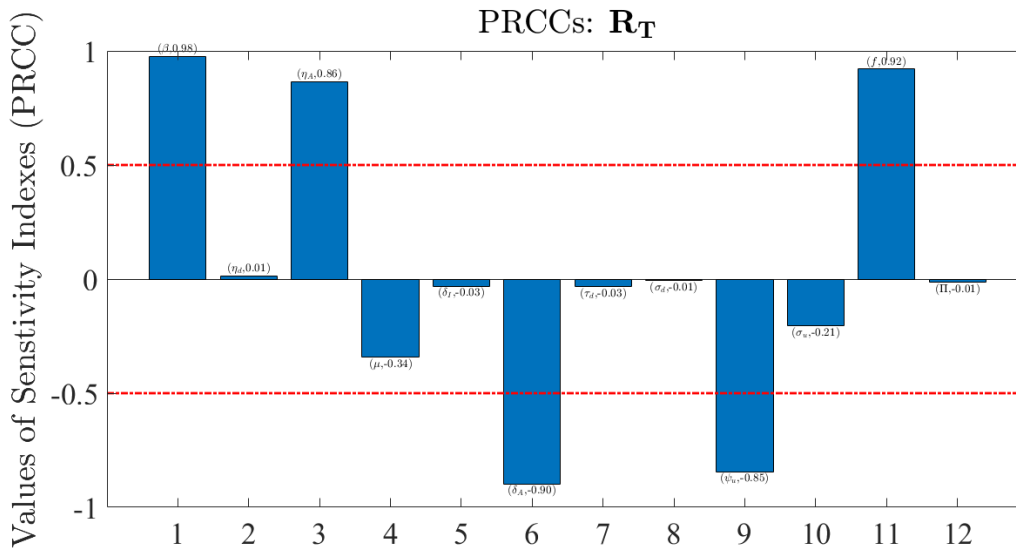
Figure 2.5: Partial Rank Correlation Coefficients (PRCCs) Depicting the Impact of the Parameters of the Model (2.3) with Respect to the Response Function ($\mathbb{R}_T$). The Parameters Used in These Simulations Are as given by the Baseline Values, and Their Corresponding Ranges Are as given in Table 2.2.

In summary, we identify, in this chapter, four parameters (i.e., $\beta, \eta_A, f, \delta_A$) that have the greatest influence on the value of the control reproduction number ($\mathbb{R}_T$), which governs the effective control of the HIV pandemic for the MSM population in the United States. Hence, to effectively control the pandemic, the control interventions and mitigation strategies should be focused on effectively targeting the aforementioned four identified parameters. Figure 2.6 depicts the distributions of each of the parameters of the model (2.3), generated from the uncertainty analysis. This figure shows that, for the parameter values and ranges used in the uncertainty analysis (given in Table 2.3), the value of the reproduction number ($\mathbb{R}_T$) of the model, for the MSM community in the State of Arizona, range from $(0.9563, 1.7818)$ with a mean value of 1.3211 at the 95% confidence interval. The probability that $\mathbb{R}_T > 1$ for the HIV dynamics in this MSM community is given to be 95.1% (hence, under the current

conditions and parameterization, HIV will remain endemic in this population).
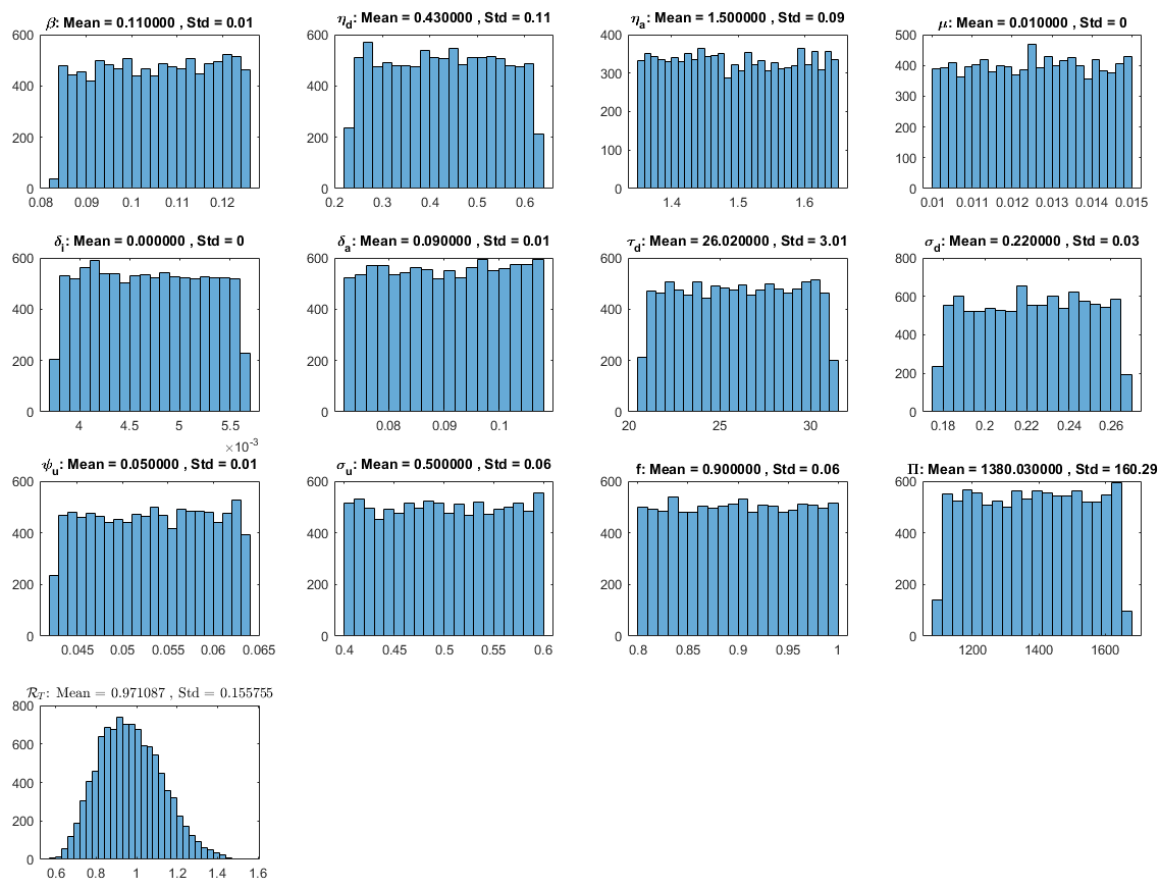
Figure 2.6: Distribution of Parameters of the Model (2.3) and the Response Function ($\mathbb{R}_T$) Generated from the Uncertainty Analysis. Parameter Values Used Are as given by the Baseline Values and Ranges in Table 2.2.

.

2.5   Numerical Simulations

The model (2.3) is now simulated, using the baseline parameter values in Table 2.2 (unless otherwise stated), to assess the impact of control interventions. To assess the impact of condom use (to prevent the transmission or acquisition of HIV infection in the MSM population), the model (2.3) is slightly modified to include the implemen-

tation of condom use strategy. Specifically, the transmission rate β is re-scaled to $\beta(1 - \varepsilon_c c_m)$, where $0 < \varepsilon_c \leq 1$ is condom efficacy and $0 \leq c_m \leq 1$ is the compliance in its usage within the MSM community). Figure 2.7 depicts a contour plot of the control reproduction number, $\mathbb{R}_T$, as a function of the condom efficacy (ε_c) and compliance (c_m). The contours show that, for the MSM community considered, $\mathbb{R}_T$ ranges from 0.2 to 1.2. Furthermore, this figure shows that the control reproduction number decreases with increasing condom efficacy and compliance. For instance, the contour plot shows that, for the case where condoms of 80% efficacy (i.e., $\varepsilon_c = 0.8$) are exclusively used in the population, HIV can be eliminated from the MSM community if at least 29.7% of the population consistently use condoms during sexual contacts. The results in Figure 2.7 clearly show that the prospects of the effective control and/or elimination of HIV in the MSM community, using a condom-based intervention, are very promising provided the condom efficacy and compliance are high enough.
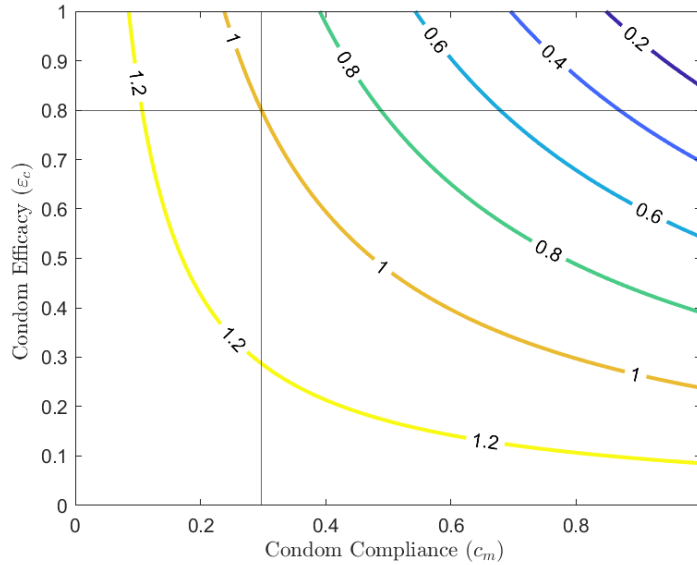
Figure 2.7: Contour Plot of the Reproduction Number ($\mathbb{R}_T$) of the Model (2.3), with β Replaced by $\beta(1 - \varepsilon_c C_m)$, as a Function of Condom Efficacy (ε_c) and Compliance (c_m). Parameter Values Are as given by Their Baseline Values in Table 2.2.

2.6 Concluding Remarks for Chapter 2

The aim of this chapter is to assess the population- level impact of public health education campaign (or awareness of HIV infection status), as a sole intervention and mitigation strategy, on the transmission dynamics and control of HIV/AIDS in an MSM community in the United States. Specifically, a basic model (i.e., a deterministic system of nonlinear differential equations), is developed, coupled with rigorous analysis and computation, to address the challenge of the spread and control of the disease. The impact of interventions based on condom use strategy for the effective control and/or elimination of HIV, is also assessed.

The model was parameterized by fitting it to the observed new yearly data (for the MSM community) for the State of Arizona for the period from 1990 to 2019. Furthermore, the model was rigorously analysed to gain insight into the main qualitative features of the model. The rigorous asymptotic stability analysis of the basic model revealed that its unique disease-free equilibrium is locally-asymptotically stable whenever the control reproduction number of the model is less than one (i.e., $\mathbb{R}_T$). It was shown that the disease-free equilibrium of the model is globally-asymptotic stable when the associated control reproduction number is less than one. The epidemiological implication of the global asymptotic stability result for the disease-free equilibrium of the model is that the HIV/AIDS pandemic can be eliminated in the United States if the associated control reproduction number can be brought to (and maintained at) a value below one (in other words, maintaining the value of $\mathbb{R}_T$ less than one is necessary and sufficient for the elimination of the HIV/AIDS pandemic in the United States).

It was also shown that the model has a unique and locally-asymptotically stable endemic equilibrium for the special case (where disease-induced mortality is negligible)

whenever the associated control reproduction number exceeds one. The epidemiological implication of this result is that, for the special case of the basic model (i.e., in the absence of the disease induced mortality), the HIV/AIDS disease will persist in the population whenever the associated reproduction number is greater than one. Furthermore, it was also shown that the unique endemic equilibrium for the special case of the model (i.e., when $f = 1$ and $\eta_A = \delta_I = \delta_A = 0$) is globally-asymptotic stable when the associated control reproduction number is greater than one.

Furthermore, using the global sensitivity analysis of the parameters of the model, we identified the parameters of the model that have the most influence on the chosen response function (hence, the burden of the HIV/AIDS in the MSM community). Specifically, we identified the most influential four PRCC-ranked parameters to be the effective contact rate (β), the modification parameter accounting for the assumption that individuals with clinical symptoms of AIDS are more infectious than HIV-infected individuals who do not display clinical symptoms of AIDS (η_A), the proportion of new HIV-infected individuals who are unaware of their HIV infection status (f) and the disease-induced mortality for individuals in the asymptomatic (AIDS) stage of HIV infection (δ_A). The numerical PRCC values indicate that reduction of the contact rate of the individuals results in the reduction of the associated reproduction number. Decrease f by implementing effective public health education campaign and counselling and encouraging minimizing risks, random and frequent HIV testing etc. η_A can be reduced by effective treatment and/or discouraging individuals in the AIDS stage from partaking in risky practices that could lead to disease transmission to their susceptible partners.

The model was re-scaled and used to assess the population-level impact of using the condoms in the MSM community as an intervention strategy. Our simulations showed that HIV/AIDS can be eliminated from the MSM community in the United States if

at least 29.7% of the population consistently use condoms (with 80% efficacy) during sexual contacts. In summary, the numerical simulation results generated from this chapter showed that the prospects for the effective control and/or elimination of HIV/AIDS in the MSM community in the United States are very promising using a condom-based intervention, provided the condom efficacy is high and the compliance is moderate enough.

Some of the limitations of the basic model developed in this chapter include: (a) not stratifying the total MSM population according to the risk of acquisition of HIV infection (i.e., splitting the MSM population into low or high risk groups, based on how much risk they take in their sexual practices), (b) the model does not incorporate the three stage-progression property (i.e., (i) acute HIV infection, (ii) chronic HIV infection, and (iii) AIDS) of transmission processes which is a well-known feature of HIV disease and (c) not explicitly incorporating PrEP (a fairly recent preventive measure against acquisition of HIV/AIDS) as a potent preventive intervention in a HIV risk-structured and staged-structured MSM population.

Chapter 3

TWO-GROUP MODEL FOR HIV DYNAMICS IN AN MSM POPULATION

3.1   Introduction

The human immunodeficiency virus (HIV), the causative agent of the acquired im-
munodeficiency syndrome (AIDS), typically leads to death within three years if un-
treated [88]. Over 40.1 million people have died of HIV/AIDS, as of July 2022,
and 38.4 million people currently live with the disease (globally). The HIV/AIDS
pandemic continues to inflict a major socio-economic burden in many parts of the
world [23, 96]. Although there is currently no safe and effective vaccine against HIV
[23], significant progress has been made, over the last three decades, in the design of
effective preventive and therapeutic therapies for the battle against the HIV/AIDS
pandemic. These therapies have essentially transformed this once highly fatal disease
into a treatable chronic condition [23]. Specifially, there have been more than 25 drugs
developed for the treatment of HIV/AIDS [112] over the last three decades. The first
antiretroviral drug (i.e., *zidovudine* (AZT)) for the treatment of AIDS was approved
in March of 1987 by the U.S. Food and Drug Administration (FDA) [130]. The most
recent drug against HIV/AIDS, *Lenacapavir(Sunlenca)*®, approved by the FDA in
December, 2022, is the second injectable anti-HIV drug, and is only approved for
individuals who are resistant to the other drugs [132]. Pre-Exposure Prophylaxis (or
PrEP, for short), a fairly recent preventive measure against acquisition of HIV/AIDS
(approved by FDA on July 16, 2012), entails taking daily medication (or a monthly
injection) to high-risk individuals who are currently HIV-negative, aimed at mini-
mizing their chance of acquiring an HIV infection,typically from their HIV-positive

partners (individuals on PrEP are also required to follow up with their healthcare provider and get tested for HIV regularly, typically every three months) [45, 23]. The FDA approved two drugs, namely *Truvada* and *Descovy*, for PrEP (Truvada in 2012 and Descovy in 2016 [125, 55]. Each of these drugs (taken by individuals who test negative for HIV) are in pill form, and must be taken once a day in conjunction with the use of condoms during sexual contact to be more effective [125]. Individuals on these drugs are regularly tested for HIV (every three months). Furthermore, both drugs have *emtricitabine*, but *Truvada* combines it with *tenefovir disoproxifumarate* while *Descovy* combines it with *tenofovir alafenamide* [10]. While *Truvada* is generally recommended for individuals who are at risk for HIV through sex and *IDU*, *Descovy* is only recommended for individuals who are at risk of HIV infection through sex [125, 121]. Data shows that it takes PrEP pills approximately 7 days of daily use to reach maximum protection for receptive anal sex and 21 days of daily use to reach maximum protection for receptive vaginal sex and *IDU* [38, 109]. There is currently no data on insertive sex [38].

Data from the CDC shows that consistent usage of PrEP medication could lead up to a 99% reduction in the risk of acquisition of HIV infection from sex and reduce the risk of getting HIV from intravenous drug use by at least 74%, compared to those who did not take them consistently [44]. Unfortunately, despite the overall progress in curbing the HIV/AIDS pandemic through the use of pharmaceutical interventions, the disease continues to affect some groups severely and disproportionately. This is largely due to alarming persistent inequity in PrEP usage. For instance, in the year 2021 alone, only 9% (42,372) of the nearly 469,000 Black people who could benefit from PrEP received a prescription, and only 16% (48,838) of the nearly 313,000 Hispanic/Latino people (who could benefit from PrEP) received a prescription [29]. These inequities in PrEP prescription and usage translates into increased HIV in-

cidence in the affected populations. For instance, the HIV incidence among Black individuals in the United States is over eight times than in the White population (HIV incidence in the Hispanic population is about four times higher than the average in the White population) [29]. Black people represented 14% of PrEP users in 2021, despite accounting for 42% of new HIV diagnoses in 2020. Similarly, Hispanic people represented 17% of PrEP users in 2021 and 27% of new HIV diagnoses in 2020, whereas White people represented 65% of PrEP users and 26% of new HIV diagnoses [4]. Finally, inequity also exists in PrEP prescription and usage by gender. In the year 2020, for example, PrEP coverage was about three times as high among males (28%), compared to among females (10%) [29]. All these inequities (by race and gender) further exacerbates and fuels the HIV/AIDS pandemic in the ethnic minority and female populations.

Several mathematical models have been developed and used to assess the impact of PrEP on HIV transmission dynamics and control of HIV/AIDS in the United States [76, 107, 93, 95, 83]. For instance, Simpson *et al.* [107] presented a novel stage-progression model for HIV/AIDS, to assess the population-level impact of the use of PrEP on the transmission dynamics of the disease within an MSM population. This study reported that the effective disease control can be achieved in the MSM community of Minnesota if $[61 - 77\%]$ of susceptible members of the MSM community are on PrEP [107]. Mitchell *et al.* [83] presented a deterministic model to assess the population level impact of PrEP for female sex workers (FSW) and men who have sex with men (MSM) upon HIV incidence and survival in Southern India. The results found in this study predicted that PrEP intervention with 40% coverage of the target population and 60% efficacy could avert over a fifth of new infections amongst the targeted population (FSW or MSM), and $[2 - 3\%]$ of new infections in the whole population. Kim *et al.* [76] presented a mathematical model of HIV prevention mea-

46

sures including PrEP on HIV incidence in South Korea. The results of this study predicted that PrEP reduced the HIV incidence by 74% comparing with the use of antiretroviral therapy (ART) within one year of diagnosis just in 10 years. Moreover, PrEP reduced the HIV incidence by 23% comparing with diagnosis within one year of infection [76]. Nsuami *et al.* [93] reported that managing HIV with early treatment can decrease transmission and possibly decrease the number of AIDS-related deaths and increase in the uptake of PrEP could significantly reduce the number of overall HIV/AIDs infections in South Africa. Omondi *et al.* [95] found that an increase in the PrEP uptake leads to a decline in the number of HIV/AIDS patients under antiretroviral therapy. Furthermore, a combination of PrEP uptake and ART would reduce the spread of the disease appreciably [95].

This chapter introduces a two-group model for the transmission dynamics of HIV/AIDS in an MSM community in the United States. The model to be developed, which incorporates the main epidemiological and biological features of the HIV disease (such as the staged-progression property of the transmission process), will be used to assess the population-level impact of the three pillars of the United States Anti-HIV Initiative to reduce HIV infections in the country by 90% by 2030 [26, 117] (namely testing, drug treatment and PrEP) in combating and mitigating the spread of the disease in an MSM population in the United States. Another novel feature of the model to be designed is that it stratifies the total MSM population according to risk of acquisition of HIV infection. That is, we split the total MSM population into those who are low- or high-risk of acquiring an HIV infection (based on how much risk they take in their sexual practices). The chapter is organized as follows. The two-group, risk-structured model is formulated in Section 3.2. Its basic qualitative properties are also presented in this section. Rigorous analysis of the model, with respect to the existence and asymptotic stability properties of its disease-free and endemic equilibria,

47

is explored in Section 3.3. The feasibility of the dynamic phenomenon of *backward bifurcation* is also rigorously explored in this section. Numerical simulations, as well as global parameter sensitivity analyses, are reported in Section 3.5. The results of this chapter are summarized in Section 3.6.

3.2 Model Formulation

The model to be developed in this chapter is that of the transmission dynamics and control of HIV/AIDS in an MSM community in the United States. In the formulation of the model, the main mode of transmission to be considered is sexual (*albeit* intravenous drug use is also an important mode of transmission in this group). Furthermore, the total susceptible MSM population will be stratified according to the risk of acquisition of HIV infection. Specifically, the susceptible population will be divided into two risk groups, low and high. The susceptible high-risk population consists of HIV negative MSM individuals who, in addition to having sexual contacts with HIV-positive individuals, are *intravenous drug users*. The low-risk, susceptible group consists of HIV-negative MSM who do not engage in risky sexual (or IDU) behavior. In addition to risk structure, another notable feature of HIV disease to be incorporated into the model is stage structure (namely the primary stage, the secondary stage and the AIDS stage). Furthermore, in addition to PrEP and treatment (given to the sexually active susceptible MSM individuals), another important feature to be included into the model is voluntary testing. The motivation for this is that a sizable percentage of HIV-infected individuals in the U.S. are unaware of their infection status. To account for this, (i.e., testing and detection), the infected MSM population will be stratified based on whether they know their infection status. In other words, we will classify the MSM infected individuals in terms of whether they are detected (via testing) or not. In this study, three main preventive and therapeutic

strategies against HIV/AIDS are considered, namely the use of PrEP to prevent susceptible MSM individuals from acquiring an HIV infection, voluntary testing aimed at detecting infected individuals who are unaware of their infection status and the treatment (using antiretroviral therapy) for those who have been detected (i.e., those who are aware of their infection status). In the model to be developed, PrEP is only administered to susceptible individuals in the high-risk category. Based on the above descriptions, the total MSM population at time t, denoted by $N(t)$, is sub-divided into the mutually-exclusive compartments of low-risk susceptible $(S_L(t))$, and high-risk susceptible $(S_H(t))$, individuals in the primary stage of infection who are unaware $(I_{1u}(t))$ or aware $(I_{1d}(t))$ of their infection status, individuals in the secondary stage who are unaware $(I_{2u}(t))$ or aware $(I_{2d}(t))$ of their infection status, individuals in the AIDS stage of infection who are unaware $(A_u(t))$ or aware $(A_d(t))$ of their infection status and effectively-treated infected individuals $(T(t))$. Thus,

$$N(t) = S_L(t) + S_H(t) + I_{1u}(t) + I_{1d}(t) + I_{2u}(t) + I_{2d}(t) + A_u(t) + A_d(t) + T(t).$$

The risk-structured and staged-structured model for HIV transmission in an MSM population (where PrEP, antiretroviral drugs and testing are administered and implemented as preventive and/or therapeutic interventions) is given by the following deterministic system of nonlinear differential equations. The flow diagram of the model (3.1) is depicted in Figure 3.1, and the description of the state variables and

parameters of the model are tabulated in Tables 3.1 and 3.2, respectively:

$$\frac{dS_L}{dt} = \Pi(1-p) + \psi_H S_H - \lambda S_L - \psi_L S_L - \mu S_L,$$

$$\frac{dS_H}{dt} = \Pi p + \psi_L S_L - \eta_H(1-\varepsilon_p c_p)\lambda S_H - \psi_H S_H - \mu S_H,$$

$$\frac{dI_{1u}}{dt} = \lambda S_L + \eta_H(1-\varepsilon_p c_p)\lambda S_H - \varepsilon_d \xi_d I_{1u} - \sigma_{1u} I_{1u} - \mu I_{1u},$$

$$\frac{dI_{1d}}{dt} = \varepsilon_d \xi_d I_{1u} - \tau_1 I_{1d} - \sigma_{1d} I_{1d} - \mu I_{1d},$$

$$\frac{dI_{2u}}{dt} = \sigma_{1u} I_{1u} - \varepsilon_d \xi_d I_{2u} - \sigma_{2u} I_{2u} - \mu I_{2u}, \tag{3.1}$$

$$\frac{dI_{2d}}{dt} = \varepsilon_d \xi_d I_{2u} + \sigma_{1d} I_{1d} - \tau_2 I_{2d} - \sigma_{2d} I_{2d} - \mu I_{2d},$$

$$\frac{dA_u}{dt} = \sigma_{2u} I_{2u} - \varepsilon_d \xi_d A_u - \mu A_u - \delta_u A_u,$$

$$\frac{dA_d}{dt} = \sigma_{2d} I_{2d} + \varepsilon_d \xi_d A_u - \tau_A A_d - \mu A_d - \delta_d A_d,$$

$$\frac{dT}{dt} = \tau_I I_{1d} + \tau_2 I_{2d} + \tau_A A_d - \mu T,$$

where the *force of infection*, $\lambda(t)$, is given by

$$\lambda(t) = \beta \frac{[I_{1u}(t) + \eta_d I_{1d}(t) + \eta_2\{I_{2u}(t) + \eta_d I_{2d}(t)\} + \eta_A\{A_u(t) + \eta_d A_d(t)\}]}{N(t)}. \tag{3.2}$$

In the model (3.1), Π is the rate at which new sexually-active MSM individuals are recruited into the population (assumed to be susceptible), and a proportion, $0 \le p < 1$, of these are assumed to be high-risk susceptible individuals. Low (high)-risk susceptible individuals change their risk behavior and become high (low)-risk at a rate of $\psi_H(\psi_L)$. Susceptible individuals acquire HIV infection at the rate $\lambda(t)$, given by model (3.1). In Equation (3.2), β is the effective contact rate, $0 < \eta_d < 1$ is the modification parameter for the assumed reduced infectiousness of detected individuals, in relation to undetected individuals (since they are on treatment, hence they have reduced viral load), $0 < \eta_2 < 1$ is the modification parameter for the reduced infectiousness of individuals in the secondary stage of infection, in relation to those in the primary stage of infection (owing to their reduced viral load), and $\eta_A > 0$

50

is the modification parameter accounting for the variability of the infectiousness of individuals in the AIDS stage of infection, in relation to those in the primary stage of infection (η_A could be less than, or greater than, unity). Natural mortality occurs in each epidemiological compartment at a rate μ. High-risk susceptible individuals acquire HIV infection at a rate $\eta_H(1 - \varepsilon_p c_p)\lambda$, where $\eta_H > 1$ is the modification parameter for the assumed increase in the likelihood of acquiring an HIV infection by high-risk susceptible individuals, in relation to low-risk susceptible individuals (due to their high-risk sexual practices), $0 < \varepsilon_p < 1$ is the efficacy of PrEP in preventing infection and $0 < c_p \leq 1$ is compliance in PrEP usage. Infected individuals who are unaware of their infection status (i.e., those in $I_{1u}(t)$, $I_{2u}(t)$ and $A_u(t)$ classes) are detected, after voluntary testing, at a rate $\varepsilon_d \xi_d$, where ξ_d is the testing/detection rate and $1 < \varepsilon_d \leq 2$ is the efficacy of the diagnostic test (PCR) administered. Individuals in the primary stage progress to the corresponding secondary stage ($I_{2u}(t)$) at a rate σ_{1u}. Detected individuals in the primary infection stage (i.e., those in the $I_{1d}(t)$ class) are treated at a rate τ_1 and progress to the corresponding secondary stage ($I_{2d}(t)$) at a rate σ_{1d}. Undetected infected individuals in the secondary stage of infection ($I_{2u}(t)$) progress to the corresponding AIDS stage of infection ($A_u(t)$) at a rate σ_{2u}. Similarly, those in the ($I_{2d}(t)$) class progress to the ($A_d(t)$) class at a rate σ_{2d}. Individuals in this ($I_{2d}(t)$) class are treated at a rate τ_2. The treatment rate of detected individuals in the AIDS stage of infection is denoted by τ_A. Individuals in the ($A_u(A_d)$) stage of HIV infection die, due to the opportunistic infections associated with AIDS, at a rate $\delta_u(\delta_d)$.
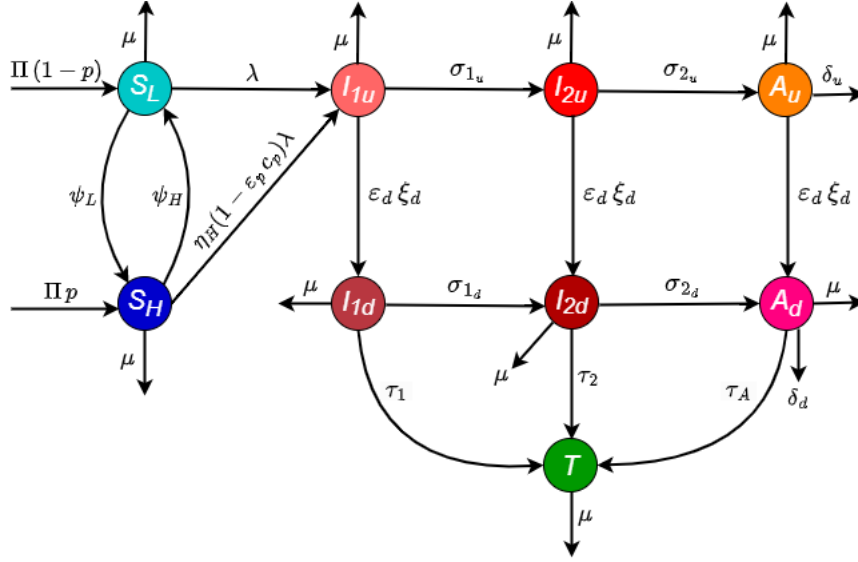
Figure 3.1: Flow Diagram of the Two-Group Model (3.1).

Parameter	Description
Π	Recruitment rate into the sexually-active MSM population
$0 \leq p < 1$	Proportion of newly sexually-active susceptible individuals that are high-risk
β	Effective contact rate
$\psi_L(\psi_H)$	Transition rate from low(high)-risk to high(low)-risk susceptible population
μ	Natural death rate
$0 < \eta_d < 1$	Modification parameter for reduced infectiousness of detected individuals, in relation to undetected individuals
$0 < \eta_2 < 1$	Modification parameter for the reduced infectiousness of individuals in secondary stage of infection, in relation to those in primary stage

$\eta_A > 0$	Modification parameter for the variables of infectiousness of individuals in the AIDS stage of infection, in relation to those in primary stage
$\eta_H > 1$	Modification parameter for the assumed increase in the likelihood of acquiring an HIV infection by high-risk susceptible individuals
$0 < \varepsilon_p < 1$	Efficacy of PrEP to prevent acquisition of HIV infection
$0 < c_p \leq 1$	Compliance in PrEP usage
$\sigma_{1u}(\sigma_{1d})$	Progression rate of undetected (detected) individuals in primary stage to the corresponding secondary stage
$\sigma_{2u}(\sigma_{2d})$	Progression rate of undetected (detected) individuals in secondary stage to the corresponding AIDS stage
ξ_d	Detection rate of diagnostic test administered
$1 < \varepsilon_d \leq 2$	Efficacy of diagnostic test to detect undetected individuals
$\tau_1(\tau_2)$	Treatment rate of detected individuals in $I_{1d}(I_{2d})$ class
τ_A	Treatment rate of detected individuals in AIDS stage of infection
$\delta_u(\delta_d)$	Disease-induced mortality rate of undetected (detected) individuals in the AIDS stage

Table 3.2: Description of Parameters of the Model (3.1).

The main assumptions made in the formulation of the model (3.1) are same as discussed in the Section 2.2. Furthermore, we have relaxed the assumption that individuals in the primary and asymptomatic stage of HIV infection are lumped into one compartment (I_u or I_d), based on whether they are aware of their infection status.

State Variable	Description
S_L	Population of low-risk susceptible individuals
S_H	Population of high-risk susceptible individuals
I_{1u}	Population of undetected HIV-infected individuals in primary stage of infection
I_{1d}	Population of detected HIV-infected individuals in primary stage of infection
I_{2u}	Population of undetected HIV-infected individuals in secondary stage of infection
I_{2d}	Population of detected HIV-infected individuals in secondary stage of infection
A_u	Population of undetected HIV-infected individuals in AIDS stage of infection
A_d	Population of detected HIV-infected individuals in AIDS stage of infection
T	Population of successfully-treated individuals

Table 3.1: Description of State Variables of the Two-Group Model (3.1).

3.2.1 Basic Qualitative Properties

In this section we assess the well-posedness of the model (3.1). We define the following biologically- feasible region for the model (3.1):

$$\Gamma = \left\{ (S_L, S_H, I_{1u}, I_{1d}, I_{2u}, I_{2d}, A_u, A_d, T) \in \mathbb{R}_+^9 : 0 \leq N \leq \frac{\Pi}{\mu} \right\}.$$

We claim the following result:

Theorem 3.2.1. *All solutions of the two-group model (3.2.1) with non-negative initial data remain non-negative for all time $t > 0$.*

Proof. Let $t_1 = sup\{t > 0 : S_L > 0, S_H > 0, I_{1u} > 0, I_{1d} > 0, I_{2u} > 0, I_{2d} > 0, A_u > 0, A_d > 0, T > 0 \in [0, t]\}$. Thus, $t_1 > 0$. It follows from the first equation of the model (3.1) that

$$\frac{dS_L}{dt} = \Pi(1-p) + \psi_H S_H - \lambda S_L - \psi_L S_L - \mu S_L \geq \Pi(1-p) - (\lambda + \psi_L + \mu)S_L,$$

which can be re-written as:

$$\frac{d}{dt}\left[S_L(t)exp\left\{\int_0^t \lambda(u)du + (\psi_L + \mu)t\right\}\right] \geq \Pi(1-p)exp\left\{\int_0^t \lambda(u)du + (\psi_L + \mu)t\right\}.$$

Hence,

$$S_L(t_1)exp\left\{\int_0^{t_1} \lambda(u)du + (\psi_L + \mu)t_1\right\} - S_L(0)$$

$$\geq \int_0^{t_1} \Pi(1-p)exp\left\{\int_0^x \lambda(\nu)d\nu + (\psi_L + \mu)x\right\}dx,$$

$$S_L(t_1) \geq exp\left\{-\int_0^{t_1} \lambda(u)du - (\psi_L + \mu)t_1\right\}$$

$$\left[S_L(0) + I\int_0^{t_1} \Pi(1-p)exp\left\{\int_0^x \lambda(\nu)d\nu + (\psi_L + \mu)x\right\}dx\right] > 0.$$

Similarly, it can be shown that all the remaining state variables of the model (3.1) are non-negative (for all non-negative initial conditions) for $t \geq 0$. Consequently, all the solutions of the model (3.1), with non-negative initial conditions, remain non-negative for all time $t \geq 0$. $\square$

Theorem 3.2.2. *The region Γ is positively-invariant and attracts all solutions of the model (3.1).*

Proof. Adding all the equations of the model (3.1) gives:

$$\frac{dN}{dt} = \Pi - \mu N - \delta_u A_u - \delta_d A_d, \tag{3.3}$$

thereby (since all state variables and parameters of the model are non-negative)

$$\frac{dN}{dt} \le \Pi - \mu N. \tag{3.4}$$

Hence if $N \le \dfrac{\Pi}{\mu}$, then $\dfrac{dN}{dt} \le 0$. Thus, it follows, by applying a standard comparison theorem [78], that:

$$N(t) \le \frac{\Pi}{\mu} + \left(N(0) - \frac{\Pi}{\mu} \right) e^{-\mu t}. \tag{3.5}$$

In particular, $N(t) \le \dfrac{\Pi}{\mu}$ if $N(0) \le \dfrac{\Pi}{\mu}$. Further, if $N(t) > \dfrac{\Pi}{\mu}$, then $dN(t)/dt < 0$. Therefore, every solution of the model (3.1) with initial conditions in Γ remains in Γ for all time. Thus, the region Γ is positively-invariant and attracting. $\qquad\square$

Since the region Γ is positively-invariant, attracting and bounded, it is therefore sufficient to study the dynamics of the model (3.1) in the feasible region, Γ [70]. The existence and asymptotic stability properties of the equilibria of the model (3.1) will now be explored.

3.3   Existence and Asymptotic Stability of Equilibria

In this section, the two group HIV/AIDS model (3.1) will be rigorously analyzed to explore the conditions for the existence and asymptotic stability of disease-free equilibrium and endemic equilibrium.

3.3.1   Disease-Free Equilibrium

The model (3.1) has a disease-free equilibrium (DFE), given by:

$$\begin{aligned}
\mathcal{E}_{DF} &= (S_L^*, S_H^*, 0, 0, 0, 0, 0, 0, 0) \\
&= \left(\frac{\Pi(\psi_H + (1-p)\mu)}{\mu K}, \frac{\Pi(p\mu + \psi_L)}{\mu K}, 0, 0, 0, 0, 0, 0, 0 \right).
\end{aligned} \tag{3.6}$$

where, $K = \mu + \psi_H + \psi_L$. The local asymptotic stability of the DFE will be explored using the next generation operator method [50, 131]. Specifically, it follows, using the notation in [131], that the non-negative matrix, F, of new infection terms, and the M-matrix, V, of linear transformation terms, associated with the model (3.1), are given, respectively, by:

$$F = \begin{bmatrix} \dfrac{\beta B^*}{N^*} & \eta_d \dfrac{\beta B^*}{N^*} & \eta_2 \dfrac{\beta B^*}{N^*} & \eta_2 \eta_d \dfrac{\beta B^*}{N^*} & \eta_A \dfrac{\beta B^*}{N^*} & \eta_A \eta_d \dfrac{\beta B^*}{N^*} \\ 0 & 0 & 0 & 0 & 0 & 0 \\ 0 & 0 & 0 & 0 & 0 & 0 \\ 0 & 0 & 0 & 0 & 0 & 0 \\ 0 & 0 & 0 & 0 & 0 & 0 \\ 0 & 0 & 0 & 0 & 0 & 0 \end{bmatrix}$$

and,

$$V = \begin{bmatrix} C_1 & 0 & 0 & 0 & 0 & 0 \\ -\varepsilon_d\,\xi_d & C_2 & 0 & 0 & 0 & 0 \\ -\sigma_{1u} & 0 & C_3 & 0 & 0 & 0 \\ 0 & -\sigma_{1d} & -\varepsilon_d\,\xi_d & C_4 & 0 & 0 \\ 0 & 0 & -\sigma_{2u} & 0 & C_5 & 0 \\ 0 & 0 & 0 & -\sigma_{2d} & -\varepsilon_d\,\xi_d & C_6 \end{bmatrix},$$

where,

$$B^* = S_L^* + \eta_H(1 - \varepsilon_p c_p)S_H^*, N^* = \frac{\Pi}{\mu}, C_1 = \varepsilon_d\,\xi_d + \sigma_{1u} + \mu, C_2 = \tau_1 + \sigma_{1d} + \mu,$$

$$C_3 = \varepsilon_d\,\xi_d + \sigma_{2u} + \mu, C_4 = \tau_2 + \sigma_{2d} + \mu, C_5 = \varepsilon_d\,\xi_d + \delta_u + \mu \tag{3.7}$$

and $C_6 = \tau_A + \delta_d + \mu$.

It is convenient to define (where ρ is the spectral radius):

$$\mathbb{R}_{T_c} = \rho(FV^{-1})$$

$$= \mathbb{R}_{I_{1u}} + \mathbb{R}_{I_{1d}} + \mathbb{R}_{I_{2u}} + \mathbb{R}_{I_{2d}} + \mathbb{R}_{A_u} + \mathbb{R}_{A_d}, \tag{3.8}$$

where,

$$\mathbb{R}_{I_{1u}} = \left(\frac{\beta B^*}{N^*}\right)\left(\frac{1}{C_1}\right),$$

$$\mathbb{R}_{I_{1d}} = \eta_d\left(\frac{\beta B^*}{N^*}\right)\left(\frac{\varepsilon_d \xi_d}{C_1 C_2}\right),$$

$$\mathbb{R}_{I_{2u}} = \eta_2\left(\frac{\beta B^*}{N^*}\right)\left(\frac{\sigma_{1u}}{C_1 C_3}\right),$$

$$\mathbb{R}_{I_{2d}} = \eta_2\eta_d\left(\frac{\beta B^*}{N^*}\right)\left(\frac{\varepsilon_d \xi_d \sigma_{1d}}{C_1 C_2 C_4} + \frac{\sigma_{1u}\varepsilon_d \xi_d}{C_1 C_3 C_4}\right), \tag{3.9}$$

$$\mathbb{R}_{A_u} = \eta_A\left(\frac{\beta B^*}{N^*}\right)\left(\frac{\sigma_{1u}\sigma_{2u}}{C_1 C_3 C_5}\right),$$

$$\mathbb{R}_{A_d} = \eta_A\eta_d\left(\frac{\beta B^*}{N^*}\right)\left(\frac{\sigma_{1u}\sigma_{2u}\varepsilon_d \xi_d}{C_1 C_3 C_5 C_6} + \frac{\varepsilon_d \xi_d \sigma_{1d}\sigma_{2d}}{C_1 C_2 C_4 C_6} + \frac{\sigma_{1u}\varepsilon_d \xi_d \sigma_{2d}}{C_1 C_3 C_4 C_6}\right).$$

In (3.9), the quantities $\mathbb{R}_{I_{1u}}, \mathbb{R}_{I_{1d}}, \mathbb{R}_{I_{2u}}, \mathbb{R}_{I_{2d}}, \mathbb{R}_{A_u}, \mathbb{R}_{A_d}$, represent, respectively, the constituent reproduction numbers for individuals in the $I_{1u}, I_{1d}, I_{2u}, I_{2d}, A_u, A_d$ classes. The result below follows from Theorem 2 of [131].

Theorem 3.3.1. *The disease-free equilibrium ($\mathcal{E}_{DF}$) of the model (3.1) is locally-asymptotically stable whenever $\mathbb{R}_{T_c} < 1$, and is unstable if $\mathbb{R}_{T_c} > 1$.*

The epidemiological implication of Theorem 3.3.1 is that a small influx of HIV-infected individuals will not generate a large outbreak in the MSM population if the quantity $\mathbb{R}_{T_c}$ can be brought to (and maintained at) a value less than one. The quantity $\mathbb{R}_{T_c}$ is the *control reproduction number* of the model (3.1). It measures the average number of new HIV cases generated by a typical infected individual introduced into the MSM population where a certain proportion of infected individuals receive anti-HIV treatment.

3.3.2 Existence and Asymptotic Stability of Endemic Equilibria

In this section, we explore conditions for the existence and asymptotic stability of endemic equilibria (i.e., equilibria where the infected components of the model are nonzero) of the model (3.1).

$$\mathcal{E}_{EE} = (S_L^{**}, S_H^{**}, I_{1u}^{**}, I_{1d}^{**}, I_{2u}^{**}, I_{2d}^{**}, A_u^{**}, A_d^{**}, T^{**}) \tag{3.10}$$

represents any arbitrary (positive) endemic equilibrium point of the model (3.1) with

$$N^{**} = S_L^{**} + S_H^{**} + I_{1u}^{**} + I_{1d}^{**} + I_{2u}^{**} + I_{2d}^{**} + A_u^{**} + A_d^{**} + T^{**} \tag{3.11}$$

and the *force of infection* now defined as:

$$\lambda^{**} = \frac{\beta}{N^{**}} \left\{ I_{1u}^{**} + \eta_d I_{1d}^{**} + \eta_2 \left(I_{2u}^{**} + \eta_d I_{2d}^{**} \right) + \eta_A \left(A_u^{**} + \eta_d A_d^{**} \right) \right\} \tag{3.12}$$

The components of the arbitrary equilibrium (obtained by solving for each of the state variables of the model (3.1) at steady-state) are given as:

$$
\begin{aligned}
S_L^{**} &= \frac{\Pi(1-p) + \psi_H S_H^{**}}{\lambda^{**} + \psi_L + \mu}, \quad S_H^{**} = \frac{\Pi p + \psi_L S_L^{**}}{\eta_H \left(1 - \varepsilon_p c_p\right) \lambda^{**} + \psi_H + \mu}, \\[2mm]
I_{1u}^{**} &= \frac{\lambda^{**} \left\{ S_L^{**} + \eta_H \left(1 - \varepsilon_p c_p\right) S_H^{**} \right\}}{C_1}, \quad I_{1d}^{**} = \frac{\varepsilon_d \xi_d \lambda^{**} \left\{ S_L^{**} + \eta_H \left(1 - \varepsilon_p c_p\right) S_H^{**} \right\}}{C_1 C_2}, \\[2mm]
I_{2u}^{**} &= \frac{\sigma_{1u} I_{1u}^{**}}{C_3}, \quad I_{2d}^{**} = \frac{\varepsilon_d \xi_d I_{2u}^{**} + \sigma_{1d} I_{1d}^{**}}{C_4}, \\[2mm]
A_u^{**} &= \frac{\sigma_{2u} I_{2u}^{**}}{C_5}, \quad A_d^{**} = \frac{\sigma_{2d} I_{2d}^{**} + \varepsilon_d \xi_d A_u^{**}}{C_6}, \quad T^{**} = \frac{\tau_1 I_{1d}^{**} + \tau_2 I_{2d}^{**} + \tau_A A_d^{**}}{\mu}.
\end{aligned}
\tag{3.13}
$$

Substituting the equations in (3.13) into (3.12) yields

$$\lambda^{**} = \frac{\lambda^{**} \Pi \mu K \left(\beta N_1 Q_1 \lambda^{**} + \mathbb{R}_{T_c} \right)}{\left[\Pi B_1 D_1 (\lambda^{**})^2 + \left\{ \Pi \mu B_2 D_2 + \Pi B_3 D_1 \right\} \lambda^{**} + \Pi \mu K D_2 \right]} \tag{3.14}$$

where,

$$N_1 = C_2\,C_3\,C_4\,C_5\,C_6 + C_3\,C_4\,C_5\,C_6\,\eta_d\,\varepsilon_d\,\xi_d + C_2\,C_4\,C_5\,C_6\,\eta_2\,\sigma_{1_u}$$

$$+ C_2\,C_4\,C_6\,\eta_A\,\sigma_{1_u}\,\sigma_{2_u} + C_5\,C_6\,\eta_2\,\eta_d\,\varepsilon_d\,\xi_d\,\sigma_{1_u}\,(C_2\,+C_3) + \eta_A\,\eta_d\,\varepsilon_d\,\xi_d\,(C_2C_5\,\sigma_{1_u}\sigma_{2_d}$$

$$+ C_3C_5\,\sigma_{1_d}\sigma_{2_d} + C_2C_4\,\sigma_{1_u}\sigma_{2_u}),$$

$$D_1 = \mu\,C_2\,C_3\,C_4\,C_5\,C_6 + \mu\,C_3\,C_4\,C_5\,C_6\,\varepsilon_d\,\xi_d + \mu\,C_2\,C_4\,C_5\,C_6\,\sigma_{1_u} + \mu\,C_2\,C_4\,C_6\,\sigma_{1_u}\,\sigma_{2_u}$$

$$+ \mu\,C_5\,C_6\,\varepsilon_d\,\xi_d\,(C_2\,\sigma_{1_u}\,+C_3\,\sigma_{1_d}) + \mu\,\varepsilon_d\,\xi_d\,(C_2C_5\,\sigma_{1_u}\sigma_{2_d} + C_3C_5\,\sigma_{1_d}\sigma_{2_d}$$

$$+ C_2\,C_4\,\sigma_{1_u}\sigma_{2_u}) + C_5\,C_6\,\varepsilon_d\,\xi_d\,(C_3\,C_4\,\tau_1 + C_2\,\tau_2 + C_3\,\sigma_{1_u}\,\tau_2) \tag{3.15}$$

$$+ \varepsilon_d\,\xi_d\,\tau_A\,(C_2\,C_5\,\sigma_{1_u}\,\sigma_{2_d} + C_2\,C_4\,\sigma_{1_u}\,\sigma_{2_u} + C_3\,C_5\,\sigma_{1_d}\,\sigma_{2_d}),$$

$$D_2 = C_1\,C_2\,C_3\,C_4\,C_5\,C_6,\ B_1 = \eta_H(1 - \varepsilon_p\,c_p),\ B_2 = \{(1-p)\eta_H(1-\varepsilon_p\,c_p) + p\},$$

$$B_3 = \psi_h + \mu(1-p) + \{\eta_h\,(1 - \varepsilon_p\,c_p)\}\,(\psi_l + \mu\,p),$$

$$Q_1 = \frac{\eta_H\,(1-\varepsilon_p\,c_p)}{K},\ \text{ and }\ K = \mu + \psi_H + \psi_L.$$

It follows that the non-zero (endemic) equilibria of the model (3.1), satisfy the following polynomial (in terms of λ^{**}),

$$a_2(\lambda^{**})^2 + a_1\lambda^{**} + a_0 = 0, \tag{3.16}$$

where,

$$a_2 = \Pi\,B_1\,D_1,\ a_1 = \Pi\,\mu\,B_2\,D_2 + \Pi\,B_3\,D_1 - \Pi\,\beta\,K\,\mu\,N_1\,Q_1,\ a_0 = \Pi\,\mu\,K\,D_2\,(1 - \mathbb{R}_{T_c}), \tag{3.17}$$

with,

$B_1,\ D_1,\ B_2,\ D_2,\ B_3,\ K,\ N_1$ as defined in (3.15). The quadratic equation (3.16) can be analyzed for the possibility of multiple endemic equilibria when $\mathbb{R}_{T_c} < 1$. It should be noted that the coefficient a_2 is always positive (since $\varepsilon_p c_p < 1$ thus $(1 - \varepsilon_p c_p) > 0$ and all the state variables are also positive) and a_0 is negative if $\mathbb{R}_{T_c} > 1$. Hence, the following result follows from the quadratic equation (3.16).

Theorem 3.3.2. *The two-group model* (3.1) *has:*

(i) a unique endemic equilibrium if $a_0 < 0 \leftrightarrow \mathbb{R}_{T_c} > 1$;

(ii) a unique endemic equilibrium if $a_1 < 0$, and $a_0 = 0$ or $a_1^2 - 4a_0a_2 = 0$;

(iii) two endemic equilibria if $a_0 > 0, a_1 < 0$, and $a_1^2 - 4a_0a_2 > 0$;

(iv) no endemic equilibrium otherwise.

Case (i) of Theorem 3.3.2 shows that the model (3.1) has a unique endemic equilibrium whenever $\mathbb{R}_{T_c} > 1$. Furthermore, Case (iii) of Theorem 3.3.2 suggests the possibility of backward bifurcation, a dynamic phenomenon characterized by the co-existence of multiple stable equilibria (a disease-free equilibrium and a stable endemic equilibrium) when the associated reproduction number of the model ($\mathbb{R}_{T_c}$) is less than unity [63]. The epidemiological implication of the phenomenon of backward bifurcation is that the requirement, while necessary, is not sufficient for disease elimination. In this case, disease elimination will depend upon the initial sizes of the sub-populations of the model [63]. Accordingly, the existence of backward bifurcation in the transmission dynamics of a disease makes it difficult to achieve effective control (or elimination) of that disease in the community. The existence of such phenomenon in the model (3.1) will be explored now.

Theorem 3.3.3. *The model* (3.1) *undergoes backward bifurcation at $\mathbb{R}_{T_c} = 1$ whenever the inequality* (D.11), *given in Appendix D, holds.*

The proof of Theorem 3.3.3, based on using center manifold theory, is given in Appendix D. Figure 3.2 depicts the backward bifurcation plots associated with the model (3.1). However, the arbitrary set of parameter values chosen to generate the backward bifurcation diagram (i.e., Figure 3.2) may not be biologically meaningful but these arbitrary set of parameter values are chosen to show the phenomenon of backward
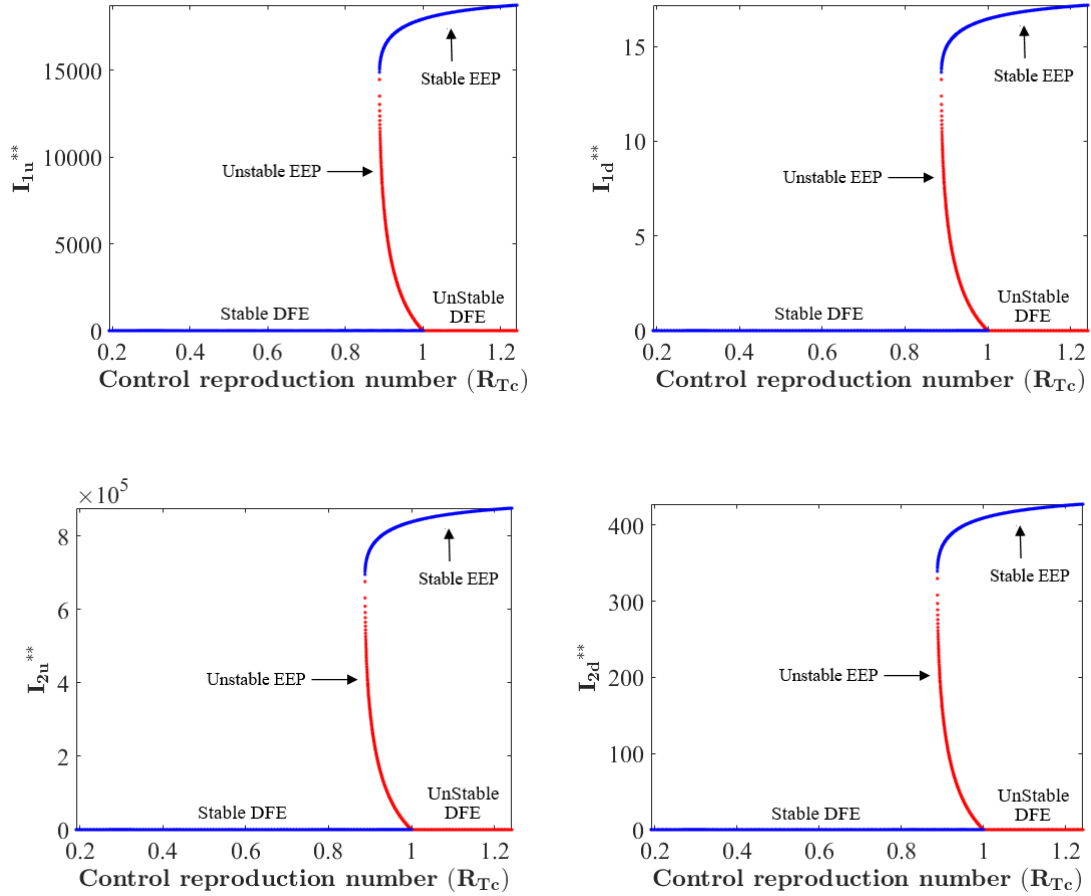
Figure 3.2: Backward Bifurcation Diagram for the Model (3.1), Showing the Profiles of the Population of (a) Undetected HIV-infected Individuals in the Primary Infection Stage of Infection (I_{1u}), (B) Detected Hiv-infected Individuals in the Primary Infection Stage of Infection (I_{1d}), (C) Undetected Hiv-infected Individuals in the Secondary Infection Stage of Infection (I_{2u}) and (D) Detected Hiv-infected Individuals in the Secondary Infection Stage of Infection (I_{2d}), as a Function of the Control Reproduction Number $\mathbb{R}_{T_c}$. Parameter Values Used Are: $\Pi = 100000, p = 0.81, \psi_l = 0.99, \psi_h = 0.0001, \sigma_{1u} = 5.1, \sigma_{1d} = 0.1, \sigma_{2u} = 0.1, \sigma_{2d} = 0.1, \xi_D = 0.01, \varepsilon_d = 0.01, \varepsilon_p = 0.01, C_p = 1, \eta_d = 0.1, \eta_2 = 0.1, \eta_a = 0.1, \eta_h = 0.009, \delta_u = 10.1, \delta_d = 0.1, \tau_1 = 0.0001, \tau_2 = 0.1, \tau_a = 0.1, \mu = 0.009, \beta = 50$. With This Arbitrary Set of Parameter Values, the Values of the Associated Backward Bifurcation Coefficients (Denoted by a and b, and given in (D.7) and (D.8)) Are $a = 9.925338500 \times 10^{-5} > 0$ and $b = 0.04638601600 > 0$, Respectively. Apart from the Efficacies (i.e., ε_d and ε_p), Modification Parameters (i.e., η_d, η_2, η_a and η_h) and the Compliance Parameter "c_p", Which Are Dimensionless, All the Other Parameters Have a Unit of *per* Year.

bifurcation associated with the model (3.1). It should be mentioned that, for computational convenience (in generating Figure 3.2), we set, the eigenvectors v_1 and v_3 in

(D.3) (given in Appendix D) to one. Similarly, we set the eigenvectors w_2 and w_3 in (D.4) to one.

To make sure that the effective control of the HIV/AIDS in a MSM population (or the elimination of the disease) is independent of the initial sizes of the subpopulations of the model (3.1), it is necessary that the disease-free equilibrium is proved to be globally-asymptotically stable when the associated control reproduction number of the model is less than unity. This will be explored below in Section 3.3.3, for the special case of the model (3.1).

3.3.3 Global Asymptotic Stability of DFE: Special Case

In this section, we explore extending the result in Theorem 3.3.1 to prove the global asymptotic stability of the DFE for the special case of the model (3.1). Consider the model (3.1) with $\varepsilon_p \, c_p = 1$ and $\delta_u = \delta_d = 0$. Setting $\delta_u = \delta_d = 0$ into the model (3.1), and adding all the equations, shows that $\dfrac{dN}{dt} = \Pi - \mu N$, from which it follows that $N(t) \to \dfrac{\Pi}{\mu}$ as $t \to \infty$. From now on, the total population at time t, $N(t)$, will be replaced by its limiting value, $N^* = \Pi/\mu$. In other words, the standard incidence formulation for the infection rate is now replaced by a mass action incidence. Consider the following feasible region for the special case of the two-group model (3.1):

$$\Gamma^* = \left\{ (S_L, S_H, I_{1_u}, I_{1_d}, I_{2_u}, I_{2_d}, A_u, A_d, T) \in \Gamma : S_L \le S_L^*, S_H \le S_H^* \right\}.$$

It can be shown that the region Γ^* is positively-invariant and attracting with respect to this special case of the model (see Appendix E). The control reproduction number of this special case of the two group model, denoted by $\hat{\mathbb{R}}_{T_c}$, is given by:

$$\hat{\mathbb{R}}_{T_c} = \rho(\hat{F}V^{-1}) = \mathbb{R}_{T_c}\big|_{\varepsilon_p \, c_p = 1, \delta_u = \delta_d = 0}. \tag{3.18}$$

We claim the following result:

Theorem 3.3.4. *Consider the special case of the model (3.1) with $\varepsilon_p\, c_p = 1$ and $\delta_u = \delta_d = 0$. The disease-free equilibrium of the special case of the model (3.1), $\mathcal{E}_{DF}$ is globally-asymptotically stable in Γ^* whenever $\mathring{\mathbb{R}}_{T_c} < 1$.*

The proof of Theorem 3.3.4, based on using a comparison theorem argument [78, 65, 104], is given in Appendix E. The result of Theorem 3.3.4 is numerically illustrated in Figure 3.3, where all initial conditions of the special case of the model converged to the disease-free equilibrium when the associated control reproduction number, $\mathring{\mathbb{R}}_{T_c}$, is less than one. The epidemiological implication of Theorem 3.3.4 is that, for the special case of the model (3.1) with $\varepsilon_p\, c_p = 1$ and $\delta_u = \delta_d = 0$, the HIV-disease can be eliminated in the United States if the threshold quantity, $\mathring{\mathbb{R}}_{T_c}$, can be brought to (and maintained at) a value less than one. In other words, for the aforementioned special case of the model (3.1), having $\mathring{\mathbb{R}}_{T_c} < 1$ is necessary and sufficient for the effective control (or elimination) of HIV in the United States.
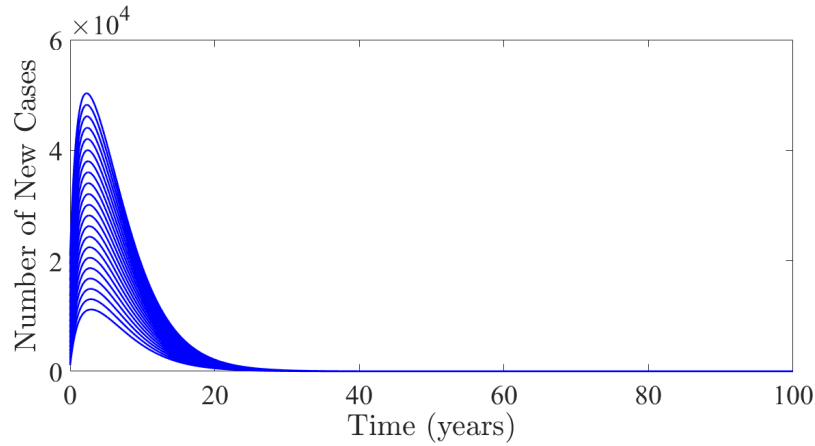
Figure 3.3: Simulations of the Model (3.1), for the Number of New Cases as a Function of Time, Showing Convergence of Initial Conditions to the Disease-free Equilibrium When $\mathring{\mathbb{R}}_{T_c} < 1$. Parameter Values Used Are as given in Table 3.3 with $\beta = 0.25$ (so That, $\mathring{\mathbb{R}}_{T_c} = 0.4649 < 1$). For These Simulations, the Associated Backward Bifurcation Coefficient, a, Takes the Value $a = -5.41730928 \times 10^{-5} < 0$, and the Associated Backward Bifurcation Coefficient, b, Takes the Value $b = 0.181937418 > 0$.

It is worth mentioning that substituting $\varepsilon_p\, c_p = 1$ and $\delta_u = \delta_d = 0$ into the expressions for the backward bifurcation coefficients (a and b) in (D.7) and (D.8), and simplifying, shows that $a = -5.41730928 \times 10^{-5} < 0$ and $b = 0.181937418 > 0$. Thus, it follows from Item (i) of Theorem 4.1 in [16] that the special case of the model (3.1) with $\varepsilon_p\, c_p = 1$ and $\delta_u = \delta_d = 0$ will not undergo backward bifurcation at $\hat{\mathbb{R}}_{T_c} = 1$ (this is in line with the global asymptotic stability result proved for the disease-free equilibrium of the special case of the model in Theorem 3.3.4; as illustrated in Figure 3.3, where all initial conditions of the model converged to the DFE when the conditions for the absence of backward bifurcation are achieved.

3.4   Global Uncertainty and Sensitivity Analysis

The model (3.1) contains 23 parameters. Although the baseline values of these parameters are available from the literature (as tabulated in Table 3.3), uncertainties are expected to arise in the estimate of these parameter values [103]. It is, therefore, crucial to assess the impact of these uncertainties on the outcome of the model simulations [103, 13, 81, 79, 107]. Furthermore, it is also important to identify the key parameters of the model that have the most influence on the dynamics of the model with respect to a chosen response function. In this section, global uncertainty and sensitivity analyses will be carried out to determine the parameters that have the most influence on the chosen response function for the model (3.1). Since the values of two of the parameters of the model (3.1), namely the demographic parameters Π and μ, are reliably known for the target (available from the population health and vital statistics data obtained from the Arizona Department of Health Services [9]), they are excluded from the global uncertainty and sensitivity analyses to be carried out in this section. That is, these analyses will be based on the remaining 21 parameters of the model (3.1)).

Parameter	Baseline Value	Reference
Π	1,379	[7, 60]
β	0.62	[62]
p	0.15	[99]
ψ_L	0.3	assumed
ψ_H	0.3	assumed
σ_{1u}	0.5	[101]
σ_{1d}	0.5	[101]
σ_{2u}	0.2223	[47]
σ_{2d}	0.2223	[47]
ξ_d	0.8	assumed
ε_d	1.5	assumed
η_d	0.43	[100]
η_2	0.5	assumed
η_A	1.5	[107]
δ_u	0.0047	[101]
δ_d	0.09	[101]
τ_1	0.54	[80]
τ_2	0.54	[80]
τ_A	0.54	[80]
η_H	1.5	assumed
ε_p	0.964	[52]
c_p	0.31	[73]
μ	0.0125	[31]

Table 3.3: Baseline Values of the Parameters of the Model (3.1). Apart from The Modification Parameters (i.e., η_d, η_2, η_a and η_h), Efficacies (i.e., ε_p and ε_d) and the Proportion "p", Which Are Dimensionless, All Other Parameters of the Model Model (3.1), Together with Their Ranges, Have Unit of *per* Year.

Parameter	Baseline Value	Range	PRCC: $\mathbb{R}_{T_c}$
β	0.62	[0.496, 0.744]	0.933*
p	0.15	[0.120, 0.180]	0.2433
ψ_L	0.3	[0.235, 0.375]	0.707*
ψ_H	0.3	[0.235, 0.375]	-0.696*
σ_{1u}	0.5	[0.400, 0.600]	-0.2072
σ_{1d}	0.5	[0.400, 0.600]	0.1618
σ_{2u}	0.222	[0.178, 0.267]	-0.1469
σ_{2d}	0.222	[0.178, 0.267]	0.0539
ξ_d	0.8	[0.640, 0.960]	-0.696*
ε_d	1.5	[1.200, 1.800]	-0.716*
η_d	0.43	[0.344, 0.516]	0.787*
η_2	0.5	[0.400, 0.600]	0.4365
η_A	1.5	[1.200, 1.800]	0.3330
δ_u	0.005	[0.004, 0.006]	-0.0359
δ_d	0.09	[0.072, 0.108]	-0.0239
τ_1	0.54	[0.440, 0.640]	-0.523*
τ_2	0.54	[0.440, 0.640]	-0.1577
τ_A	0.54	[0.440, 0.640]	-0.2104
η_H	1.5	[1.200, 1.800]	0.907*
ε_p	0.964	[0.771, 1.157]	-0.667*
c_p	0.31	[0.248, 0.372]	-0.665*

Table 3.4: Table of PRCC Values of the Parameters in the Expression for the Control Reproduction Number, $\mathbb{R}_{T_c}$, of the Model (3.1). PRCC Values above 0.5 in Magnitude Are Highlighted with a ($*$), Implying That These Parameters Are Highly-correlated (i.e., Either Positively-correlated or Negatively-correlated with the Response Function). Apart from the Modification Parameters, (i.e., η_d, η_2, η_a and η_h), Efficacies (i.e., ε_p and ε_d) and the Proportion "p" Which Are Dimensionless, All the Other Parameters and Their Ranges Have Unit of *per* Year.

Global uncertainty analysis is conducted for the model (3.1) to assess the variability in the outcome variable (i.e., a response function) arising due to the uncertainty in estimating the input values (i.e., due to uncertainty in estimating the values of the 21 parameters of the model, in this case). The Latin Hypercube Sampling (LHS) technique is used to explore the effect of the uncertainty in estimating the values of the 21 parameters [81, 13]. The practical implementation of this stratified Monte Carlo sampling method (an extension of Latin Square sampling [13]), in the context of the model (3.1), involves defining a baseline value and range for each of the 21 parameters, and generating multiple runs for a chosen response function (we choose the control reproduction number, $\mathbb{R}_{T_c}$, as the response function [107]) and generating a random sample of size $10,000$ (using the LHS approach) for each of the parameters using a uniform distribution. The results of the uncertainty analysis, depicted by histograms for the 21 parameters in Figures 3.4 (a) and (b)[107, 13], show that, for the parameter values and ranges used in the uncertainty analysis (see Table 3.4), the value of the response function (i.e., the control reproduction number, $\mathbb{R}_{T_c}$, of the model (3.1) for HIV dynamics in the MSM community in the State of Arizona) lie in the range $\mathbb{R}_{T_c} \in (0.5845, 1.3377)$, with a mean value of $\mathbb{R}_{T_c} = 0.8919$ at the 95% confidence interval. Hence, since the mean value of the control reproduction number, $\mathbb{R}_{T_c}$, is less than one, it follows from Theorem 3.3.4 that the disease can be eliminated from the MSM population. Furthermore, it follows from this figure that the probability that the control reproduction number $(\mathbb{R}_{T_c})$ will exceed one (so that the disease will persist in the MSM population) is 27% (this probability is calculated by using the 10,000 random samples generated to calculate $\mathbb{R}_{T_c}$; the probability is then obtained by dividing the total number of times $\mathbb{R}_{T_c}$ exceeds one by the sample size, 10,000).

Global parameter sensitivity analysis is now carried out to determine the key param-
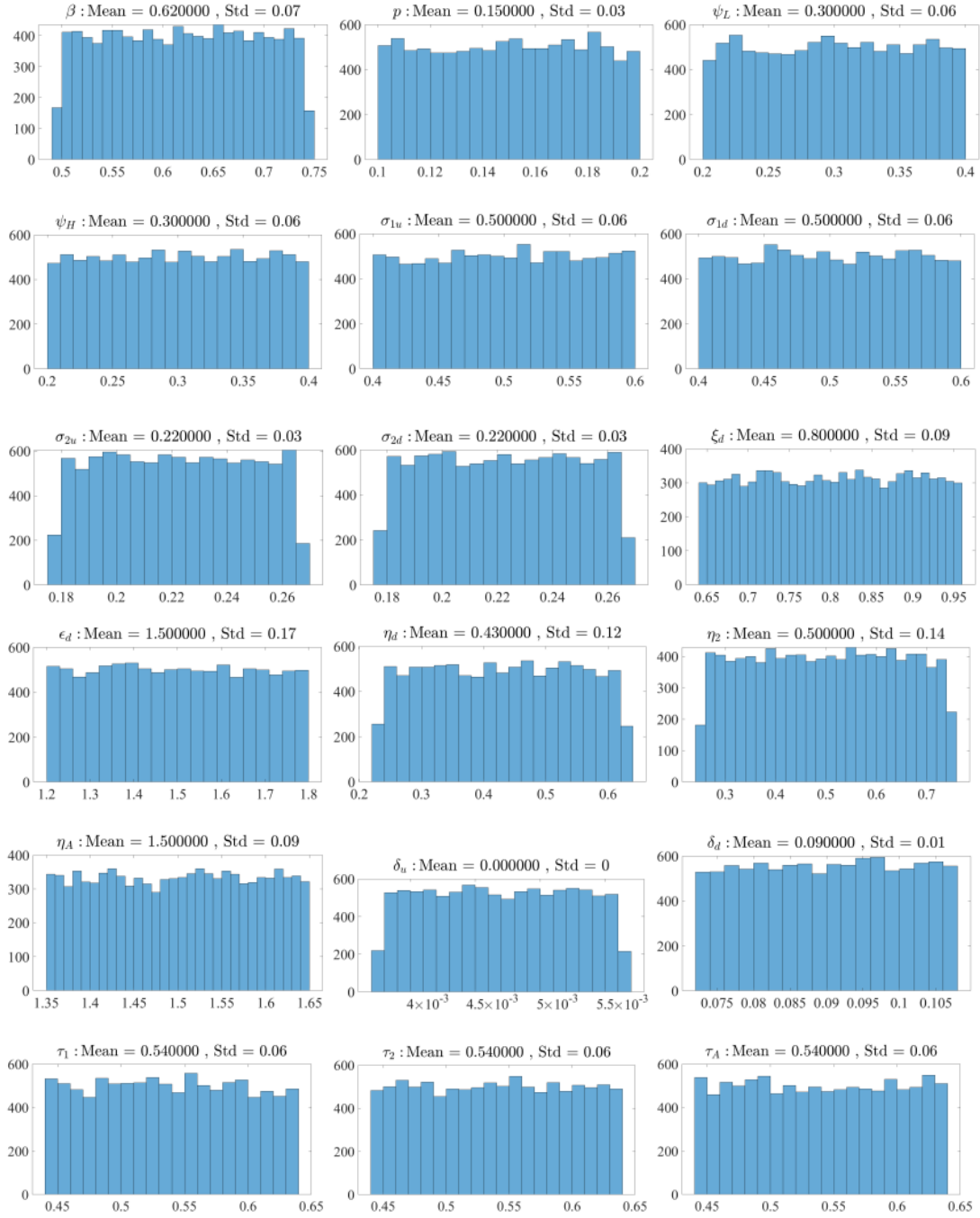
Figure 3.4: (a) Distribution of Parameters of the Model (3.1) and the Response Function ($\mathbb{R}_{T_c}$) Generated from the Uncertainty Analysis. Parameter Values Used Are given by the Baseline Values and Ranges in Table 3.4.
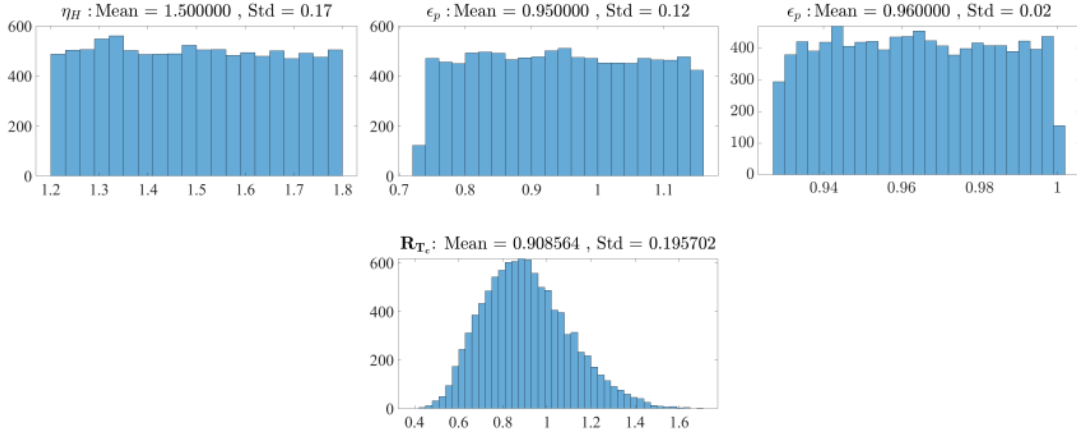
Figure 3.4: (b) Distribution of Parameters of the Model (3.1) and the Response Function ($\mathbb{R}_{T_c}$) Generated from the Uncertainty Analysis. Parameter Values Used Are given by the Baseline Values and Ranges in Table 3.4.

eters of the model (3.1) that have the most influence on the aforementioned response function ($\mathbb{R}_{T_c}$). The overall methodology and process of carrying out the global parameter sensitivity analysis is the same as discussed in the Section 2.4, and is not repeated here (except that the sensitivity analysis here uses the baseline values and ranges of the parameters of the model (3.1) given in Table 3.4, and 1,000 random samples are generated from the range of each parameter using the LHS approach). The results of the sensitivity analysis conducted on the model (3.1), with respect to the response function $\mathbb{R}_{T_c}$, are depicted in Figure 3.5 (see also Table 3.4). It follows from this figure that the top five PRCC-ranked parameters that have the most influence on the response function ($\mathbb{R}_{T_c}$) are:

1. The effective contact rate (β).

2. The modification parameter for the assumed increase in the likelihood of acquiring an HIV infection by high-risk susceptible individuals (η_H).

3. The modification parameter for reduced infectiousness of detected individuals, in relation to undetected individuals (η_d).

70

4. The efficacy of diagnostic test to detect undetected infectious individuals (ε_d).

5. Transition rate of susceptible individuals from the low-risk to the high-risk susceptible compartment (ψ_L).

Therefore, it follows from the global parameter sensitivity analysis that HIV can be effectively controlled in the MSM population by implementing intervention and mitigation measures that focus on the following strategies:

(i) Reducing the effective contact rate (i.e., reduce β). This can be achieved by minimizing the number of sexual partners, consistently using condoms during sexual intercourse and avoiding needle-sharing by injection-drug MSM users.

(ii) Reducing the increased likelihood of high-risk susceptible individuals from acquiring an HIV infection, in comparison to low-risk susceptible individuals (i.e., reduce η_H). This can be achieved by encouraging high-risk individuals to get tested frequently to keep them aware of their HIV infection status (and risk), reducing their number of sexual partners, using sterilized needles (by high-risk susceptible injection-drug MSM users), and using condoms consistently during sexual intercourse.

(iii) Reducing the value of the modification parameter for the assumed reduction of infectiousness of detected individuals, in comparison to undetected infectious individuals (i.e., reduce η_d). This can be achieved by encouraging individuals to get tested frequently and to immediately treat the detected infected individuals (in addition to counselling them to desist from risky practices that could lead them to infect their susceptible partners).

(iv) Increasing the efficacy of diagnostic tests (i.e., increase ε_d). This can be achieved by using high-quality HIV diagnostic tests (with high specificity and sensitivity,

71

including DNA-based HIV tests, such as NAT [87, 35]).

(v) Reducing the increase in risky behavior (i.e., reduce ψ_L). This can be achieved by implementing effective public health education and counselling campaigns that discourage low-risk individuals from engaging in risky behavior that increases their likelihood of acquiring an HIV infection. In other words, effective strategies that encourages positive change of behavior (so that low-risk individuals do not change their behavior and transition to the high-risk HIV-susceptible class) should be implemented.
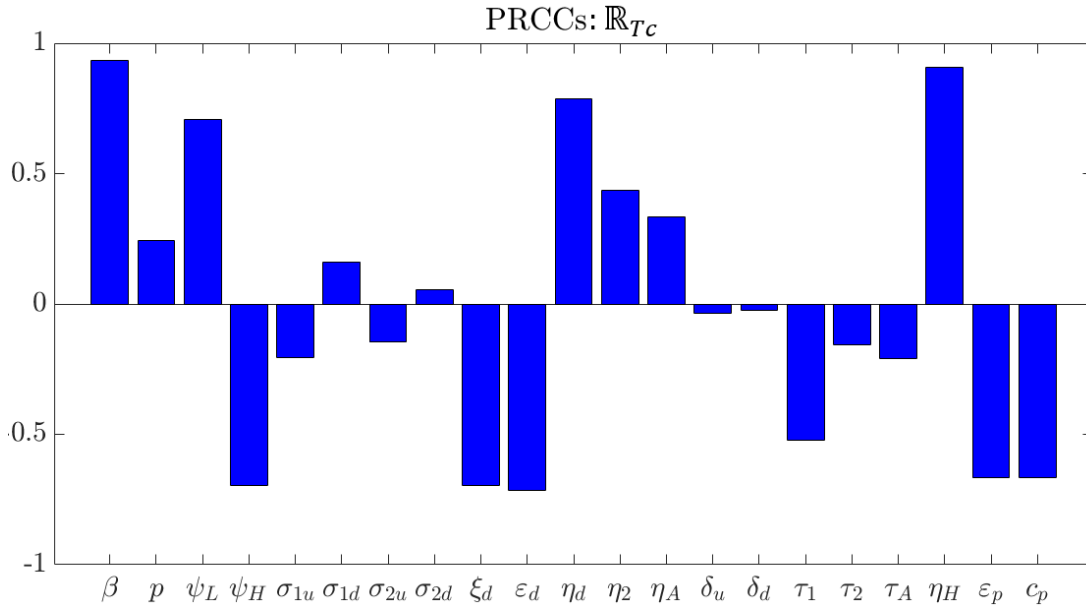
Figure 3.5: Partial Rank Correlation Coefficients (PRCCs) Depicting the Impact of the Parameters of the Model (3.1) with Respect to the Response Function (or Burden of the HIV/AIDS in the MSM Community) ($\mathbb{R}_{T_c}$). The Parameters Used in These Simulations Are as given by the Baseline Values, and Their Corresponding Ranges Are as given in Table 3.4.

It should be mentioned that other notable influential parameters (with respect to the response function, but not as influential as the aforementioned top-five) of the model are the transition rate of susceptible individuals from high-risk to low-risk class (ψ_H),

the detection rate of diagnostic test administered the compliance in PrEP usage (ξ_d), the efficacy of PrEP to prevent high-risk susceptible individuals from acquiring an HIV infection (ε_p), the compliance in PrEP usage (c_p) and the treatment rate of detected individuals in I_{1d} class (τ_1).

In summary, based on the sensitivity analysis conducted in this section, this study identifies five parameters of the model (3.1), namely, β, η_H, η_d, ε_d and ψ_L, that have the greatest influence on the value of the chosen response function of the model (i.e., the control reproduction number, ($\mathbb{R}_{T_c}$), which governs the persistence or effective control of the HIV/AIDS pandemic for the MSM population in the State of Arizona). Hence, in order to effectively curtail the HIV/AIDS epidemic in the MSM population, the control and mitigation interventions implemented in the MSM community should focus on effectively targeting the aforementioned top-five PRCC-ranked parameters. Furthermore, based on the results of the uncertainty analysis depicted in Figures 3.4(a) and (b), this study suggests that, under the current conditions and parameterizations, the HIV epidemic has a relatively small probability of remaining endemic in this MSM population, and that the disease can be eliminated from the MSM population (since the mean reproduction number is less than one).

3.5   Numerical Simulations

The model (3.1) will now be simulated to assess the population-level impact of the effective contact rate, the compliance of PrEP coverage, the duration before detection of undetected individuals, treatment, modification parameters (η_d and η_H) and behaviour change on the dynamics of HIV/AIDS in an MSM community in the State of Arizona. Unless otherwise stated, the simulations will be carried out using the baseline values of the parameters tabulated in Table 3.3.

3.5.1 Assessing the Impact of Heterogeneity in Effective Contact Rate

The model (3.1) will now be simulated to assess the community-wide impact of heterogeneity in the effective contact rate on the efficacy of PrEP and compliance of PrEP coverage. Figure 3.6 depicts the contour plots of the control reproduction number $(\mathbb{R}_{T_c})$ of the model (3.1), as a function of the efficacy of PrEP (ε_p) and compliance in PrEP usage (c_p). For all the simulations depicted in Figures $3.6(a) - (c)$, all the parameters are maintained at their baseline values, as tabulated in Table 3.3. It follows from the contour plot depicted in Figure $3.6(a)$ that the value of $\mathbb{R}_{T_c}$ decreases with the increasing efficacy of PrEP and compliance in PrEP usage. Figure $3.6(b)$ further shows that if β is increased by 2-fold from its baseline value (while PrEP efficacy is maintained at its baseline value of 96%, as given in Table 3.3), at least 40% of the high-risk susceptible MSM population needs to be on PrEP to bring (and maintain) the control reproduction number $(\mathbb{R}_{T_c})$ to a value below one. However, if β is increased by 5-fold from its baseline value (with PrEP efficacy maintained at 96%), then the PrEP compliance needed to bring (and maintain) the control reproduction number to a value below one dramatically increases to 86% (Figure $3.6(c)$).

In summary, the contour plots depicted in Figure 3.6 show that, for baseline PrEP efficacy, the level of PrEP compliance needed to bring (and maintain) the control reproduction number to a value less than one increases significantly with increasing the value of the effective contact rate (β) in the MSM community.

3.5.2 Assessing the Effect of Compliance of PrEP Coverage

The model (3.1) is further simulated to assess the population-level impact of PrEP compliance on the dynamics of HIV in the MSM population. Specifically, simulations are carried out for the yearly and cumulative yearly cases of HIV in the MSM

74
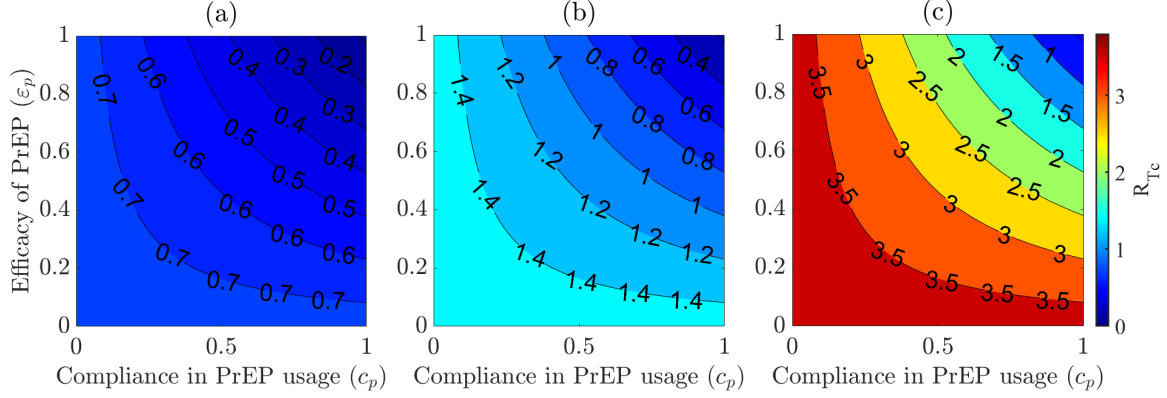
Figure 3.6: Contour Plots of the Control Reproduction Number ($\mathbb{R}_{T_c}$) of the Model (3.1), as a Function of the Efficacy of Prep (ε_p) and Compliance in Prep Usage (c_p). (a) the Effective Contact Rate (β) Kept at Its Baseline. (b) the Effective Contact Rate (β) Increased by 2-fold from Its Baseline Value. (c) the Effective Contact Rate (β) Increased by 5-fold from Its Baseline Value. Other Parameter Values Used in the Simulations Are as given by Their Baseline Values in Table 3.3.

population, as a function of PrEP compliance coverage (c_p), while keeping all the other parameters of the model at their baseline values (tabulated in Table 3.3). The results obtained are depicted in Figure 3.7. In particular, Figure 3.7(a) show a significant decrease in the average yearly new cases at the peak recorded with increasing coverage in PrEP compliance (i.e., compare the peaks for the magenta, yellow and green curves in Figure 3.7(a), with the peaks of the blue curve, which represents the worst-case scenario where PrEP-based intervention is not implemented in the MSM community). For instance, this figure shows that if the compliance in PrEP usage is 30%, then about 10.8% of the yearly new HIV/AIDS cases recorded at the peak could have been prevented, in comparison to the worst-case scenario (i.e., compare the peaks of the blue and magenta curves in Figure 3.7(a)). If compliance in PrEP usage is increased to 50%, then about 19.1% of the yearly new HIV/AIDS cases recorded at the peak could have been averted, in comparison to the worst-case scenario (i.e., compare the peaks of the blue and gold curves in Figure 3.7(a)). Finally, if the com-

pliance in PrEP usage is further increased to 80%, about 34.2% of the new yearly HIV/AIDS cases recorded at the peak could have been averted, in comparison to the worst-case scenario (i.e., compare peaks of blue and green curves in Figure 3.7(a)). Similar reductions are observed with respect to the cumulative number of yearly new cases, for the aforementioned levels of compliance of PrEP coverage considered in these simulations, in comparison to the worst-case scenario (as illustrated in Figure 3.7(b)).
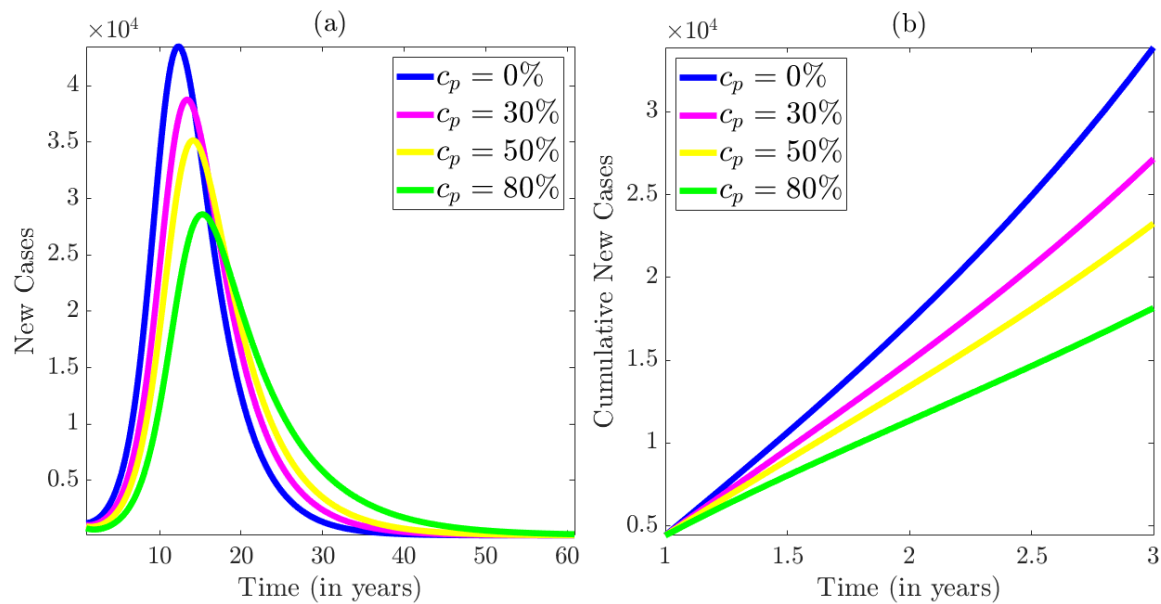
Figure 3.7: Simulations of the Model (3.1), Showing (a) New Cases of HIV/AIDS and (b) Cumulative New Cases of HIV/AIDS in the MSM Population in the State of Arizona, as a Function of Time, for Various Values of the Compliance in Prep Usage (c_p). Values of the Other Parameters of the Model (3.1) Used in These Simulations Are as given by Their Respective Baseline Values Tabulated in Table 3.3.

In summary, the simulations in this section show that increasing PrEP coverage in the high-risk susceptible MSM population resulted in a marked reduction in the average number of new yearly (and cumulative yearly) cases recorded at the peak, in comparison to the worst-case scenario when no PrEP-based intervention is implemented in the MSM community.

3.5.3 Assessing the Effect of Duration Before Detection of Undetected Individuals

The model (3.1) is now simulated to assess the effect of the average duration before the detection of undetected infectious individuals $(1/\xi_d)$ and the efficacy of the diagnostic test (ε_d) on the dynamics of HIV/AIDS in the MSM community in the State of Arizona. The simulations are carried out using the baseline values of the other parameters of the model, tabulated in Table 3.3. The results obtained, depicted by the contour plot of the control reproduction number of the model, as a function of $1/\xi_d$ and ε_d (in Figure 3.8), show that regardless of the values of the efficacy of the diagnostic test, early detection of undetected infectious individuals significantly reduces the control reproduction number (hence, reduce the disease burden). Thus, it can be concluded from Figure 3.8 that, for the baseline value of the efficacy of diagnostic test to detect undetected individuals (i.e., $\varepsilon_d = 1.5$), the control reproduction number can be brought to a value below one if (on average) undetected infected individuals can be detected and treated within about 4 years, and the corresponding value of the detection rate of diagnostic test administered is 0.281 (i.e., $\xi_d = 0.281$).

3.5.4 Assessing the Effect of Treatment

The model (3.1) is simulated, using the baseline parameter values in Table 3.3, to assess the effect of treatment of detected individuals in the population of HIV-infected individuals in the MSM community during primary and secondary infection stages of infection (i.e., we are assessing the impact of treating detected individuals in the I_{1d} and I_{2d} classes), on the dynamics of HIV/AIDS in the MSM community. Figure 3.9 depicts a contour plot of the control reproduction number of the model (3.1), as a function of the duration before treatment of detected HIV-infected individuals in the primary infection stage of the infection $(1/\tau_1)$ and the duration before treatment
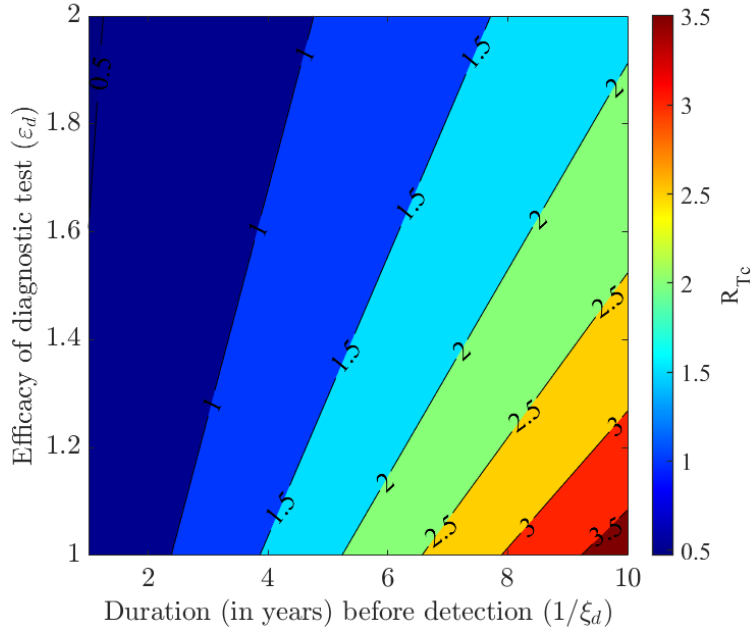
Figure 3.8: Contour Plot of the Control Reproduction Number ($\mathbb{R}_{T_c}$) of the Model (3.1), as A Function of Efficacy of Diagnostic Test to Detect Undetected Individuals (ε_d) and the Duration Before Detection ($1/\xi_d$). Parameter Values Used Are as given by Their Baseline Values in Table 3.3.

of detected HIV-infected individuals in the secondary infection stage of the infection ($1/\tau_2$). The parameter values used in the simulations to generate the contour plots in Figure 3.9 are as given by their baseline values as tabulated in Table 3.3. This figure 3.9 shows that the value of the control reproduction number ($\mathbb{R}_{T_c}$) decreases as the the duration before treatment of detected individuals in the I_{1d} and I_{2d} classes decreases. Hence, it can be concluded that, for the range of the duration before the treatment of detected individuals in I_{2d} class is between 1 year to 12 years (i.e., $1 < 1/\tau_2 < 12$), if the average duration before treatment of detected individuals in the population of detected HIV-infected individuals in the primary infection stage of infection is about 9 years or less, then HIV can be effectively controlled in the MSM community (since the control reproduction number, $\mathbb{R}_{T_c}$, of the model takes a value below one).

In summary, even for the scenario when the duration before treatment of HIV-infected

individuals in I_{2d} class is between 1 to 12 years, the prospects for the effective control and elimination of HIV/AIDS in the MSM community is promising if the average duration before the treatment of detected individuals in the primary stage of the HIV-infection is about 9 years or less.

Figure 3.9: Contour Plot of the Control Reproduction Number ($\mathbb{R}_{T_c}$) of the Model (3.1), as A Function of the Duration Before Treatment of Detected Individuals in Primary Stage of Infection ($1/\tau_1$) and the Duration Before Treatment of Detected Individuals in Secondary Stage of Infection ($1/\tau_2$). Parameter Values Used Are as given by Their Baseline Values in Table 3.3.

3.5.5 Assessing the Effect of Modification Parameters (η_d and η_H)

The combined population-level impact of the modification parameters for reduced infectiousness of detected individuals, in relation to undetected individuals (η_d) and the modification parameter for the assumed increase in the likelihood of acquiring an HIV infection by high-risk susceptible individuals (η_H) is monitored by simulating the model (3.1) using the baseline parameters in Table 3.3. The results obtained, depicted

by the contour plots in Figure 3.10, show a significant decrease in the value of the control reproduction number ($\mathbb{R}_{T_c}$) with decreasing values of the modification parameter η_H (where the reproduction number decreases from 1.6 to 0.45, as η_H decreases from 3 to 2.5), regardless of the values of the modification parameter for reduced infectiousness of detected individuals, in relation to undetected individuals (η_d). Thus, it can be concluded that, for the baseline value of the modification parameter for the reduced infectiousness of detected individuals, in relation to undetected individuals (i.e., $\eta_d = 0.43$), the value of the modification parameter for the assumed increase in the likelihood of acquiring an HIV infection by high-risk susceptible individuals need to be 2.9 or less in order to reduce the control reproduction number ($\mathbb{R}_{T_c}$) below one (i.e., for this setting, high-risk susceptible individuals should not be more than 10% more likely to acquire HIV infection, in comparison to their low-risk counterparts).

3.5.6   Assessing the Effect of Behaviour Change

The model (3.1) is further simulated to assess the effect of negative behavior change (from low-risk to high-risk susceptible population) and positive behavior change (from high-risk to low-risk susceptible population) on the dynamics of HIV/AIDS in the MSM community. The simulations are carried out using the baseline values of the parameters of the model (tabulated in Table 3.3). Figure 3.11 depicts the contour plot of the control reproduction number of the model (3.1), as a function of the transition rate from low-risk to high-risk susceptible population (ψ_L) and the transition rate from high-risk to low-risk susceptible population (ψ_H). It follows from the contour plots depicted in Figure 3.11(a) that the value of the control reproduction number ($\mathbb{R}_{T_c}$) decreases with the decreasing values of the transition rate from low-risk to high-risk susceptible population and with the increasing values of the transition rate from high-risk to low-risk susceptible population. Furthermore, our simulations show
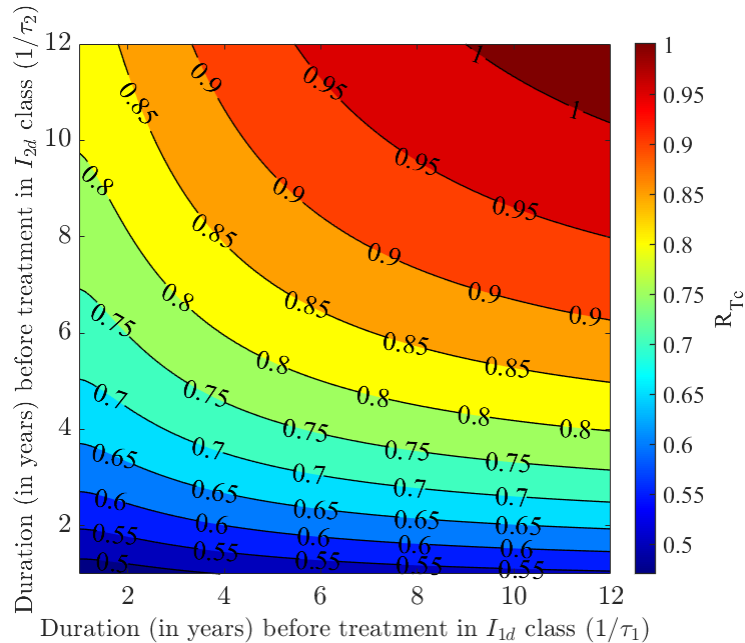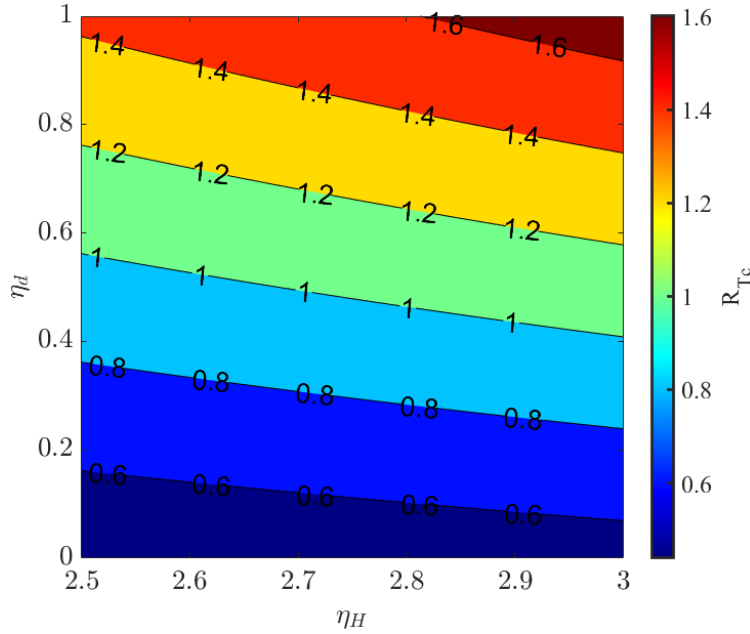
Figure 3.10: Contour Plot of the Control Reproduction Number ($\mathbb{R}_{T_c}$) of the Model (3.1), as a Function of the Modification Parameter for the Assumed Reduction in the Infectiousness of Detected Individuals, in Relation to Undetected Individuals (η_d) and the Modification Parameter for the Assumed Increase in the Likelihood of Acquiring an HIV Infection by High-risk Susceptible Individuals (η_h). Parameter Values Used Are as given by Their Baseline Values in Table 3.3.

that if the transmission rate β is increased by 2-fold from its baseline value, and the value of ψ_L is kept at baseline, then the value of ψ_H needs to be at least 0.40 *per* year (i.e., if the duration before the transition of susceptible individuals from high-risk to low-risk susceptible population is at most 2.5 years), to bring the control reproduction number ($\mathbb{R}_{T_c}$) below one (Figure 3.11(*b*)). However, if β is increased by 5-fold from its baseline value then the transition rate of susceptible individuals from low-risk to high-risk susceptible population (ψ_L) needs to be below 0.07 *per* year (regardless of the value of the transition rate from high-risk to low-risk susceptible population) to bring the control reproduction number below unity (Figure 3.11(*c*)). In other words, the prospects of eliminating HIV/AIDS in the MSM population is promising if the duration before the transition of susceptible individuals from low-risk to high-risk

81

susceptible population is at least 15 years (i.e., if low-risk individuals take at least 15 years before they change their risky behavior and transition to the high-risk group). In summary, it follows from the results depicted in Figure 3.11 that the value of the control reproduction number ($\mathbb{R}_{T_c}$) decreases significantly with increasing values of the transition rate from high-risk to low-risk susceptible population (ψ_H) even if the effective contact rate (β) is increasing. Furthermore, if the effective contact rate (β) is increased by 5-fold from its baseline value, then the value of the transition rate from low-risk to high-risk susceptible population (ψ_L) must be reduced significantly to have any realistic chance for the effective control or elimination of the disease in the MSM community.
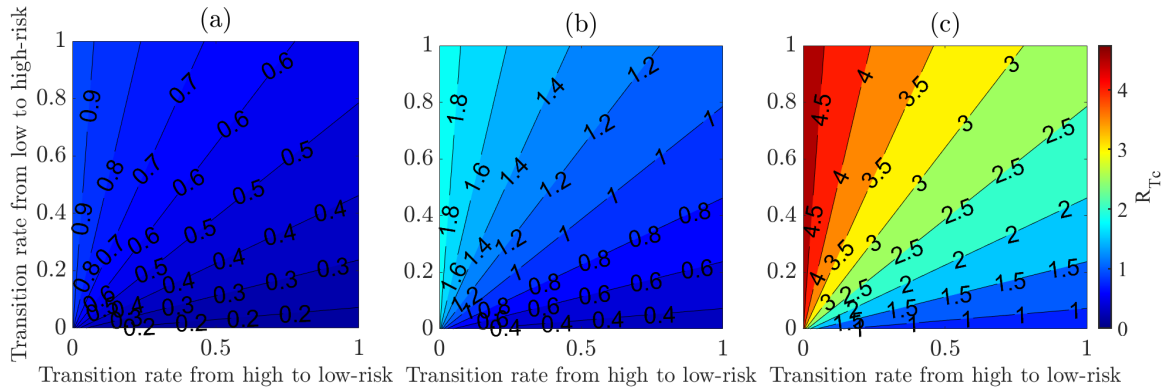
Figure 3.11: Contour Plot of the Control Reproduction Number ($\mathbb{R}_{T_c}$) of the Model (3.1), as A Function of the Transition Rate from Low-risk to High-risk Susceptible Population (ψ_l) and the Transition Rate from High-risk to Low-risk Susceptible Population (ψ_h) When (a) the Effective Contact Rate (β) Is at the Baseline, (b) the Effective Contact Rate (β) Is Increased by 2-fold from the Baseline Value, (c) the Effective Contact Rate (β) Is Increased by 5-fold from the Baseline Value. The Units of ψ_l and ψ_h Are *per* Year. The Other Parameter Values Used Are as given by Their Baseline Values in Table 3.3.

3.6   Concluding Remarks for Chapter 3

This chapter is based on the use of mathematical modeling approaches to assess the combined impacts of risk-structure and the use of pre-exposure prophylaxis (PrEP)

on the spread and control of HIV/AIDS in a sexually-active MSM population in the United States. Specifically, a novel two-group model (low-risk and high-risk), which takes the form of a 9-dimensional deterministic system of nonlinear differential equations is developed. This model, which extends numerous other HIV transmission models in the literature, was rigorously analysed to gain insight into its qualitative features. The analyses revealed that the disease-free equilibrium of the model is locally-asymptotically stable whenever the associated control reproduction number of the model (denoted by $\mathbb{R}_{T_c}$) is less than one. Using the theory of center manifold, it was shown that the model undergoes the dynamic phenomenon of backward bifurcation when the associated reproduction number ($\mathbb{R}_{T_c}$) is less than unity under certain conditions. The epidemiological implication of the backward bifurcation phenomenon is that the usual epidemiological requirement of having the control reproduction number of the model being less than unity, while necessary, is no longer sufficient for the elimination of the disease in the community. Furthermore, when the phenomenon of backward bifurcation occurs, more control measures need to be implemented to further reduce the control reproduction number. A sufficient condition for the presence of backward bifurcation in the model was identified, namely the imperfect nature of the efficacy and compliance of PrEP in the MSM community. The disease-free equilibrium for the special case of the model with perfect PrEP efficacy and compliance and no disease-induced mortality (i.e., the special case of the two-group model with $\varepsilon_p c_p = 1$ and $\delta_u = \delta_d = 0$), where backward bifurcation does not occur, is shown to be globally-asymptotically stable when the associated control reproduction number of the model is less than one. The epidemiological implication of this global asymptotic stability result for the special case of the model is that the HIV/AIDS pandemic can be eliminated from the MSM community in the State of Arizona if the control measures implemented can bring (and maintain) the associated

reproduction number to a value less than one. The HIV/AIDS pandemic will persist in the MSM community if the control measures are unable to bring (and maintain) the control reproduction number to a value less than one.

Global uncertainty analysis was also conducted to assess the impact of the uncertainties in the estimates of the parameters of the two group model [13, 81]. Our simulations for parameter uncertainty show that the reproduction number ($\mathbb{R}_{T_c}$) lie between (0.6354, 1.2502) with a mean value of 0.8923 (i.e., $\mathbb{R}_{T_c} = 0.8923$). Thus, under the current conditions and parameterizations, the HIV epidemic can be eliminated from the MSM community (since elimination of the disease requires the reproduction number to be less than unity). In other words, it is less likely for the disease to persist in the MSM community since the probability that the control reproduction number will exceed one is about 27%.

Furthermore, using the global sensitivity analysis of the model, we identified the parameters of the model that have the most influence on the control reproduction number of the model, $\mathbb{R}_{T_c}$. Specifically, the top-five PRCC ranked parameters that had the most impact on the control reproduction number are; the effective contact rate (β), the modification parameter for the assumed increase in the likelihood of acquiring an HIV infection by high-risk susceptible individuals (η_H), the modification parameter for reduced infectiousness of detected individuals, in relation to undetected individuals (η_d), the efficacy of diagnostic test to detect undetected individuals (ε_d) and the transition rate from low-risk to high-risk susceptible population (ψ_L). The numerical PRCC values indicate that reduction of β, η_H, η_d and ψ_L, and increasing ε_d, results in the reduction of $\mathbb{R}_{T_c}$. The parameter β can be reduced by minimizing the number of sexual partners, consistently using condoms during sexual intercourse and avoiding injection-drug by MSM users. The parameter η_H can be reduced by

encouraging high-risk susceptible individuals to get tested frequently to keep them aware about their HIV-infection status (and risk), using sterilized needles (by high-risk susceptible injection-drug MSM users), using condoms consistently during sexual intercourse and reducing the number of sexual partners. ψ_L can be reduced by a change of behaviour *via* public health education campaigns to give awareness about the consequences of unsafe sexual intercourse and the effects of sharing needles (in other word, by promoting counselling campaigns that discourage low-risk individuals from engaging in risky behavior). Furthermore, by decreasing the value of the modification parameter for reduced infectiousness of detected individuals (i.e., by encouraging individuals to get tested frequently and to immediately treat the detected infected individuals) and by increasing the efficacy of diagnostic test to detect undetected individuals (i.e., by using high-quality HIV diagnostic tests, such as NAT [87, 35]), will ultimately reduce $\mathbb{R}_{T_c}$.

We carried out extensive numerical simulations to assess the impact of heterogeneity in effective contact rate and the efficacy of PrEP and compliance in PrEP usage on the dynamics of HIV/AIDS disease in the MSM community. These simulations showed, as expected, that the control reproduction number $(\mathbb{R}_{T_c})$ decreases significantly with the increasing efficacy of PrEP and compliance in PrEP usage, even if the effective contact rate is increasing. For instance, if the effective contact rate (β) is increased by 2-fold from its baseline value for the efficacy of PrEP set at about 96%, at least 40% of the compliance in PrEP usage is needed to bring the control reproduction number $(\mathbb{R}_{T_c})$ below one. However, if β is increased by 5-fold from its baseline value for the efficacy of PrEP set at about 96% then the compliance in PrEP usage drastically increases to 86% to bring the control reproduction number below unity. Furthermore, we also simulated the model to assess the effect of compliance of PrEP coverage on the peak yearly new cases. The numerical simulations showed a marked decrease in the

average yearly new cases at the peak recorded when the compliance in PrEP coverage is increased in comparison to the corresponding scenario when no PrEP compliance is implemented. Specifically, for the scenario when the compliance in PrEP usage is 50%(80%) then about 19.1%(34.2%) of the yearly new HIV/AIDS cases recorded at the peak will have been prevented, in comparison to the the worst-case scenario where PrEP-based intervention is not implemented in the MSM community. This study also showed that, for the baseline value of the modification parameter for the reduced infectiousness of detected individuals, in relation to undetected individuals, the prospects of HIV/AIDS pandemic elimination in the MSM community is possible if high-risk susceptible individuals should not be more than 10% more likely to acquire HIV infection, in comparison to their low-risk counterparts.

This study also addressed an important question related to the community-wide impact of behaviour change (i.e., negative or positive behaviour change) in the MSM population on the dynamics of HIV/AIDS pandemic in the State of Arizona (specifically, the duration before the transition of the susceptible individuals from high-risk to low-risk susceptible population or vice versa). The numerical simulations showed that the value of the control reproduction number $(\mathbb{R}_{T_c})$ decreases significantly with the decreasing values of transition rate from low-risk to high-risk susceptible population (ψ_L) even if the effective contact rate (β) has increased up to 5-fold from its baseline value. It was also shown that for the scenario when the effective contact rate is increased by 2-fold from its baseline value and the value of the transition rate from low-risk to high-risk susceptible population is kept at the baseline value then for the HIV pandemic elimination, the duration before the transition of susceptible individuals from high-risk to low-risk susceptible population needs be at most 2.5 years. Furthermore, if the effective contact rate (β) is increased by 5-fold from its baseline value then low-risk individuals take at least 15 years before they change their risky

behavior and transition to the high-risk group (regardless of the value of the transition rate from high-risk to low-risk susceptible population), in order to eliminate the HIV/AIDS disease from the MSM community.

Some of the limitations of the two group model presented in this study include not incorporating different detection rates of diagnostic test administered for the HIV-infected individuals in the primary, secondary and AIDS stage of infection. Furthermore, the model does not incorporate the condom use strategy (which remains the most effective HIV prevention strategy) along with the use of pre-exposure prophylaxis (PrEP) on the spread and control of HIV/AIDS in an MSM population.

REFERENCES

[1] O. A. Aguirrebengoa, M. V. García, J. A. P. Nuñez, T. P. López, M. G. Lotero, C. E. Garcia, M. R. Utrilla, V. E. Pérez, J. D. R. Guerrero, and C. R. Martín. Implementing Pre-Exposure Prophylaxis could prevent most new HIV infections in transsexual women and men who have sex with men. `https://pubmed.ncbi.nlm.nih.gov/30982539/`, 2019. (Accessed April 5, 2023).

[2] AIDSmap. The stages of HIV infection. `https://www.aidsmap.com/about-hiv/stages-hiv-infection`, 2020. (Accessed April 5, 2023).

[3] AIDSVu. HIV U.S. Map. `https://www.map.aidsvu.org/map`, 2020. (Accessed April 5, 2023).

[4] AIDSVu. Inequities among Black and Hispanic Americans. `https://www.aidsvu.org/prep-use-race-ethnicity-launch-22/`, 2022. (Accessed April 5, 2023).

[5] AIDSVu. Local data Arizona. `https://www.aidsvu.org/local-data/united-states/west/arizona`, 2022. (Accessed April 5, 2023).

[6] Arizona Department of Health Services. HIV/AIDS in Arizona Integrated Epidemiologic Profile. `https://www.azdhs.gov/documents/preparedness/epidemiologydisease-control/disease-integrated-services/hiv-epidemiology/reports/2012/2009-2012-integrated-epidemiologic-profile.pdf`, 2015. (Accessed April 5, 2023).

[7] Arizona Department of Health Services. HIV/AIDS in Arizona. `https://www.azdhs.gov/documents/preparedness/epidemiology-diseasecontrol/disease-integrated-services/hiv-epidemiology/reports/2021/annualreport.pdf`, 2021. (Accessed December 30, 2022).

[8] Arizona Department of Health Services. HIV/AIDS in Arizona Annual Report 2021. https://www.azdhs.gov/documents/preparedness/epidemiology-disease-control/disease-integrated-services/hiv-epidemiology/reports/ 2021/annual-report.pdf, 2021. (Accessed April 5, 2023).

[9] Arizona Department of Health Services. Population Health and Vital Statistics in Arizona. `https://pub.azdhs.gov/health-stats/menu/info/trend/index.php?pg=births`, 2023. (Accessed June 02, 2023).

[10] Biktarvy. Biktarvy. `https://www.biktarvy.com`, 2022. (Accessed April 5, 2023).

[11] A. Bingham, R. K. Shrestha, N. Khurana, E. U. Jacobson, and F. P. G. Estimated lifetime HIV-Related medical costs in the United States. `https://pubmed.ncbi.nlm.nih.gov/33492100/`, 2021. (Accessed May 15, 2023).

[12] K. W. Blayneh, A. B. Gumel, S. Lenhart, and T. Clayton. Backward bifurcation and optimal control in transmission dynamics of West Nile virus. *Bulletin of Mathematical Biology*, 72:1006–1028, 2010.

[13] S. M. Blower and H. Dowlatabadi. Sensitivity and uncertainty analysis of complex models of disease transmission: an HIV model, as an example. *International Statistical Review/Revue Internationale de Statistique*, pages 229–243, 1994.

[14] S. Broder. The development of antiretroviral therapy and its impact on the HIV-1/AIDS pandemic. *Antiviral Research*, 85(1):1–18, 2010.

[15] J. Carr. *Applications of Centre Manifold Theory*, volume 35. Springer Science & Business Media, 2012.

[16] C. Castillo-Chavez and B. Song. Dynamical models of Tuberculosis and their applications. *Mathematical Bioscience & Engineering*, 1(2):361–404, 2004.

[17] Centers for Disease Control and Prevention. Basic statistics. `https://www.cdc.gov/hiv/basics/statistics.html`, 2020. (Accessed December, 2020).

[18] Centers for Disease Control and Prevention. HIV and injection drug use. `https://www.cdc.gov/hiv/basics/hiv-transmission/injection-drug-use.html`, 2020.

[19] Centers for Disease Control and Prevention. HIV modes of transmission. `https://www.cdc.gov/hiv/basics/transmission.html`, 2020. (Accessed December, 2020).

[20] Centers for Disease Control and Prevention. HIV-related death rate in U.S. fell by half from 2010 to 2017. `https://www.cdc.gov/nchhstp/newsroom/2020/hiv-related-deathrate-press-release.html`, 2020. (Accessed April 5, 2023).

[21] Centers for Disease Control and Prevention. HIV testing. `https://www.cdc.gov/hiv/testing/`, 2020. (Accessed April 5, 2023).

[22] Centers for Disease Control and Prevention. HIV transmission. `https://www.cdc.gov/hiv/basics/transmission.html`, 2020. (Accessed December, 2020).

[23] Centers for Disease Control and Prevention. HIV transmission. `https://www.cdc.gov/hiv/basics/transmission.html`, 2020. (Accessed Feb 25, 2023).

[24] Centers for Disease Control and Prevention. New hope for stopping HIV. `https://www.cdc.gov/vitalsigns/hivtesting/index.html`, 2020. (Accessed April 5, 2023).

[25] Centers for Disease Control and Prevention. Sexually transmitted infections treatment guidelines, 2021. `https://www.cdc.gov/hiv/basics/transmission.html`, 2020. (Accessed Feb 25, 2023).

[26] Centers for Disease Control and Prevention. About Ending HIV Epidemic in the U.S. Initiative. `https://www.cdc.gov/endhiv/about.html`, 2021. (Accessed April 5, 2023).

[27] Centers for Disease Control and Prevention. Basic statistics. `https://www.cdc.gov/hiv/basics/statistics.html`, 2021. (Accessed April 5, 2023).

[28] Centers for Disease Control and Prevention. PrEP for HIV Prevention in the U.S. `https://www.cdc.gov/hchstp/newsroom/fact-sheets/hiv/prep-for-hiv-preventionin-the-US-factsheet.html`, 2021. (Accessed April 5, 2023).

[29] Centers for Disease Control and Prevention. PrEP for HIV Prevention in the U.S. `https://www.cdc.gov/nchhstp/newsroom/fact-sheets/hiv/PrEP-for-hiv-prevention-in-the-US-factsheet.html`, 2021. (Accessed March 27, 2023).

[30] Centers for Disease Control and Prevention. About PrEP. `https://www.cdc.gov/hiv/basics/prep/about-prep.html`, 2022. (Accessed on january 15, 2023).

[31] Centers for Disease Control and Prevention. Deaths and mortality. `https://www.cdc.gov/nchs/fastats/deaths.htm`, 2022. (Accessed April 5, 2023).

[32] Centers for Disease Control and Prevention. Guidelines for Using Antiretroviral Agents Among HIV-infected Adults and Adolescents. `https://www.cdc.gov/MMWR/preview/mmwrhtml/rr5107a1.html`, 2022. (Accessed April 5, 2023).

[33] Centers for Disease Control and Prevention. Hiv cost effectiveness. `https://www.cdc.gov/hiv/programresources/guidance/costeffectiveness/index.html`, 2022. (Accessed May 15, 2023).

[34] Centers for Disease Control and Prevention. Hiv Prevention. `https://www.cdc.gov/hiv/basics/prevention.html`, 2022. (Accessed April 5, 2023).

[35] Centers for Disease Control and Prevention. HIV testing. `https://www.cdc.gov/hiv/testing/index.html`, 2022. (Accessed June 2, 2023).

[36] Centers for Disease Control and Prevention. How effective is PrEP. `https://www.cdc.gov/hiv/basics/prep-effectiveness.html`, 2022. (Accessed April 5, 2023).

[37] Centers for Disease Control and Prevention. Pre-Exposure Prophylasis (PrEP). `https://www.cdc.gov/hiv/clinicians/prevention/prep.html`, 2022. (Accessed April 5, 2023).

[38] Centers for Disease Control and Prevention. Prep effectiveness. `https://www.cdc.gov/hiv/basics/prep/prep-effectiveness.html`, 2022. (Accessed April 5, 2023).

[39] Centers for Disease Control and Prevention. Statistics Overview. `https://www.cdc.gov/hiv/statistics/overview/index.html`, 2022. (Accessed April 5, 2023).

[40] Centers for Disease Control and Prevention. Basic statistics. `https://www.cdc.gov/hiv/statistics.html`, 2023. (Accessed January 15, 2023).

[41] Centers for Disease Control and Prevention. HIV and African American People. `https://www.cdc.gov/hiv/group/racialethnic/africanamericans/index`, 2023. (Accessed April 5, 2023).

[42] Centers for Disease Control and Prevention. HIV and African Americans: HIV Diagnoses. `https://www.cdc.gov/hiv/group/racialethnic/africanamericans/diagnoses.html`, 2023. (Accessed April 5, 2023).

[43] Centers for Disease Control and Prevention. HIV declines among young people. `https://www.cdc.gov/media/releases/2023/p0523-hiv-declines-among-young-people.html`, 2023. (Accessed June 6, 2023).

[44] Centers for Disease Control and Prevention. Pre-exposure prophylaxis (prep). `https://www.cdc.gov/hiv/risk/prep/index.html`, 2023. (Accessed Feb 27, 2023).

[45] Centers for Disease Control and Prevention. PrEP for HIV Prevention in the U.S. `https://www.cdc.gov/nchhstp/newsroom/fact-sheets/hiv/PrEP-for-hiv-prevention-in-the-US-factsheet.html`, 2023. (Accessed Feb 27, 2023).

[46] Centers for Disease Control and Prevention. "HIV Basic Statistics". `https://www.cdc.gov/hiv/statistics/overview/index.html.`, 2023. (Accessed January 15, 2023).

[47] L. Chen, J. Yang, R. Zhang, Y. Xu, J. Zheng, J. Jiang, J. Jiang, L. He, N. Wang, P. C. Yeung, et al. Rates and risk factors associated with the progression of HIV to AIDS among HIV patients from Zhejiang, China between 2008 and 2012. *AIDS Research and Therapy*, 12(1):1–8, 2015.

[48] M. Clinic. HIV/AIDS Overview and Symptoms, 2022. (Accessed Feb 25, 2023).

[49] D. Hamby. A review of techniques for parameter Sensitivity Analysis of Environmental Models. *Environmental Monitoring and Assessment*, 32(2):135–154, 1994.

[50] O. Diekmann and J. A. P. Heesterbeek. *Mathematical Epidemiology of Infectious Diseases: Model Building, Analysis and Interpretation*, volume 5. John Wiley & Sons, 2000.

[51] J. S. Eggleton and S. Nagalli. Highly Active Antiretroviral Therapy (HAART). *StatPearls [Internet]*, 2020.

[52] R. W. Eisinger, C. W. Dieffenbach, and A. S. Fauci. HIV viral load and transmissibility of HIV infection: undetectable equals untransmittable. *JAMA*, 321(5):451–452, 2019.

[53] L. Esteva, A. B. Gumel, and C. V. De LeóN. Qualitative study of transmission dynamics of drug-resistant Malaria. *Mathematical and Computer Modelling*, 50(3-4):611–630, 2009.

[54] L. Esteva and C. Vargas. Influence of vertical and mechanical transmission on the dynamics of Dengue Disease. *Mathematical Biosciences*, 167(1):51–64, 2000.

[55] Food and Drug Administration. FDA approves second drug to prevent HIV infection as part of ongoing efforts to end the HIV epidemic. `https://www.fda.gov/news-events/press-announcements/fda-approves-second-drug-prevent-hiv-infection-part-ongoing-efforts-end-hiv-epidemic`, 2019. (Accessed April 5, 2023).

[56] C. for Disease Control (CDC et al. First 100,000 cases of Acquired Immunodeficiency Syndrome–United States. *MMWR. Morbidity and mortality weekly report*, 38(32):561–563, 1989.

[57] K. F. Foundation. Black Americans and HIV/AIDS the basics. `https://www.KFF.org/hivaids/fact-sheet/black-americansandhivaidsthebasics`, 2020. (Accessed April 5, 2023).

[58] GileadHIV.com. History of the HIV Epidemic Progress through Innovation and Activism. `https://www.gileadhiv.com/landscape/history-of-hiv/`, 2023. (Accessed April 5, 2023).

[59] R. M. Granich, C. F. Gilks, C. Dye, K. M. De Cock, and B. G. Williams. Universal voluntary HIV testing with immediate antiretroviral therapy as a strategy for elimination of HIV transmission: a mathematical model. *The Lancet*, 373(9657):48–57, 2009.

[60] J. A. Grey, K. T. Bernstein, P. S. Sullivan, D. W. Purcell, H. W. Chesson, T. L. Gift, and E. S. Rosenberg. Estimating the population sizes of men who have sex with men in U.S. states and counties using data from the American Community Survey. *JMIR Public Health and Surveillance*, 2(1):e5365, 2016.

[61] I. S. S. Group. Initiation of antiretroviral therapy in early asymptomatic HIV infection. *New England Journal of Medicine*, 373(9):795–807, 2015.

[62] A. Gumel, C. C. McCluskey, and P. van den Driessche. Mathematical study of a staged-progression HIV model with imperfect vaccine. *Bulletin of Mathematical Biology*, 68(8):2105–2128, 2006.

[63] A. B. Gumel. Causes of backward bifurcations in some epidemiological models. *Journal of Mathematical Analysis and Applications*, 395(1):355–365, 2012.

[64] A. B. Gumel, E. A. Iboi, C. N. Ngonghala, and E. H. Elbasha. A Primer on using mathematics to understand COVID-19 Dynamics: Modeling, analysis and simulations. *Infectious Disease Modelling*, 6:148–168, 2021.

[65] A. B. Gumel, E. A. Iboi, C. N. Ngonghala, and G. A. Ngwa. Toward achieving a vaccine-derived herd immunity threshold for covid-19 in the U.S. *Frontiers in Public Health*, 9:709369, 2021.

[66] A. B. Gumel, C. C. McCluskey, and P. van den Driessche. Mathematical study of a staged-progression HIV model with imperfect vaccine. *Bulletin of Mathematical Biology*, 68:2105–2128, 2006.

[67] H. Guo and M. Y. Li. Global dynamics of a staged-progression model for HIV/AIDS with amelioration. *Nonlinear Analysis: Real World Applications*, 12(5):2529–2540, 2011.

[68] J. Hale. *Ordinary Differential Equations*. John Wiley and Sons, New York, 1969.

[69] E. A. Hernandez-Vargas and R. H. Middleton. Modeling the three stages in HIV infection. *Journal of Theoretical Biology*, 320:33–40, 2013.

[70] H. W. Hethcote. The mathematics of infectious diseases. *SIAM review*, 42(4):599–653, 2000.

[71] H. W. Hethcote and H. R. Thieme. Stability of the endemic equilibrium in epidemic models with subpopulations. *Mathematical Biosciences*, 75(2):205–227, 1985.

[72] History.com. History Silence Crisis Timeline. `https://www.History.com/topics/1980s/hiv-aids-crisis-timeline`, 2023. (Accessed April 5, 2023).

[73] J. E. Hood, S. E. Buskin, J. C. Dombrowski, D. A. Kern, E. A. Barash, D. A. Katzi, and M. R. Golden. Dramatic increase in Preexposure Prophylaxis use among MSM in Washington State. *AIDS*, 30(3):515–519, 2016.

[74] J. M. Hyman, J. Li, and E. A. Stanley. The differential infectivity and staged progression models for the transmission of HIV. *Mathematical Biosciences*, 155(2):77–109, 1999.

[75] T. Kelesidis and R. J. Landovitz. Preexposure Prophylaxis for HIV Prevention. *Current HIV/AIDS Reports*, 8(2):94–103, 2011.

[76] S. B. Kim, M. Yoon, N. S. Ku, M. H. Kim, J. E. Song, J. Y. Ahn, S. J. Jeong, C. Kim, H.-D. Kwon, J. Lee, et al. Mathematical modeling of HIV prevention measures including pre-exposure prophylaxis on HIV incidence in South Korea. *PloS one*, 9(3):e90080, 2014.

[77] J. P. La Salle. *The Stability of Dynamical Systems*. SIAM, 1976.

[78] V. Lakshmikantham and S. Leela. *Differential and Integral inequalities: Theory and Applications: volume I: Ordinary Differential Equations.* Academic press, 1969.

[79] S. Marino, I. B. Hogue, C. J. Ray, and D. E. Kirschner. A methodology for performing Global Uncertainty and Sensitivity Analysis in Systems Biology. *Journal of Theoretical Biology*, 254(1):178–196, 2008.

[80] N. C. McCann, T. H. Horn, E. P. Hyle, and R. P. Walensky. HIV Antiretroviral therapy costs in the United States, 2012-2018. *JAMA Internal Medicine*, 180(4):601–603, 2020.

[81] R. G. McLeod, J. F. Brewster, A. B. Gumel, and D. A. Slonowsky. Sensitivity and uncertainty analyses for a SARS model with time-varying inputs and outputs. *Mathematical Biosciences and Engineering*, 3(3):527–544, 2006.

[82] D. Y. Melesse and A. B. Gumel. Global asymptotic properties of an SEIRS model with multiple infectious stages. *Journal of Mathematical Analysis and Applications*, 366(1):202–217, 2010.

[83] K. M. Mitchell, H. J. Prudden, B. M. Ramesh, R. Washington, S. Isac, S. Rajaram, F. Terris-Prestholt, and P. Vickerman. Mathematical modelling of the impact of PrEP for female sex workers and men who have sex with men upon HIV incidence and survival in Southern India. *AIDS research and human retroviruses*, 30(S1):A161–A162, 2014.

[84] S. M. Moghadas, A. B. Gumel, R. G. McLeod, and R. Gordon. Could condoms stop the AIDS epidemic? *Journal of Theoretical Medicine*, 5(3-4):171–181, 2003.

[85] Z. Mukandavire, W. Garira, and J. Tchuenche. Modelling effects of public health educational campaigns on HIV/AIDS transmission dynamics. *Applied Mathematical Modelling*, 33(4):2084–2095, 2009.

[86] National Institute of Health. HIV and Women. `https://www.hivinfo.nih.gov/understanding-hiv/fact-sheets/hiv-and-women`, 2021. (Accessed April 5, 2023).

[87] National Institute of Health. HIV-Testing. `https://www.hivinfo.nih.gov/understanding-hiv/fact-sheets/hiv-testing`, 2021. (Accessed June 2, 2023).

[88] National Institute of Health. FDA approved HIV medicines. `https://www.https://hivinfo.nih.gov/understanding-hiv/fact-sheets/fda-approved-hiv-medicines`, 2022. (Accessed April 5, 2023).

[89] National Institute of Health. HIV Infection. `https://www.hivinfo.nih.gov/understanding-hiv/fact-sheets/stages-hiv-infection`, 2023. (Accessed April 5, 2023).

[90] National Institutes of Health. Nih announces restructured HIV clinical trials networks. https://www.nih.gov/news-events/news-releases/nih-announces-restructured-{HIV}-clinical-trials-networks, 2020. (Accessed April 5, 2023).

[91] C. N. Ngonghala, H. B. Taboe, S. Safdar, and A. B. Gumel. Unraveling the dynamics of the Omicron and Delta variants of the 2019 coronavirus in the presence of vaccination, mask usage, and antiviral treatment. *Applied Mathematical Modelling*, 114:447–465, 2023.

[92] NHS. HIV/AIDS prevention. https://www.nhs.uk/conditions/hiv-and-aids/prevention/, 2021. (Accessed Feb 25, 2023).

[93] M. U. Nsuami and P. J. Witbooi. A model of HIV/AIDS population dynamics including ARV treatment and pre-exposure prophylaxis. *Advances in Difference Equations*, 2018:1–12, 2018.

[94] E. Omondi, R. Mbogo, and L. Luboobi. Mathematical modelling of the impact of testing, treatment and control of HIV transmission in Kenya. *Cogent Mathematics & Statistics*, 5(1):1475590, 2018.

[95] E. Omondi, R. Mbogo, and L. Luboobi. A mathematical model of hiv transmission between commercial sex workers and injection drug users. *Research in Mathematics*, 9(1):2082044, 2022.

[96] Our World in Data. HIV/AIDS. https://ourworldindata.org/hiv-aids, 2019. (Accessed Feb 25, 2023).

[97] A. S. Perelson and P. W. Nelson. Mathematical analysis of HIV-1 dynamics in vivo. *SIAM Review*, 41(1):3–44, 1999.

[98] Pinterest. HIV Global Map. https://www.pinterest.com/pin/hiv, 2020. (Accessed April 5, 2023).

[99] M. A. Pitasi, K. P. Delaney, E. Oraka, H. Bradley, E. A. DiNenno, J. T. Brooks, and J. Prejean. Interval since last HIV test for men and women with recent risk for HIV infection—United States, 2006–2016. *Morbidity and Mortality Weekly Report*, 67(24):677, 2018.

[100] C. Podder, O. Sharomi, A. Gumel, and E. Strawbridge. Mathematical analysis of a model for assessing the impact of antiretroviral therapy, voluntary testing and condom use in curtailing the spread of HIV. *Differential Equations and Dynamical Systems*, 19(4):283–302, 2011.

[101] J. Poorolajal, E. Hooshmand, H. Mahjub, N. Esmailnasab, and E. Jenabi. Survival rate of AIDS disease and mortality in HIV-infected patients: a meta-analysis. *Public Health*, 139:3–12, 2016.

[102] R. Taylor. Interpretation of the correlation coefficient: a basic review. *J. Diagn. Med. Sonogr.*, 6(1):35–39, 1990.

[103] S. Safdar and A. B. Gumel. *Book chapter in "Mathematical Modelling from the Next Generation", Fields Institute for Research in the Mathematical Sciences seminar series. Jummy David and Jianhong Wu, editors. (To appear).* Springer, 2023.

[104] S. Safdar, C. N. Ngonghala, and A. B. Gumel. Mathematical assessment of the role of waning and boosting immunity against the BA. 1 Omicron variant in the United States. *Mathematical Biosciences and Engineering*, 20(1):179–212, 2023.

[105] M. A. Safi and A. B. Gumel. Global asymptotic dynamics of a model for quarantine and isolation. *Discrete & Continuous Dynamical Systems-B*, 14(1):209, 2010.

[106] O. Sharomi, C. Podder, A. Gumel, S. Mahmud, and E. Rubinstein. Modelling the transmission dynamics and control of the novel 2009 swine influenza (H1N1) pandemic. *Bulletin of Mathematical Biology*, 73:515–548, 2011.

[107] L. Simpson and A. B. Gumel. Mathematical assessment of the role of Pre-Exposure Prophylaxis on HIV transmission dynamics. *Applied Mathematics and Computation*, 293:168–193, 2017.

[108] H. L. Smith and P. Waltman. *The theory of the Chemostat: Dynamics of Microbial Competition*, volume 13. Cambridge University Press, 1995.

[109] STDcenterNY. Everything you need to know about preventing HIV with PrEP. `https://www.stdcenterny.com/articles/hiv-prep-mediation-practical-guide.html`, 2022. (Accessed April 5, 2023).

[110] H. R. Thieme. Local stability in epidemic models for heterogeneous populations. In *Mathematics in Biology and Medicine*, pages 185–189. Springer, 1985.

[111] A. Tripathi, R. Naresh, and D. Sharma. Modeling the effect of screening of unaware infectives on the spread of HIV infection. *Applied Mathematics and Computation*, 184(2):1053–1068, 2007.

[112] A. Tseng, J. Seet, and E. J. Phillips. The evolution of three decades of antiretroviral therapy: challenges, triumphs and the promise of the future. *British Journal of Clinical Pharmacology*, 79(2):182–194, 2015.

[113] UNAIDS. UNAIDS Fact-Sheet. `https://www.unaids.org/en/resources/fact-sheet`, 2023. (Accessed April 5, 2023).

[114] U.S. Department of Health & Human Services. Clinical Overview of HIV Disease. `https://www.fda.gov/news-events/fda-brief/fda-brief-fda-continues-encourageongoing-education-about-benefits-and-risks-associated-{PrEP}`, 2009. (Accessed April 5, 2023).

[115] U.S. Department of Health & Human Services. HHS Agencies Involved in Ending the HIV Epidemic. `https://www.hiv.gov/federal-response/ending-the-hiv-epidemic/federalaction/agencies`, 2020. (Accessed April 5, 2023).

[116] U.S. Department of Health & Human Services. What is HIV? `https://www.hiv.gov/hiv-basics/overview/about-hiv-and-aids/what-are-hiv-and-aids`, 2020. (Accessed April 5, 2023).

[117] U.S. Department of Health & Human Services. About ending the HIV epidemic: Plan for America. `https://www.hiv.gov/federal-response/ending-the-hiv-epidemic/overview`, 2021. (Accessed April 5, 2023).

[118] U.S. Department of Health & Human Services. Budget. `https://www.hiv.gov/federal-response/national-hiv-aids-strategy/national-hivaids-strategies-2010-2021`, 2021. (Accessed April 5, 2023).

[119] U.S. Department of Health & Human Services. Data and Trends. `https://www.hiv.gov/hiv-basics/overview/data-and-trends/statistics`, 2021. (Accessed April 5, 2023).

[120] U.S. Department of Health & Human Services. HIV Care Continuum. `https://www.hiv.gov/federal-response/policies-issues/hiv-aids-carecontinuum`, 2021. (Accessed April 5, 2023).

[121] U.S. Department of Health & Human Services. Pre-exposure Prophylaxis. `https://www.hivinfo.hiv.gov/understanding-hiv/fact-sheets/pre-exposure-prophylaxis-prep`, 2021. (Accessed November 25, 2022).

[122] U.S. Department of Health & Human Services. U.S. Statistics: Fast facts. `https://www.hiv.gov/hiv-basics/overview/data-and-trends/statistics`, 2021. (Accessed April 5, 2023).

[123] U.S. Department of Health & Human Services. Global statistics. `https://www.hiv.gov/hiv-basics/overview/data-and-trends/global-statistics`, 2022. (Accessed November 25, 2022).

[124] U.S. Department of Health & Human Services. Pre-Exposure Prophylaxis. `https://www.hiv.gov/hiv-basics/hiv-prevention/using-hiv-medication-to-reducerisk/pre-exposure-prophylaxis`, 2022. (Accessed April 5, 2023).

[125] U.S. Department of Health & Human Services. Pre-exposure Prophylaxis. `https://www.hiv.gov/hiv-basics/hiv-prevention/using-hiv-medication-to-reduce-risk/pre-exposure-prophylaxis`, 2022.

[126] U.S. Department of Health & Human Services. The Affordable Care Act and HIV/AIDS. `https://www.hiv.gov/federal-response/policies-issues/the-affordable-care-actand-HIV-AIDS`, 2022. (Accessed April 5, 2023).

[127] U.S. Department of Health & Human Services. Impact on Racial and Ethnic Minorities. `https://www.hiv.gov/hiv-basics/overview/data-and-trends/impact-on-racial-and-ethnic-minorities`, 2023. (Accessed April 5, 2023).

[128] U.S. Food and Drug Administration. FDA in brief: FDA continues to encourage ongoing education about the benefits and risks associated with PrEP, including additional steps to help reduce the risk of getting HIV. `https://www.fda.gov/news-events/fda-brief/fda-brief-fda-continues-encourageongoing-education-about-benefits-and-risks-associated-prep`, 2019. (Accessed Feb 09, 2023).

[129] U.S. Food and Drug Administration. FDA approves first injectable treatment for [HIV pre-exposure Prevention. `https://www.fda.gov/news-events/press-announcements/fda-approves-first-injectable-treatment-hiv-pre-exposure-prevention`, 2021. (Accessed Feb 09, 2023).

[130] U.S. Food and Drug Administration. The History of FDA's role in preventing the spread of HIV/AIDS. `https://www.fda.gov/about-fda/fda-history-exhibits/history-fdas-role-preventing-spread-hivaids`, 2023. (Accessed Feb 27, 2023).

[131] P. van den Driessche and J. Watmough. Reproduction numbers and sub-threshold endemic equilibria for compartmental models of disease transmission. *Mathematical Biosciences*, 180(1-2):29–48, 2002.

[132] WebMED. New HIV Treatments in Development. `https://www.webmed.com/hiv-aids/new-hiv-treatments-development`, 2023. (Accessed April 5, 2023).

[133] World Health Organization. The Global Health Observatory. `https://www.who.int/data/gho/data/themes/hiv-aids`, 2022. (Accessed Feb 25, 2023).

[134] World Health Organization. Global HIV, Hepatitis and STIs programmes. `https://www.who.int/teams/global-hiv-hepatitis-and-stis-programmes/populations/men-who-have-sex-with-men`, 2023. (Accessed March 4, 2023).

[135] World Health Organization. Hiv. `https://www.who.int/data/gho/data/themes/hiv-aids`, 2023. (Accessed April 5, 2023).

[136] T. T. Yusuf and F. Benyah. Optimal strategy for controlling the spread of HIV/AIDS disease: a case study of South Africa. *Journal of Biological Dynamics*, 6(2):475–494, 2012.

APPENDIX A

PROOF OF THEOREM 2.3.2

Proof. Consider the model (2.3) and let $\mathbb{R}_T < 1$. The proof is based on using a comparison theorem [78]. The equations for the infected compartments of the model (2.3) can be re-written in terms of the next generation matrices (F and V as defined in Equations (2.10) and (2.11), respectively) as below:

$$\frac{d}{dt} \begin{bmatrix} I_u(t) \\ I_d(t) \\ A_u(t) \\ A_d(t) \end{bmatrix} = (F - V) \begin{bmatrix} I_u(t) \\ I_d(t) \\ A_u(t) \\ A_d(t) \end{bmatrix} - M \begin{bmatrix} I_u(t) \\ I_d(t) \\ A_u(t) \\ A_d(t) \end{bmatrix}, \tag{A.1}$$

where,

$$M = \left(1 - \frac{S}{N}\right) \begin{bmatrix} f\beta & f\beta\eta_d & f\beta\eta_A & f\beta\eta_A\eta_d \\ (1-f)\beta & (1-f)\beta\eta_d & (1-f)\beta\eta_A & (1-f)\beta\eta_A\eta_d \\ 0 & 0 & 0 & 0 \\ 0 & 0 & 0 & 0 \end{bmatrix}. \tag{A.2}$$

Since $S(t) \leq N(t)$ for all $t > 0$ in Ω, it follows that the matrix M, defined in Equation (A.2), is non-negative. Hence, the Equation (A.1) can be re-written in terms of the following inequality:

$$\frac{d}{dt} \begin{bmatrix} I_u(t) \\ I_d(t) \\ A_u(t) \\ A_d(t) \end{bmatrix} \leq (F - V) \begin{bmatrix} I_u(t) \\ I_d(t) \\ A_u(t) \\ A_d(t) \end{bmatrix}. \tag{A.3}$$

It should be recalled from the local asymptotic stable result for the disease-free equilibrium (given in Theorem 2.3.1) that all eigenvalues of the next generation matrix FV^{-1} are negative if $\mathbb{R}_T < 1$, which implies that $F - V$ is a stable matrix. Thus, it can be concluded that the linearized differential inequality system (A.3) is stable whenever the spectral radius of FV^{-1} is less than unity (i.e., $\rho(FV^{-1}) < 1$). Hence, it follows that (for the linear system of ordinary differential equations (A.3)):

$$(I_u(t), I_d(t), A_u(t), A_d(t)) \to (0, 0, 0, 0), \text{ as } t \to \infty.$$

Substituting $I_u(t) = I_d(t) = A_u(t) = A_d(t) = 0$ into the differential equations for the rate of change of the $S(t)$ and $T(t)$ compartments of the model (2.3) shows that:

$$T(t) \to 0 \text{ and } S(t) \to S^* \text{ as } t \to \infty.$$

Thus, the DFE $(\mathcal{E}_0)$ of the model (2.3), is globally-asymptotically stable in Ω whenever $\mathbb{R}_T < 1$. $\qquad\square$

APPENDIX B

PROOF OF THEOREM 2.3.4

Proof. Consider the special case of the model (2.3) with $\delta_I = \delta_A = 0$. As in Section 2.3.2, setting $\delta_I = \delta_A = 0$ in the model (2.3) shows that $N(t) \to N^{**} = \Pi/\mu$, as $t \to \infty$. As shown in Theorem 2.3.3, this special case of the model has a unique endemic equilibrium whenever $\tilde{\mathbb{R}}_T > 1$. The Krasnoselskii sub-linearity trick [71] (see also [110, 54, 53, 105, 82]) will be used to prove Theorem 2.3.4. To implement this method, it is convenient to first replace $S(t)$ in the model by the following relation:

$$S(t) = N^{**} - [I_u(t) + I_d(t) + A_u(t) + A_d(t) + T(t)]. \tag{B.1}$$

Using the relation (B.1) in the model (2.3) gives the following equivalent model (for the special case with $\delta_I = \delta_A = 0$):

$$
\begin{aligned}
\frac{dI_u}{dt} &= f\lambda^{**}(N^{**} - I_u - I_d - A_u - A_d - T) - (\psi_u + \sigma_u + \mu)I_u, \\
\frac{dI_d}{dt} &= (1-f)\lambda^{**}S + \psi_u I_u - (\sigma_d + \tau_d + \mu)I_d, \\
\frac{dA_u}{dt} &= \sigma_u I_u - (\psi_u + \mu)A_u, \\
\frac{dA_d}{dt} &= \sigma_d I_d + \psi_u A_u - (\tau_d + \mu)A_d, \\
\frac{dT}{dt} &= \tau_d(I_d + A_d) - \mu T,
\end{aligned}
\tag{B.2}
$$

where λ^{**} (the force of infection of the unique endemic equilibrium for this special case of the model) is given by:

$$\lambda^{**} = \frac{\beta \left[I_u + \eta_d I_d + \eta_A (A_u + \eta_d A_d)\right]}{N^{**}}. \tag{B.3}$$

The unique endemic equilibrium associated with the reduced system (B.2) now has the form:

$$\tilde{E} = (I_u^{**}, I_d^{**}, A_u^{**}, A_d^{**}, T^{**})$$

Linearizing the system (B.2) around the unique endemic equilibrium, gives [71, 110,

54, 53, 105, 82]:

$$
\begin{cases}
\dfrac{dI_u}{dt} = (f\alpha - \hat{K}_1)I_u + f\beta I_d + f\gamma A_u + f\theta A_d - fa_1 T, \\[2mm]
\dfrac{dI_d}{dt} = \left[(1-f)\alpha + \psi_u\right]I_u + \left[(1-f)\beta - \hat{K}_2\right]I_d + \left[(1-f)\gamma\right]A_u \\[1mm]
\qquad\quad + \left[(1-f)\theta\right]A_d - fa_1 T, \\[2mm]
\dfrac{dA_u}{dt} = \sigma_u I_u - \hat{K}_3 A_u, \\[2mm]
\dfrac{dA_d}{dt} = \sigma_d I_d + \psi_u A_u - \hat{K}_4 A_d, \\[2mm]
\dfrac{dT}{dt} = \tau_d(I_d + A_d) - \mu T,
\end{cases}
\tag{B.4}
$$

where, $\alpha = a_2 - a_1$, $\beta = \eta_d a_2 - a_1$, $\gamma = \eta_A a_2 - a_1$, $\theta = \eta_A \eta_d a_2 - a_1$,
$$a_1 = \frac{\beta\left[I_u + \eta_d I_d + \eta_A(A_u + \eta_d A_d)\right]}{N^{**}}, a_2 = \frac{\beta S^{**}}{N^{**}},$$
with, $\hat{K}_1 = \psi_u + \sigma_u + \mu$, $\hat{K}_2 = \sigma_d + \tau_d + \mu$, $\hat{K}_3 = \psi_u + \mu$, and $\hat{K}_4 = \tau_d + \mu$.

Furthermore, the Jacobian of the linearized system (B.4), evaluated at $\tilde{E}$, is given by:

$$
J(\tilde{E}) =
\begin{bmatrix}
f\alpha - \hat{K}_1 & f\beta & f\gamma & f\theta & -fa_1 \\[2mm]
(1-f)\alpha + \psi_u & (1-f)\beta - \hat{K}_2 & (1-f)\gamma & (1-f)\theta & -fa_1 \\[2mm]
\sigma_u & 0 & -\hat{K}_3 & 0 & 0 \\[2mm]
0 & \sigma_d & \psi_u & -\hat{K}_4 & 0 \\[2mm]
0 & \tau_d & 0 & \tau_d & -\mu
\end{bmatrix}
$$

Suppose the system (B.4) has a solution of the form [71, 110, 54, 53, 105, 82]:

$$
\mathbf{Z}(t) = \mathbf{Z}_0 e^{\omega t}, \tag{B.5}
$$

with $\mathbf{Z}_0 \in \mathbb{C} - \{0\}$, where $\mathbf{Z}_0 = (Z_1, Z_2, Z_3, Z_4, Z_5), \omega, Z_i \in \mathbb{C}$ (for $i = 1, 2, ..., 5$) and $\mathbb{C}$ denotes the complex numbers. Substituting the solution of the form (B.5) into the

linearized system (B.4) gives [71, 110, 54, 53, 105, 82]:

$$\begin{cases} \omega Z_1 &= (f\alpha - \hat{K}_1)Z_1 + f\beta Z_2 + f\gamma Z_3 + f\theta Z_4 - fa_1 Z_5, \\[2mm] \omega Z_2 &= \left[(1-f)\alpha + \psi_u\right] Z_1 + \left[(1-f)\beta - \hat{K}_2\right] Z_2 + \left[(1-f)\gamma\right] Z_3 + \left[(1-f)\theta\right] Z_4 \\[1mm] & \quad - \ fa_1 Z_5, \\[2mm] \omega Z_3 &= \sigma_u Z_1 - \hat{K}_3 Z_3, \\[2mm] \omega Z_4 &= \sigma_d Z_2 - \hat{K}_4 Z_4 + \psi_u Z_3, \\[2mm] \omega Z_5 &= \tau_d Z_2 + \tau_d Z_4 - \mu Z_5. \end{cases}$$

(B.6)

The system (B.6) can be simplified by moving all the negative terms in the last five equations of (B.6) to the respective left-hand sides [71, 110, 54, 53, 105, 82]. Additionally, the last three equations are then re-written in terms of Z_1 and substituted into the first two equations of (B.6), and all its negative terms are moved to the left-hand side as well. Finally, adding the first and second equations of (B.6), and moving all the negative terms to the left-hand side, leads to the following system [71, 110, 54, 53, 105, 82]:

$$[1 + F_3(\omega)] Z_3 = (MZ)_3,$$
$$[1 + F_4(\omega)] Z_4 = (MZ)_4,$$
$$[1 + F_5(\omega)] Z_5 = (MZ)_5.$$
$$[1 + F_1(\omega)]Z_1 + [1 + F_2(\omega)]Z_2 = (MZ)_1 + (MZ)_2,$$

(B.7)

where,

$$F_1(\omega) = \frac{\omega}{\hat{K}_1} + \frac{fa_1}{\hat{K}_1} + \frac{fa_1\sigma_u}{\hat{K}_1(\omega + \hat{K}_3)} + \frac{fa_1\psi_u\sigma_u}{\hat{K}_1(\omega + \hat{K}_3)(\omega + \hat{K}_4)}$$
$$+ \frac{fa_1\psi_u\sigma_u\tau_d}{\hat{K}_1(\omega + \mu)(\omega + \hat{K}_3)(\omega + \hat{K}_4)} + \frac{fa_2}{\hat{K}_1} + \frac{a_1}{\hat{K}_1} + \frac{(f\eta_A a_2 + a_1)\sigma_u}{\hat{K}_1(\omega + \hat{K}_3)}$$
$$+ \frac{(f\eta_A\eta_d a_2 + a_1)\sigma_u\psi_u}{\hat{K}_1(\omega + \hat{K}_3)(\omega + \hat{K}_4)} + \frac{fa_1\tau_d\psi_u\sigma_u}{\hat{K}_1(\omega + \mu)(\omega + \hat{K}_3)(\omega + \hat{K}_4)},$$

$$F_2(\omega) = \frac{\omega}{\hat{K}_2} + \frac{fa_1}{\hat{K}_2} + \frac{fa_1\sigma_d}{\hat{K}_2(\omega + \hat{K}_4)} + \frac{fa_1\tau_d}{\hat{K}_2(\omega + \mu)} + \frac{fa_1\tau_d\sigma_d}{\hat{K}_2(\omega + \mu)(\omega + \hat{K}_4)}$$
$$+ \frac{f\eta_d a_2}{\hat{K}_2} + \frac{a_1}{\hat{K}_2} + \frac{(a_1 + f\eta_A\eta_d a_2)\sigma_d}{\hat{K}_2(\omega + \hat{K}_4)} + \frac{fa_1\tau_d}{\hat{K}_2(\omega + \mu)} + \frac{fa_1\tau_d\sigma_d}{\hat{K}_2(\omega + \mu)(\omega + \hat{K}_4)},$$

$$F_3(\omega) = \frac{\omega}{\hat{K}_3}, \quad F_4(\omega) = \frac{\omega}{\hat{K}_4}, \quad F_5(\omega) = \frac{\omega}{\mu}.$$

with,

$$M = \begin{bmatrix} \dfrac{fa_2}{\hat{K}_1} & \dfrac{f\eta_d a_2}{\hat{K}_1} & \dfrac{f\eta_A a_2}{\hat{K}_1} & \dfrac{f\eta_A\eta_d a_2}{\hat{K}_1} & 0 \\[2ex] \dfrac{(1-f)a_2 + \psi_u}{\hat{K}_2} & \dfrac{(1-f)\eta_d a_2}{\hat{K}_2} & \dfrac{(1-f)\eta_A a_2}{\hat{K}_2} & \dfrac{(1-f)\eta_A\eta_d a_2}{\hat{K}_2} & 0 \\[2ex] \dfrac{\sigma_u}{\hat{K}_3} & 0 & 0 & 0 & 0 \\[2ex] 0 & \dfrac{\sigma_d}{\hat{K}_4} & \dfrac{\psi_u}{\hat{K}_4} & 0 & 0 \\[2ex] 0 & \dfrac{\tau_d}{\mu} & 0 & \dfrac{\tau_d}{\mu} & 0 \end{bmatrix}.$$

It can be verified that the associated endemic equilibrium point represented as, $\tilde{E} = (I_u^{**}, I_d^{**}, A_u^{**}, A_d^{**}, T^{**})$, satisfies $\tilde{E} = M\tilde{E}$ [71, 110, 54, 53, 105, 82]. The notation $(M\mathbf{Z})_i$, $(i = 1, 2, ..., 5)$ denotes the ith coordinate of the vector $M\mathbf{Z}$, and the matrix M has non-negative entries [71, 110, 105]. If $\mathbf{Z}$ is a solution of (B.7), then it is possible to find a minimal positive real number r such that [71, 110, 54, 53, 105, 82]

$$\|\mathbf{Z}\| = r\tilde{E} \tag{B.8}$$

106

where, $\|\mathbf{Z}\| = (\|Z_1\|, \|Z_2\|, \|Z_3\|, \|Z_4\|, \|Z_5\|)$ with lexicographic order, and $\|.\|$ is a norm in $\mathbb{C}$. The main goal is to show that $Re(\omega) < 0$. This will be proved by contradiction [71, 110, 54, 53, 105, 82]. Suppose, now, that $Re(\omega) \geq 0$ and consider the following cases.

Case 1: $\omega = 0$.

For this case, (B.6) is a homogeneous linear system in the variables Z_i with $(i = 1, ..., 5)$, and the determinant of this homogeneous linear system is given by:

$$\Delta = \left[(\mu c_1 c_2 c_3 c_4) \left(\frac{S^{**}(\tilde{\mathbb{R}}_T)}{N^{**}} - 1 \right) \right] - A_2 \tag{B.9}$$

where,

$$A_2 = f(1 - 2f)\{a_1^2(\hat{K}_4 + \sigma_d)(\hat{K}_3 + \sigma_u)\tau_d\} + a_1[\hat{K}_1\hat{K}_3(\hat{K}_4 + \sigma_d)\{(1 - f)\mu + f\tau_d\}$$

$$+ f\{\hat{K}_3(\hat{K}_4 + \sigma_d)(\mu + \tau_d)\psi_u\} + (2f - 1)a_2\tau_d\{(\hat{K}_4 + \sigma_d)(\hat{K}_3 + \eta_a\sigma_u)$$

$$+ (\eta_A - 1)\eta_d\sigma_u\psi_u\}\{\hat{K}_2(\mu\hat{K}_4(\hat{K}_3 + \sigma_u) + \sigma_u(\mu + \tau_d)\psi_u\}].$$

To finally determine the sign of Δ, the sign of $\left(\dfrac{S^{**}(\tilde{\mathbb{R}}_T)}{N^{**}} - 1 \right)$ must be obtained. This is done below. Solving the expressions for $\dfrac{N^{**}}{S^{**}}$ at the unique endemic steady-state $\tilde{E}_1$ gives:

$$\frac{N^{**}}{S^{**}} = \frac{S^{**} + I_u^{**} + I_d^{**} + A_u^{**} + A_d^{**} + T^{**}}{S^{**}}. \tag{B.10}$$

Substituting the expressions for $S^{**}, I_u^{**}, I_d^{**}, A_u^{**}, A_d^{**}$ and T^{**} from (2.16), and after some algebraic manipulations, gives:

$$\frac{S^{**}}{N^{**}} = \frac{1}{\tilde{\mathbb{R}}_T}, \tag{B.11}$$

so that $\dfrac{S^{**}}{N^{**}} - \dfrac{1}{\tilde{\mathbb{R}}_T} = 0$. Thus, equation (B.9) becomes

$$\Delta = -A_2 < 0.$$

107

Since the determinant (Δ) is negative, it follows that the system (B.6) has a unique solution, given by $\mathbf{Z} = 0$ (which corresponds to the DFE (E_0)).

Case 2: $\omega \neq 0$.

By assumption, we have that $Re(\omega) > 0$. Then, the remaining task is to show that the system has no non-trivial solution when $Re(\omega) > 0$. Clearly, we have that $F_i(\omega) > 0 \ \forall i = 1, 2, ..., 5$, which implies that $|F_i(\omega) + 1| > 1$. We then define $F(\omega) = min(|F_i(\omega) + 1|) \ \forall i = 1, 2, ..., 5$. Then, $1 < F(\omega)$ and hence $\dfrac{r}{F(\omega)} < r$. Since r is a minimal positive real number such that $\|\mathbf{Z}\| \leq r\tilde{E}$ [71, 110, 54, 53, 105, 82]. This implies that:

$$\|\mathbf{Z}\| > \frac{r}{F(\omega)}\tilde{E}. \tag{B.12}$$

On the other hand, by taking the norm of both sides of the third equation in (B.6), and noting that M is a non-negative matrix [71, 110, 54, 53, 105, 82], we have:

$$F(\omega)\|Z_1\| \leq |1 + F_1(\omega)|\|Z_1\| = \|(MZ)_1\| \leq M\|Z_1\| \leq rM(\tilde{E})_1 = r(\tilde{E})_1 = rI_u^{**}$$
$$\tag{B.13}$$

It follows from (B.13) that $\|Z_1\| \leq \dfrac{r}{F(\omega)}I_u^{**}$, which contradicts (B.12). Hence, $Re(\omega) < 0$. Thus, all eigenvalues of the characteristic equation associated with the linearized system (B.4) will have negative real part, so that the unique endemic equilibrium, $\tilde{E}$, is LAS whenever $\tilde{\mathbb{R}}_T > 1$. This completes the proof. $\qquad\square$

APPENDIX C

PROOF OF THEOREM 2.3.6

Proof. Let $\mathcal{E}_{1r} = (S^{***}, I_u^{***}, I_d^{***}, A_u^{***}, A_d^{***}, T^{***})$ represents the unique endemic equilibrium of the reduced model (2.20). Let $\hat{\mathbb{R}}_T > 1$, so that the associated unique (positive) endemic equilibrium exists. Further, consider the following candidate non-linear Lyapunov function of the Goh-Volterra type:

$$
\begin{aligned}
\mathcal{L} &= \mathcal{L}(S, I_u, I_d, A_u, A_d, T) \\
&= a_1 \left(S - S^{***} \ln S\right) + a_2 \left(I_u - I_u^{***} \ln I_u\right) + a_3 \left(I_d - I_d^{***} \ln I_d\right) \\
&+ a_4 \left(A_u - A_u^{***} \ln A_d\right) + a_5 \left(A_d - A_d^{***} \ln A_d\right) + a_6 \left(T - T^{***} \ln T\right),
\end{aligned}
$$

where the coefficients a_i (with $i = 1, \cdots, 6$) are non-negative real numbers to be determined. The derivative of the candidate Lyapunov function, is given by:

$$
\begin{aligned}
\frac{d\mathcal{L}}{dt} &= a_1 \frac{dS}{dt}\left(1 - \frac{S^{***}}{S}\right) + a_2 \frac{dI_u}{dt}\left(1 - \frac{I_u^{***}}{I_u}\right) + a_3 \frac{dI_d}{dt}\left(1 - \frac{I_d^{***}}{I_d}\right) \\
&+ a_4 \frac{dA_u}{dt}\left(1 - \frac{A_u^{***}}{A_u}\right) + a_5 \frac{dA_d}{dt}\left(1 - \frac{A_d^{***}}{A_d}\right) + a_6 \frac{dT}{dt}\left(1 - \frac{T^{***}}{T}\right),
\end{aligned}
$$

which becomes

$$
\begin{aligned}
\frac{d\mathcal{L}}{dt} &= a_1 \left(1 - \frac{S^{***}}{S}\right)\left[\Pi - (\lambda + \mu)S\right] + a_2 \left(1 - \frac{I_u^{***}}{I_u}\right)(\lambda S - K_5 I_u) \\
\\
&+ a_3 \left(1 - \frac{I_d^{***}}{I_d}\right)\left[\psi_u I_u - K_6 I_d\right] \\
\\
&+ a_4 \left(1 - \frac{A_u^{***}}{A_u}\right)(\sigma_u I_u - K_7 A_u) + a_5 \left(1 - \frac{A_d^{***}}{A_d}\right)(\sigma_d I_d + \psi_u A_u - K_8 A_d) \\
\\
&+ a_6 \left(1 - \frac{T^{***}}{T}\right)\left[\tau_d(I_d + A_d) - \mu T\right],
\end{aligned}
$$

(C.1)

The following relations hold for the limiting model (2.20) at the unique endemic

equilibrium ($\mathcal{E}_{1r}$):

$$\Pi \quad = \quad (\lambda^{***} + \mu)\, S^{***},\ \lambda^{***} S^{***} = k_5 I_u^{***},\ \psi_u I_u^{***} = K_6 I_d^{***}$$

$$\sigma_u I_u^{***} \quad = \quad K_7 A_u^{***},\ \sigma_d I_d^{***} + \psi_u A_u^{***} = K_8 A_d^{***},\ \text{and}\ \ \tau_d\left(I_d^{***} + A_d^{***}\right) = \mu T^{***}, \tag{C.2}$$

where,

$$\lambda^{***} = (\mu\beta)\left[\frac{I_u^{***} + \eta_d I_d^{***}}{\Pi}\right]. \tag{C.3}$$

Substituting the expressions in Eq (C.2), with Eq (C.3), into Eq (C.1), and simplifying, gives:

$$\begin{aligned}
\frac{d\mathcal{L}}{dt} &= a_1\left(1 - \frac{S^{***}}{S}\right)\left[(\lambda^{***} + \mu)S^{***} - (\lambda + \mu)S\right] \\
&+ a_2\left(1 - \frac{I_u^{***}}{I_u}\right)\left[\lambda S - \frac{\lambda^{***}S^{***}}{I_u^{***}}I_u\right] + a_3\left(1 - \frac{I_d^{***}}{I_d}\right)\left[\psi_u I_u - \left(\frac{\psi_u I^{***}}{I_d^{***}}\right)I_d\right] \\[2ex]
&+ a_4\left(1 - \frac{A_u^{***}}{A_u}\right)\left[\sigma_u I_u - \frac{\sigma_u I_u^{***}}{A_u^{***}}A_u\right] \\[2ex]
&+ a_5\left(1 - \frac{A_d^{***}}{A_d}\right)\left[\sigma_d I_d + \psi_u A_u - \left(\frac{\sigma_d I_d^{***} + \psi_u A_u^{***}}{A_d^{***}}\right)A_d\right] \\[2ex]
&+ a_6\left(1 - \frac{T^{***}}{T}\right)\left[\tau_d(I_d + A_d) - \frac{\tau_d(I_d^{***} + A_d^{***})}{T^{***}}T\right],
\end{aligned}$$

which simplifies to

$$\frac{d\mathcal{L}}{dt} = a_1\left(1 - \frac{S^{***}}{S}\right)\left[(\lambda^{***}S^{***} - \lambda S) - \mu(S - S^{***})\right]$$

$$+\ a_2\left(1 - \frac{I_u^{***}}{I_u}\right)\left[\lambda S - \frac{\lambda^{***}S^{***}}{I_u^{***}}I_u\right] + a_3\left(1 - \frac{I_d^{***}}{I_d}\right)\left[\psi_u\left(I_u - \frac{I_u^{***}I_d}{I_d^{***}}I_d\right)\right]$$

$$+\ a_4\left(1 - \frac{A_u^{***}}{A_u}\right)\sigma_u\left[I_u - \frac{I_u^{***}}{A_u^{***}}A_u\right]$$

$$+\ a_5\left(1 - \frac{A_d^{***}}{A_d}\right)\left[\sigma_d\left(I_d - \frac{I_d^{***}A_d}{A_d^{***}}\right) + \psi_u\left(A_u - \frac{A_u^{***}A_d}{A_d^{***}}\right)\right]$$

$$+\ a_6\left(1 - \frac{T^{***}}{T}\right)\tau_d\left[I_d + A_d - \frac{(I_d^{***} + A_d^{***})}{T^{***}}T\right],$$

which upon further simplifications and re-grouping gives:

$$\frac{d\mathcal{L}}{dt} = -\mu a_1\frac{(S - S^{***})^2}{S} + \frac{\mu\beta}{\Pi}I_u^{***}S^{***}(a_1 + a_2) + \frac{\mu\beta\eta_d}{\Pi}S^{***}I_d^{***}(a_1 + a_2) \quad (C.4)$$

$$+\ \frac{\mu\beta}{\Pi}SI_u(-a_1 + a_2) + \frac{\mu\beta\eta_d}{\Pi}SI_d(-a_1 + a_2)$$

$$+\ \left[a_1\frac{\mu\beta}{\Pi}S^{***} - a_2\frac{\mu\beta}{\Pi}S^{***}\left(\frac{I_d^{***}}{I_u^{***}} + 1\right) + a_3\psi_u + a_4\sigma_u\right]I_u$$

$$+\ \left[a_1\frac{\mu\beta\eta_d}{\Pi}S^{***} - a_3\psi_u\frac{I_u^{***}}{I_d^{***}} + a_5\sigma_d + a_6\tau_d\right]I_d + \left[] - a_4\sigma_u\frac{I_u^{***}}{A_u^{***}} + a_5\psi_u\right]A_u$$

$$+\ \left[] - a_5\sigma_d\frac{I_d^{***}}{A_d^{***}} - a_5\psi_u\frac{A_u^{***}}{A_d^{***}} + a_6\tau_d\right]A_d - a_6\tau_d\left[\frac{I_d^{***}}{T^{***}} + \frac{A_d^{***}}{T^{***}}\right]T \quad (C.5)$$

$$-\ a_1\frac{\mu\beta}{\Pi}\frac{(S^{***})^2}{S}I_u^{***}$$

$$-\ a_1\frac{\mu\beta\eta_d}{\Pi}\frac{(S^{***})^2}{S}I_d^{***} - a_2\frac{\mu\beta}{\Pi}SI_u^{***} - a_2\frac{\mu\beta\eta_d}{\Pi}\frac{I_u^{***}}{I_u}SI_d \quad (C.6)$$

$$-\ a_3\psi\frac{I_d^{***}}{I_d}I_u + a_3\psi_u I_u^{***} - a_4\sigma_u\frac{A_u^{***}}{A_u}I_u + a_4\sigma_u I_u^{***} - a_5\sigma_d\frac{A_d^{***}}{A_d}I_d + a_5\sigma_d I_d^{***}$$

$$-\ a_5\psi_u\frac{A_d^{***}}{A_d}A_u + a_5\psi_u A_u^{***}a_6\tau_d\frac{T^{***}}{T}I_d + a_6\tau_d I_d^{***} - a_6\tau_d\frac{T^{***}}{T}A_d + a_6\tau_d A_d^{***}.$$

We can choose a_i for $i = 1, \cdots 6$ so that

$$a_1 \frac{\mu\beta}{\Pi} S^{***} - a_2 \frac{\mu\beta}{\Pi} S^{***} \left(\frac{I_d^{***}}{I_u^{***}} + 1 \right) + a_3 \psi_u + a_4 \sigma_u = 0,$$

$$a_1 \frac{\mu\beta\eta_d}{\Pi} S^{***} - a_3 \psi_u \frac{I_u^{***}}{I_d^{***}} + a_5 \sigma_d + a_6 \tau_d = 0,$$

$$-a_4 \sigma_u \frac{I_u^{***}}{A_u^{***}} + a_5 \psi_u = 0, \qquad \text{(C.7)}$$

$$-a_5 \sigma_d \frac{I_d^{***}}{A_d^{***}} - a_5 \psi_u \frac{A_u^{***}}{A_d^{***}} + a_6 \tau_d = 0,$$

$$a_6 \tau_d \left[\frac{I_d^{***}}{T^{***}} + \frac{A_d^{***}}{T^{***}} \right] = 0.$$

From Eq. (C.7), we can clearly see that $a_4 = a_5 = a_6 = 0$. Moreover,

$$a_1 \frac{\mu\beta\eta_d}{\Pi} S^{***} = a_3 \psi_u \frac{I_u^{***}}{I_d^{***}} \quad \text{or} \quad a_3 = a_1 \frac{\mu\beta\eta_d}{\psi_u \Pi} S^{***} \frac{I_d^{***}}{I_u^{***}} \quad \text{and} \quad a_2 = a_1 \frac{I^{***} + \eta_d I_d^{***}}{I^{***} + I^{***}}.$$

$$\text{(C.8)}$$

Thus, Eq. (C.7) reduces to:

$$\begin{aligned} \frac{d\mathcal{L}}{dt} &= -\mu a_1 \frac{(S - S^{***})^2}{S} + \frac{\mu\beta}{\Pi} I_u^{***} S^{***} (a_1 + a_2) + \frac{\mu\beta\eta_d}{\Pi} S^{***} I_d^{***} (a_1 + a_2) \\ &+ \frac{\mu\beta\eta_d}{\Pi} S I_u (-a_1 + a_2) + \frac{\mu\beta\eta_d}{\Pi} S I_d (-a_1 + a_2) - a_1 \frac{\mu\beta}{\Pi} \frac{(S^{***})^2}{S} I_u^{***} \\ &- a_1 \frac{\mu\beta\eta_d}{\Pi} \frac{(S^{***})^2}{S} I_d^{***} - a_2 \frac{\mu\beta}{\Pi} S I_u^{***} - a_2 \frac{\mu\beta\eta_d}{\Pi} \frac{I_u^{***}}{I_u} S I_d - a_3 \psi \frac{I_d^{***}}{I_d} I_u + a_3 \psi_u I_u^{***}. \end{aligned}$$
$$\text{(C.9)}$$

By using Eq. (C.8) in Eq. (C.10), and after further computation, we obtain.

$$\begin{aligned} \frac{d\mathcal{L}}{dt} &= a_1 \frac{\mu\beta}{\Pi} S^{***} I^{***} \left(2 - \frac{S^{***}}{S} - \frac{S}{S^{***}} \right) \\ &+ a_1 \frac{\mu\beta\eta_d}{\Pi} S^{***} I_d^{***} \left(3 - \frac{S^{***}}{S} - \frac{I_u I_d^{***}}{I_u^{***} I_d} - \frac{S I_d I_u^{***}}{S^{***} I_d^{***} I_u} \right) \\ &- \mu a_1 \frac{(S - S^{***})^2}{S}. \end{aligned}$$
$$\text{(C.10)}$$

Since the arithmetic mean exceeds the geometric mean, the following inequalities hold:

$$2 - \frac{S^{***}}{S} - \frac{S}{S^{***}} \leq 0 \text{ and } 3 - \frac{S^{***}}{S} - \frac{I_u I_d^{***}}{I_u^{***} I_d} - \frac{S I_d I_u^{***}}{S^{***} I_d^{***} I_u} \leq 0.$$

113

Furthermore, $\mu a_1 \dfrac{(S - S^{***})^2}{S} > 0$ for any arbitrary $a_1 > 0$. Hence, it follows from Eq. (C.10) that $\dfrac{d\mathcal{L}}{dt} \leq 0$.

Therefore, by the Lyapunov function and the LaSalle's principle [68, 77] every solution to the equation in the reduced model (2.20), with Eq. (C.3), approaches the unique endemic equilibrium, $\mathcal{E}_{1r}$, as $t \to \infty$ for $\hat{\mathbb{R}}_T > 1$. $\qquad \square$

APPENDIX D

PROOF OF THEOREM 3.3.3

Proof. The proof is based on the center manifold theory [15, 131]. To apply this theory, it is convenient, first of all, to let $S_L = x_1$, $S_H = x_2$, $I_{1_u} = x_3$, $I_{1_d} = x_4$, $I_{2_u} = x_5$, $I_{2_d} = x_6$, $A_u = x_7$, $A_d = x_8$ and $T = x_9$. The model 3.1 can be re-written in the general form (by using the aforementioned transformation of variables); $\frac{dX}{dt} = (f_1, f_2, f_3, f_4, f_5, f_6, f_7, f_8, f_9)^T$, with $X = (x_1, x_2, x_3, x_4, x_5, x_6, x_7, x_8, x_9)^T$. Specifically, the model (3.1) can be written in terms of the transformed variables as:

$$
\begin{cases}
\dfrac{d\,x_1}{d\,t} = f_1 & = & \Pi(1-p) + \psi_H x_2 - \lambda x_1 - k_1 x_1, \\[2mm]
\dfrac{d\,x_2}{d\,t} = f_2 & = & \Pi p + \psi_L x_1 - \eta_H(1 - \varepsilon_p c_p)\lambda x_2 - k_2 x_2, \\[2mm]
\dfrac{d\,x_3}{d\,t} = f_3 & = & \lambda x_1 + \eta_H(1 - \varepsilon_p c_p)\lambda x_2 - k_3 x_3, \\[2mm]
\dfrac{d\,x_4}{d\,t} = f_4 & = & \varepsilon_d \xi_d x_3 - k_4 x_4, \\[2mm]
\dfrac{d\,x_5}{d\,t} = f_5 & = & \sigma_{1u} x_3 - k_5 x_5, \\[2mm]
\dfrac{d\,x_6}{d\,t} = f_6 & = & \varepsilon_d \xi_d x_5 + \sigma_{1d} x_4 - k_6 x_6, \\[2mm]
\dfrac{d\,x_7}{d\,t} = f_7 & = & \sigma_{2u} x_5 - k_7 x_7, \\[2mm]
\dfrac{d\,x_8}{d\,t} = f_8 & = & \sigma_{2d} x_6 + \varepsilon_d \xi_d x_7 - k_8 x_8, \\[2mm]
\dfrac{d\,x_9}{d\,t} = f_9 & = & \tau_I x_4 + \tau_2 x_6 + \tau_A x_8 - k_9 x_9,
\end{cases}
\tag{D.1}
$$

where,

$$
\lambda = \beta \left[\frac{x_3 + \eta_d x_4 + \eta_2(x_5 + \eta_d x_6) + \eta_A(x_7 + \eta_d x_8)}{N} \right], k_1 = \psi_L + \mu, k_2 = \psi_H + \mu,
$$

$$
k_3 = \varepsilon_d \xi_d + \sigma_{1u} + \mu, k_4 = \tau_1 + \sigma_{1d} + \mu, k_5 = \varepsilon_d \xi_d + \sigma_{2u} + \mu, k_6 = \tau_2 + \sigma_{2d} + \mu,
$$

$$
k_7 = \varepsilon_d \xi_d + \mu + \delta_u, k_8 = \tau_A + \mu + \delta_d, k_9 = \mu.
\tag{D.2}
$$

Evaluating the Jacobian of the transformed system (D.1) at the DFE $(\mathcal{E}_{DF})$, is given by:

$$J(\mathcal{E}_{DF}) = \begin{pmatrix} -k_1 & \psi_H & -J_1 & -\eta_d\,J_1 & -\eta_2\,J_1 & -\eta_2\,\eta_d\,J_1 & -\eta_A\,J_1 & -\eta_A\,\eta_d\,J_1 & 0 \\ \psi_L & -k_2 & J_2 & -\eta_d\,J_2 & -\eta_2\,J_2 & -\eta_2\,\eta_d\,J_2 & -\eta_A\,J_2 & -\eta_A\,\eta_d\,J_2 & 0 \\ 0 & 0 & J_3 - k_3 & \eta_d\,J_3 & \eta_2\,J_3 & \eta_2\,\eta_d\,J_3 & \eta_A\,J_3 & \eta_A\,\eta_d\,J_3 & 0 \\ 0 & 0 & \xi_d\,\varepsilon_d & -k_4 & 0 & 0 & 0 & 0 & 0 \\ 0 & 0 & \sigma_{1_u} & 0 & -k_5 & 0 & 0 & 0 & 0 \\ 0 & 0 & 0 & \sigma_{1_d} & \xi_d\,\varepsilon_d & -k_6 & 0 & 0 & 0 \\ 0 & 0 & 0 & 0 & \sigma_{2_u} & 0 & -k_7 & 0 & 0 \\ 0 & 0 & 0 & 0 & 0 & \sigma_{2_d} & \xi_d\,\varepsilon_d & -k_8 & 0 \\ 0 & 0 & 0 & \tau_1 & 0 & \tau_2 & 0 & \tau_A & -k_9 \end{pmatrix},$$

where,

$$J_1 = \frac{\beta\{(1-p)\mu + \psi_H\}}{\mu + \psi_H + \psi_L}, \quad J_2 = \frac{\beta\,\eta_H(1 - \varepsilon_p c_p)(\mu p + \psi_L)}{\mu + \psi_H + \psi_L} \text{ and } J_3 = J_1 + J_2.$$

Consider the case when $\mathbb{R}_{T_c} = 1$ and choosing β as the bifurcation parameter, and solving for β when $\mathbb{R}_{T_c} = 1$ (i.e., at the bifurcation point) gives:

$$\beta = \frac{C_1\,C_2\,C_3\,C_4\,C_5\,C_6\,N^*}{B^*\{T_1 + T_2 + T_3 + T_4 + T_5 + T_6\}} = \beta^*,$$

where,

$B^* = S_L^* + \eta_H(1 - \varepsilon_p c_p)S_H^*$, $N^* = \dfrac{\Pi}{\mu}$, $T_1 = C_2\,C_3\,C_4\,C_5\,C_6$, $T_2 = C_3\,C_4\,C_5\,C_6\,\eta_d\,\varepsilon_d\,\xi_d$,

$T_3 = C_2\,C_4\,C_5\,C_6\,\eta_2\,\sigma_{1_u}$, $T_4 = C_5\,C_6\,\eta_2\,\eta_d\,\varepsilon_d\,\xi_d\,(C_3\,\sigma_{1_d} + C_2\,\sigma_{1_u})$, $T_5 = C_2\,C_4\,C_6\,\eta_A\,\sigma_{1_u}\,\sigma_{2_u}$,

$T_6 = \eta_A\,\eta_d\,\varepsilon_d\,\xi_d\,(C_2\,C_4\,\sigma_{1_u}\,\sigma_{1_d} + C_3\,C_5\,\sigma_{1_d}\,\sigma_{2_d} + C_2\,C_5\,\sigma_{1_u}\,\sigma_{2_d})$ and C_1, C_2, C_3, C_4, C_5, C_6 are as defined in (3.7).

Let J_{β^*} denotes the Jacobian of the system (D.1) evaluated at the DFE ($\mathcal{E}_{DF}$). It can be seen that the system (D.1), with $\beta = \beta^*$, has a simple eigenvalue with zero real part and all other eigenvalues having negative real part [12]. Hence, the center manifold theory [15, 16] can be applied to analyze the dynamics of the model (3.1) near the bifurcation point (where $\beta = \beta^*$). To apply the theory (in particular, the approach in [16]), the following computations (associated with the left and right eigenvectors

of J_{β^*}, corresponding to the zero eigenvalue) are necessary.

<div align="center">Computation of left and right eigenvectors of J_{β^*}</div>

It can be seen that the left eigenvector of J_{β^*}, corresponding to the zero eigenvalue, is given by:

$\mathbf{v} = [v_1, v_2, v_3, v_4, v_5, v_6, v_7, v_8, v_9]$, where (noting that J_1, J_2 and J_3 are defined above),

$$v_1 > 0 \quad (\text{free}), \quad v_2 = \frac{\psi_H\, v_1}{k_2}, \quad v_3 > 0 \quad (\text{free}), \quad v_9 = 0,$$

$$v_8 = \frac{\beta\, \eta_a\, \eta_d(-J_1\, v_1 - J_2\, v_2 + J_3\, v_3)}{k_8},$$

$$v_6 = \frac{\beta\, \eta_a\, \eta_d(-J_1\, v_1 - J_2\, v_2 + J_3\, v_3) + \sigma_{2_d}\, v_8}{k_6}, \tag{D.3}$$

$$v_7 = \frac{\beta\, \eta_a\, (-J_1\, v_1 - J_2\, v_2 + J_3\, v_3) + \varepsilon_d\, \xi_d\, v_8}{k_7},$$

$$v_4 = \frac{\beta\, \eta_d(-J_1\, v_1 - J_2\, v_2 + J_3\, v_3) + \sigma_{1_d}\, v_6}{k_4},$$

$$v_5 = \frac{\beta\, \eta_d(-J_1\, v_1 - J_2\, v_2 + J_3\, v_3) + \sigma_{1_d}\, v_6 + \sigma_{2_u}\, v_7}{k_5}.$$

Furthermore, the right eigenvector of J_{β^*}, corresponding to the zero eigenvalue, is given by:

$\mathbf{w} = [w_1, w_2, w_3, w_4, w_5, w_6, w_7, w_8, w_9]^T$, where,

$$w_1 = \frac{-\beta\, J_1\, (w_3 + \eta_d\, w_4 + \eta_2\, w_5 + \eta_2\, \eta_d\, w_6 + \eta_A\, w_7 + \eta_A\, \eta_d w_8) + \psi_H w_2}{k_1},$$

$$w_2 > 0, (\text{free}), w_3 > 0 \ (\text{free}), w_4 = \frac{\varepsilon_d\, \xi_d\, w_3}{k_4},$$

$$w_5 = \frac{\sigma_{1_u}\, w_3}{k_5}, w_7 = \frac{\sigma_{2_u}\, w_5}{k_7}, w_6 = \frac{\sigma_{1_d}\, w_4 + \varepsilon_d\, \xi_d\, w_5}{k_6}, \tag{D.4}$$

$$w_8 = \frac{\sigma_{2_d}\, w_6 + \varepsilon_d\, \xi_d\, w_7}{k_8}, w_9 = \frac{\tau_1\, w_4 + \tau_2\, w_6 + \tau_A\, w_8}{k_9},$$

$$w_9 = \frac{\tau_1\, w_4 + \tau_2\, w_6 + \tau_A\, w_8}{k_9}.$$

For computational convenience, we set, without loss of generality, the components of the left eigenvectors v_1 and v_3 in (D.3) to one. Similarly, we set the components w_2 and w_3, of the right eigenvector, given in (D.4) to unity.

Computation of backward bifurcation coefficients, a and b

The local bifurcation analysis near the bifurcation point ($\beta = \beta^*$) is determined by the signs of two bifurcation coefficients, denoted by a and b [15, 16]. Following [16], the expressions for these bifurcation coefficients are, respectively, given by:

$$a = \sum_{k,i,j=1}^{n} v_k w_i w_j \frac{\partial^2 f_k}{\partial x_i \partial x_j}(\mathcal{E}_{DF}, \beta^*), \tag{D.5}$$

and,

$$b = \sum_{k,i=1}^{n} v_k w_i \frac{\partial^2 f_k}{\partial x_i \partial \beta}(\mathcal{E}_{DF}, \beta^*). \tag{D.6}$$

It can be shown, by substituting the expressions for the eigenvectors (w_k and v_k; $k = 1, \cdots, 9$) given in (D.3) and (D.4) and the partial derivatives of the functions f_k ($k = 1, \cdots, 9$) defined in (D.1) into the expressions (D.5) and (D.6), that the bifurcation coefficients now become:

$$a = \frac{1}{\Pi\left(\mu + \psi_H + \psi_L\right)} \left[2\,\mu\,\beta\,(C)\left\{(P + Q + R) - (S + T + U)\right\}\right] \tag{D.7}$$

and,

$$b = \frac{C\left(X - Y\right)}{\mu + \psi_H + \psi_L}, \tag{D.8}$$

where,

$$C = w_3 + \eta_d \, w_4 + \eta_2 \, w_5 + \eta_2 \, \eta_d \, w_6 + \eta_A \, w_7 + \eta_A \, \eta_d \, w_8,$$

$$P = v_1(w_2 \, \mu + w_3 \, \mu + w_4 \, \mu + w_5 \, \mu + w_6 \, \mu + w_7 \, \mu + w_8 \, \mu + w_9 \, \mu + w_2 \, \psi_H + w_3 \, \psi_H$$

$$+ \, w_4 \, \psi_H + w_5 \, \psi_H + w_6 \, \psi_H + w_7 \, \psi_H + w_8 \, \psi_H + w_9 \, \psi_H + w_9 \, \psi_H$$

$$+ \, w_2 \, \psi_H + w_7 \, \mu + w_9 \, \mu),$$

$$Q = v_2 \, \eta_H \, (1 - \varepsilon_p \, c_p)(w_1 \, \mu \, p + w_2 \, \mu \, p + w_3 \, \mu \, p + w_4 \, \mu \, p + w_5 \, \mu \, p + w_6 \, \mu \, p$$

$$+ \, w_7 \, \mu \, p + w_8 \, \mu \, p + w_9 \, \mu \, p + w_1 \, \psi_L + w_3 \, \psi_L + w_4 \, \psi_L + w_5 \, \psi_L + w_6 \, \psi_L$$

$$+ \, w_7 \, \psi_L + w_8 \, \psi_L + w_9 \, \psi_L),$$

$$R = v_3 \{ \eta_H \, (1 - \varepsilon_p \, c_p)(w_2 \, \psi_H + w_2 \, \mu) + w_1 \, \mu \, p + w_2 \, \mu \, p + w_3 \, \mu \, p + w_4 \, \mu \, p \qquad \text{(D.9)}$$

$$+ \, w_5 \, \mu \, p + w_6 \, \mu \, p + w_7 \, \mu \, p + w_8 \, \mu \, p + w_9 \, \mu \, p \},$$

$$S = v_1 \, \mu \, p \, (w_1 + w_2 + w_3 + w_4 + w_5 + w_6 + w_7 + w_8 + w_9) + v_1 \, w_1 \, \psi_L,$$

$$T = v_2 \, w_2 \, \eta_H \, (1 - \varepsilon_p \, c_p)(\psi_H + \mu),$$

$$U = v_3 \, [\{ \eta_H \, (1 - \varepsilon_p \, c_p) \, (w_1 + w_2 + w_3 + w_4 + w_5 + w_6 + w_7 + w_8 + w_9) \, (\mu \, p + \psi_L) \}$$

$$+ \, \{ (w_2 + w_3 + w_4 + w_5 + w_6 + w_7 + w_8 + w_9)(\mu + \psi_H) \}],$$

$$X = [\{ \eta_H \, (1 - \varepsilon_p \, c_p) \, v_3(\mu \, p + \psi_L) \} + v_1 \, \mu \, p + v_3 \, (\psi_H + \mu)],$$

$$Y = [\{ \eta_H \, (1 - \varepsilon_p \, c_p) \, v_2(\mu \, p + \psi_L) \} + v_3 \, \mu \, p + v_1 \, (\psi_H + \mu)].$$

It follows from Item (i) of Theorem 4.1 of [16] that the model (3.1) will undergo a backward bifurcation at $\mathbb{R}_{T_c} = 1$ whenever the bifurcation coefficients, a and b (given by (D.7) and (D.8), respectively), are positive. It can be shown that the bifurcation coefficient b is automatically positive as follows. First of all, using the definitions for X and Y in (D.9), the quantity $X - Y$ can be simplified to:

$$X - Y = \eta_H \, (1 - \varepsilon_p \, c_p) \, (\mu \, p + \psi_L)(1 - v_2), \qquad \text{(D.10)}$$

which is positive since $\eta_H > 0$, $0 < \varepsilon_p\, c_p < 1$, $\mu > 0$, $p > 0$, $\psi_L > 0$ and the eigenvector $0 < v_2 < 1$ (from (D.3)). Since $X - Y > 0$, $\mu > 0$, $\psi_H > 0$, $\psi_L > 0$ and $C > 0$, it follows from (D.8) that the bifurcation coefficient b is automatically positive. Hence, since the bifurcation coefficient b is always positive, we only need to show that the coefficient a is positive for backward bifurcation to occur. In particular, it can be shown from Equation (D.7), and noting the definitions in (D.9) and the expressions for the eigenvectors in (D.3) and (D.4), that the backward bifurcation coefficient a is positive provided the following inequality holds:

$$P + Q + R > S + T + U. \tag{D.11}$$

Thus, it follows from Item (i) of Theorem 4.1 of [16]), that the model (3.1) will undergo a backward bifurcation at $\mathbb{R}_{T_c} = 1$ whenever inequality (D.11) holds. $\qquad\square$

APPENDIX E

PROOF OF THEOREM 3.3.4

Proof. Before proving the result of Theorem 3.3.4, it is necessary to establish the following intermediate results.

<center>*Proof of positive invariance and attractivity of Γ^**</center>

Since $N(t) \leq \Pi/\mu$ for all t in Γ^*, it follows from the first equation of the two-group HIV model (3.1) that:

$$
\begin{aligned}
\frac{dS_L}{dt} &\leq \Pi(1-p) + \left(\frac{\Pi}{\mu} - S_L\right)\psi_H - (\psi_L + \mu)S_L, \\
&\leq \Pi(1-p) + \left(\frac{\Pi}{\mu}\right)\psi_H - (\psi_H + \psi_L + \mu)\,S_L, \\
&\leq \frac{\Pi}{\mu}\{\mu(1-p) + \psi_H\} - (\psi_H + \psi_L + \mu)\,S_L, \\
&\leq (\psi_H + \psi_L + \mu)\,(S_L^* - S_L).
\end{aligned}
$$

Hence, if $S_L(t) > S_L^*$, then $\dfrac{dS_L}{dt}$ is negative. Thus, $S_L(t) \leq S_L^*$ for all t, provided that $S_L(0) \leq S_L^*$. Using similar approach for the second equation of the model (3.1), and using the above bound, we get the following bound:

$$
\begin{aligned}
\frac{dS_H}{dt} &\leq \Pi\,p + \left(\frac{\Pi}{\mu}\right)\psi_L - (\psi_H + \mu)V, \\
&\leq \Pi\,p + \left(\frac{\Pi}{\mu}\right)\psi_L - (\psi_H + \psi_L + \mu)\,S_L, \\
&\leq (\psi_H + \psi_L + \mu)\,(S_H^* - S_H).
\end{aligned}
$$

Similarly, we have $S_H(t) \leq S_H^*$ for all t, provided that $S_H(0) \leq S_H^*$. It follows from these bounds that:

$$
\Gamma^* = \{(S_L(t), S_H(t), I_{1u}(t), I_{1d}(t), I_{2u}(t), I_{2d}(t), A_u(t), A_d(t), T(t)) \in \Gamma : S_L \leq S_L^*, S_H \leq S_H^*\}
$$

<div align="right">(E.1)</div>

is positively-invariant and attracts all initial solutions in Γ^*.

<center>123</center>

Next generation matrices for the special case of the model (3.1)

For the special case of the model (3.1), the associated next generation matrix of new infection terms, denoted by $\hat{F}$, and the associated next generation matrix of linear transition terms, denoted by $\hat{V}$, are given as:

$$
\hat{F} = \begin{bmatrix}
\dfrac{\beta S_L^*}{N^*} & \eta_d \dfrac{\beta S_L^*}{N^*} & \eta_2 \dfrac{\beta S_L^*}{N^*} & \eta_2 \eta_d \dfrac{\beta S_L^*}{N^*} & \eta_A \dfrac{\beta S_L^*}{N^*} & \eta_A \eta_d \dfrac{\beta S_L^*}{N^*} \\
0 & 0 & 0 & 0 & 0 & 0 \\
0 & 0 & 0 & 0 & 0 & 0 \\
0 & 0 & 0 & 0 & 0 & 0 \\
0 & 0 & 0 & 0 & 0 & 0 \\
0 & 0 & 0 & 0 & 0 & 0
\end{bmatrix}
$$

and,

$$
\hat{V} = \begin{bmatrix}
\hat{C}_1 & 0 & 0 & 0 & 0 & 0 \\
-\varepsilon_d \xi_d & \hat{C}_2 & 0 & 0 & 0 & 0 \\
-\sigma_{1u} & 0 & \hat{C}_3 & 0 & 0 & 0 \\
0 & -\sigma_{1d} & -\varepsilon_d \xi_d & \hat{C}_4 & 0 & 0 \\
0 & 0 & -\sigma_{2u} & 0 & \hat{C}_5 & 0 \\
0 & 0 & 0 & -\sigma_{2d} & -\varepsilon_d \xi_d & \hat{C}_6
\end{bmatrix},
$$

where

$\hat{C}_1 = \varepsilon_d \xi_d + \sigma_{1u} + \mu, \hat{C}_2 = \tau_1 + \sigma_{1d} + \mu, \hat{C}_3 = \varepsilon_d \xi_d + \sigma_{2u} + \mu, \hat{C}_4 = \tau_2 + \sigma_{2d} + \mu,$
$\hat{C}_5 = \varepsilon_d \xi_d + \mu$ and $\hat{C}_6 = \tau_A + \mu.$

Proof of Theorem 3.3.4

Consider the model (3.1) with $\varepsilon_m c_m = 1$ and $\delta_u = \delta_d = 0$. We further assume that $\hat{\mathbb{R}}_{T_c} < 1$. The proof is also based on using a comparison theorem [78, 65, 104]. The

124

equations for the infected compartments of the special case of the model (3.1) can be re-written as:

$$\frac{d}{dt}\begin{bmatrix} I_{1_u}(t) \\ I_{1_d}(t) \\ I_{2_u}(t) \\ I_{2_d}(t) \\ A_u(t) \\ A_d(t) \end{bmatrix} = (\hat{F} - \hat{V}) \begin{bmatrix} I_{1_u}(t) \\ I_{1_d}(t) \\ I_{2_u}(t) \\ I_{2_d}(t) \\ A_u(t) \\ A_d(t) \end{bmatrix} - M \begin{bmatrix} I_{1_u}(t) \\ I_{1_d}(t) \\ I_{2_u}(t) \\ I_{2_d}(t) \\ A_u(t) \\ A_d(t) \end{bmatrix}, \qquad (\text{E.2})$$

where the next generation matrices $\hat{F}$ and $\hat{V}$ are as defined in Equation (E) and the matrix M is defined as:

$$M = \beta\,(S_L^* - S_L) \begin{bmatrix} 1 & \eta_d & \eta_2 & \eta_2\eta_d & \eta_A & \eta_A\eta_d \\ 0 & 0 & 0 & 0 & 0 & 0 \\ 0 & 0 & 0 & 0 & 0 & 0 \\ 0 & 0 & 0 & 0 & 0 & 0 \\ 0 & 0 & 0 & 0 & 0 & 0 \\ 0 & 0 & 0 & 0 & 0 & 0 \end{bmatrix}. \qquad (\text{E.3})$$

Since $S_L \le S_L^*$ for all $t > 0$ in Γ^*, it follows that the matrix M is non-negative. Hence, Equation (E.2) can be re-written in terms of the following inequality:

$$\frac{d}{dt}\begin{bmatrix} I_{1_u}(t) \\ I_{1_d}(t) \\ I_{2_u}(t) \\ I_{2_d}(t) \\ A_u(t) \\ A_d(t) \end{bmatrix} \le (\hat{F} - \hat{V}) \begin{bmatrix} I_{1_u}(t) \\ I_{1_d}(t) \\ I_{2_u}(t) \\ I_{2_d}(t) \\ A_u(t) \\ A_d(t) \end{bmatrix}. \qquad (\text{E.4})$$

It should be recalled from the local asymptotic stable result for the disease-free equilibrium of the model (3.1) (given in Theorem 3.3.1) that all eigenvalues of the associated

next generation matrix FV^{-1} are negative if $\mathbb{R}_{T_c} < 1$ (i.e., $F - V$ is a stable matrix). It follows that the eigenvalues of the next generation matrix $\hat{F}\hat{V}^{-1}$, associated with this special case of the model (3.1), are also negative if $\hat{\mathbb{R}}_{T_c} < 1$ (i.e., $\hat{F} - \hat{V}$ is also a stable matrix). Thus, the linearized differential inequality system (E.4) is stable whenever $\rho(\hat{F}\hat{V}^{-1}) < 1$. Consequently [106, 66, 104, 91],

$$(I_{1u}(t), I_{1d}(t), I_{2u}(t), I_{2d}(t), A_u(t), A_d(t)) \to (0, 0, 0, 0, 0, 0), \text{ as } t \to \infty.$$

Substituting $I_{1u}(t) = I_{1d}(t) = I_{2u}(t) = I_{2d}(t) = A_u(t) = A_d(t) = 0$ into the differential equations for the rate of change of the $S_L(t), S_H(t)$ and $T(t)$ compartments of the model (3.1) shows that:

$$S_L(t) \to S_L^*, S_H(t) \to S_H^* \text{ and } T \to 0 \text{ as } t \to \infty.$$

Thus, the disease-free equilibrium $(\mathcal{E}_{DF})$ of the special case of the model (3.1), with $\varepsilon_p c_p = 1$ and $\delta_u = \delta_d = 0$ is globally-asymptotically stable in Γ^* whenever $\hat{\mathbb{R}}_{T_c} < 1$. $\qquad\square$